Quantum Information Theory and The Black Hole Information Paradox

by

Md Reshad Ur Rahman
18311003
Josh Munshi
17111003

A thesis submitted to the Department of Mathematics and Natural Sciences
in partial fulfillment of the requirements for the degree of
Bachelor of Science in Physics

Department of Mathematics and Natural Sciences
Brac University
October 2020

Declaration

It is hereby declared that

1. The thesis submitted is my/our own original work while completing degree at Brac University.
2. The thesis does not contain material previously published or written by a third party, except where this is appropriately cited through full and accurate referencing.
3. The thesis does not contain material which has been accepted, or submitted, for any other degree or diploma at a university or other institution.
4. We have acknowledged all main sources of help.

Student's Full Name & Signature:

Md Reshad Ur Rahman	Josh Munshi
18311003	17111003

Approval

The thesis/project titled "Quantum Information Theory and The Black Hole Information Paradox" submitted by

1. Md Reshad Ur Rahman (18311003)
2. Josh Munshi (17111003)

Of Summer, 2020 has been accepted as satisfactory in partial fulfillment of the requirement for the degree of Bachelor of Science in Physics on October 10, 2020.

Examining Committee:

Supervisor:
(Member)

Dr. Tibra Ali
Professor and Associate Dean
Department of Mathematics and Natural Sciences
Brac University

Program Coordinator:
(Member)

Dr. Firoze Haque
Associate Professor
Department of Mathematics and Natural Sciences
Brac University

Head of Department:
(Chair)

Dr. A F M Yusuf Haider
Professor and Chairperson
Department of Mathematics and Natural Sciences
Brac University

Abstract

This thesis discusses the information-theoretic concepts of Black Holes. Its primary focus is describing black hole dynamics with unitary operators within the perspective of quantum information theory and AdS/CFT arguments on why black hole evaporation is likely to be unitary. This thesis also provides mathematical backgrounds of classical black holes and quantum field theory in curved space. Then we introduced entanglement entropy and compared the shell of photons in a pure state to free harmonic oscillators. Afterward, we introduce an interaction term in the hamiltonian for $t > 0$, which we call a sudden quench. Finally, we have calculated the time evolved entanglement entropy for N-quenched oscillators and graphically demonstrated the entanglement entropy for various N. We want to model the time dependent entanglement entropy S_1 between the internal and emitted radiation of a black hole. As for a future project, we want to regularize a quantum field to the Hamiltonian of N-quenched oscillators and compute the entanglement entropy S_2 that results from tracing degrees of freedom inside an imaginary sphere. Hence, as S_1 increases with time as the photons' shell begins to collapse, we have a comparable situation, using the ideas about holography, with the time evolution of the S_2.

Keywords: *AdS/CFT, Classical Black Holes, Curved Spacetime, Entanglement Entropy, Quantum Field Theory, Quantum Information Theory, Holography, Quench*

Acknowledgement

We would like to thank all the people that have supported us in this journey. We are truly and deeply grateful to our thesis advisor Dr. Tibra Ali and our greatest inspiration Dr. Mahbub Alam Majumdar for guiding us throughout this project.

We are most grateful to our family members for providing all the support that we needed throughout this journey. Without their support and encouragement none of this would have been possible. We would like to express gratitude to all our friends and seniors that supported us throughout our undergraduate life.

We would like to thank Professor and Chairperson Dr. A.F.M Yusuf Haider for his advice, support and time to help inspire us. We would like to thank Dr. Firoze H. Haque for motivating and introducing us to the fundamental courses that were essential in order to start this project.

We are extremely grateful to Assistant Professor Mohammad Hassan Murad and Dr. Sharmina Hussain for helping us grow a strong background in Mathematics. We would like to thank Assistant Professor Muhammad Lutfor Rahman for helping us enjoy the Applied Physics courses. We are very grateful to Senior Lecturer Mohammad Mosaddidur Rahman to guide us through his teaching and course advising. We acknowledge all the other faculty members who have equally helped us make it so far with a wide understanding and applications of Physics.

Our undergraduate journey has been memorable and joyous for all your support and inspiration.

Table of Contents

List of Figures

List of Tables

Chapter 1

Introduction

The first concept of something similar to a black hole came in as early as 1784. John Mitchell proposed that if the gravitational force of a star exceeds a certain amount, the escape velocity of the star will exceed the speed of light. Surprisingly he obtained the correct result of the radius r_h of the horizon but for the wrong reasons[26]; using the conservation of energy in Newtonian Mechanics:

$$\frac{1}{2}mc^2 - \frac{GMm}{r_h} = 0,$$
$$r_h = \frac{2GM}{c^2},$$

where M is the mass of the dark star, G is the gravitational constant and c is the speed of light.

This thesis has two portions: a portion where we review the concepts of information paradox from many perspectives, and the other portion is our original work of calculating the entanglement entropy of N-quenched oscillators. First, we start with classical black holes, then introduce quantum field theory on a black hole background and explain why it leads to difficulties. Second, to overcome that problem, we review the S-matrix, the Page curve, and quantum information-theoretic arguments on the information paradox while assuming that evaporation is unitary. Third, we introduce the AdS/CFT arguments on why black hole evaporation is likely to be unitary, and then we use the holographic principle to compare the entanglement entropy between subsystems of oscillators and the Bekenstein-Hawking entropy of a black hole. We also reviewed the calculation for the entanglement entropy for the quenched double oscillator. Finally, we wrote down our original calculation of the entanglement entropy of quenched N-oscillators.

1.1 Motivation

Srednicki's idea about holographic entanglement entropy[30] is the primary impetus behind our project. The black hole at a specific time t has a horizon area A, which is proportional to its intrinsic Bekenstein-Hawking entropy. Srednicki

showed that the entanglement entropy is a more general concept and that the entanglement entropy that results by tracing out degrees of freedom within a sphere in flat spacetime also depends on its area, suggesting an inherent link between the entanglement entropy between subsystems of harmonic oscillators and the intrinsic entropy of a black hole. Another thing to note is that a paper that studied the entanglement tsunami[18] connects the time evolution of entanglement entropy in a strongly coupled holographic system to its dual: black hole formation from a collapsing shell of matter. Initially, the shell is in a pure state, and therefore, is comparable to a system of free harmonic oscillators. As the black hole begins to form, the entanglement entropy between the late and early radiation begins to rise. We want to study the entanglement entropy of a mathematical model starting from a system of decoupled harmonic oscillators at $t = 0$ and introducing an interaction term for $t > 0$; a situation called the 'sudden quench.' The time evolution of the entanglement entropy between the subsystems should then be of interest to compare with the entanglement entropy between the black hole's early and late radiation.

1.2 Literature Review

While writing the review portion of the thesis, we required assistance from numerous sources. To write "Chapter (2): Classical Black Holes", we adopted the Schwarzchild metric from Jerusalem lecture notes [11]. Then we used Carrol's textbook [7] to calculate the fully contracted Reimann Tensor. We relied on the lecture note: Quantum Black Holes [32] for working out the formalism. Finally, to discuss the collapse of a shell, we used on Susskind's lecture on black holes and holography [31].

In "Chapter (3): Quantum Field Theory," we used Peskin and Schroeder's textbook for the Hamiltonian, followed by Krishnan's lecture on quantum field theory, black holes, and holography [17] for tortoise coordinates. We adopted the covariant form as the transition from flat spacetime to curved with Carrol's textbook. Furthermore, we related black holes with the remaining chapter with the help of Jeruslam lecture notes.

For "Chapter (4): Quantum Information Theory in a Black Hole Background", we explained concepts from quantum information theory and complex Gaussian variables using Ong's thesis on evolution of black holes in AdS space[22]. We worked through different variations of Page's Theorem with Jerusalem lecture notes. Additionally, this thesis reviewed information-theoretic arguments on Black Hole with Preskill and Haydens' article titled "Black Holes as mirrors"[12].

We did the CFT portion of "Chapter (5): AdS/CFT and Holography" from "Introduction to the Maldacena conjecture on AdS/CFT"[25]. Also, we worked out the AdS portion from the Jerusalem lecture notes. Then we combined our understanding to review AdS/CFT with TASI lectures [1] and Natsuume's user guide[20]. Afterward, we turned our attention to mathematical models of black holes in AdS/CFT and gave arguments supporting unitary evaporation from Lowe [19]. We took the holographic entanglement entropy bound from
Zwiebach's and Jerusalem lecture notes [33]. To review some mathematical back-

ground, we have consulted lectures of Kaplan[16] and Ammon[4]. In the end, we reviewed the holographic entanglement entropy formula by Ryu and Takayanagi [28] along with its heuristic derivation[21].

In "Chapter (6): Entanglement Entropy between Subsystem of Oscillators", we worked through the properties of entanglement entropy with Schumacher's textbook[29], Polak's textbook[27], and Headrick's lecture[14]. To work out the calculation and to use holographic ideas on black holes, we used Srednicki's paper [30].

For "Chapter (7): Calculation of Entropy of Quenched Double Oscillators", we reviewed the calculation for the entanglement entropy of the quenched double oscillator, written by Ali and Moynihan[3]. Here, we have worked with the same ansatz as that of Srednicki's work for the coupled two oscillators; however, we adopted the contour-integral representation of Hermite polynomials from Ali and Moynihan's work. Their paper went on to pave the foundation for our work to generalization to $N \geq 2$.

Finally, in our original work, "Chapter (8): Calculation of Entropy of Quenched N-Oscillators," we adopted our Hamiltonian for $t > 0$ from Ali's work on circuit complexity[2]. Then we went on to work with normal modes defined by Jefferson's article[15]. Srednicki had done similar work for a static case, whereas our results are time-dependent. We relied on essential concepts such as time evolution from using propagators in normal modes, the reduced density operator's eigenbasis, and the contour-integral representation to solve our ansatz from Ali and Moynihan's calculation we reviewed in chapter (7). Furthermore, we also showed that our graphical demonstration for $N = 2$ is in exact agreement with their work.

Chapter 2

Classical Black Holes

2.1 The Schwarzschild Black Hole

The metric for the geometry of the Schwarzschild spacetime is [11]

$$ds^2 = -\frac{r-2GM}{r}dt^2 + \frac{r}{r-2GM}dr^2 + r^2 d\Omega^2, \tag{2.1}$$

where M is a parameter with dimensions of mass, G is Newton's gravitational constant, and $d\Omega^2 = \left(d\theta^2 + sin^2\theta d\phi^2\right)$ is the unit metric on two sphere $\mathbb{S}^2$. The coordinate t is the time measured by an observer at $r \gg 2GM$, which means at a fixed time t the spacetime consists of concentric two spheres $\mathbb{S}^2$ of a surface area of $4\pi r^2$.

To check for singularity, we compute the fully contracted Riemann Tensor[7]:

$$R^{\mu\nu\alpha\beta}R_{\mu\nu\alpha\beta} = \frac{48G^2M^2}{r^6}. \tag{2.2}$$

Equation (2.2) is divergent only when $r = 0$. Hence, $r = 0$ is the only singularity of the Schwarzschild geometry. Furthermore, the metric diverges as it should on the singularity.

The Schwarzschild radius is given by $r_s \equiv 2GM$. At $r_s = 2GM$, the signs of the coefficient of dt^2 and dr^2 swap; therefore, r coordinate becomes timelike, and t coordinate becomes spacelike. Hence, any test particle at $r_s < 2GM$, regardless of its mass, will continue to evolve towards the singularity $r = 0$. The mathematical surface of $\mathbb{S}^2$ at $r_s = 2GM$ is called the event horizon of the Schwarzschild black hole.

2.2 Kruskal-Szekres Extention

For the radial null geodesic[32], $ds^2 = 0$ and the angles θ and ϕ are constant $\implies d\Omega^2 = 0$.

$$-\frac{r-2GM}{r}dt^2 + \frac{r}{r-2GM}dr^2 = 0 \tag{2.3}$$

$$\therefore \frac{dt}{dr} = \pm \frac{r}{r - 2GM} \tag{2.4}$$

Integrating to find t,

$$\begin{aligned} t &= \pm \int \frac{rdr}{r - 2GM} \\ &= \pm \left(r + 2GM \ln\left(-2GM + r\right)\right) + C. \end{aligned} \tag{2.5}$$

From here and onwards, the Schwarzchild radius is $r_s = 2GM$ is set to $r_s = 1$. Hence,

$$\begin{aligned} t &= \pm r + \ln(r-1) + C \\ &= \pm r_* + C, \end{aligned} \tag{2.6}$$

where,

$$r_* \equiv r + \ln(r-1), \tag{2.7}$$

$$dr_* = \frac{rdr}{r-1}. \tag{2.8}$$

The metric has become

$$ds^2 = \left(\frac{r-1}{r}\right)\left(-dt^2 + dr_*^2\right) + r^2 d\Omega^2. \tag{2.9}$$

We define newer coordinates in terms of u and v:

$$\begin{aligned} u &\equiv t + r_*, \\ v &\equiv t - r_*. \end{aligned} \tag{2.10}$$

Now, the metric becomes

$$ds^2 = -\left(\frac{r-1}{r}\right) dudv + r^2 d\Omega^2. \tag{2.11}$$

Note that,

$$\begin{aligned} \frac{1}{2}(v-u) &= r_* \\ &= r + \ln\left(r-1\right). \end{aligned} \tag{2.12}$$

Again, we define new coordinates,

$$\begin{aligned} v' &\equiv \exp\left(\frac{v}{2}\right) \\ &= \sqrt{r-1}\exp\left(\frac{r+t}{2}\right), \end{aligned} \tag{2.13}$$

$$\begin{aligned} u' &\equiv -\exp\left(-\frac{u}{2}\right) \\ &= \sqrt{r-1}\exp\left(\frac{r-t}{2}\right). \end{aligned} \tag{2.14}$$

However,

$$du'dv' = \frac{1}{4}\exp(r)(r-1)dudv. \tag{2.15}$$

The Schwarzchild metric is now

$$ds^2 = -\frac{4}{r}\exp(-r)du'dv' + r^2 d\Omega^2. \tag{2.16}$$

Defining newer coordinates,
when $r > r_s$,

$$\begin{aligned} T &\equiv \frac{1}{2}\left(u' + v'\right) \\ &= \sqrt{r-1}\exp\left(\frac{r}{2}\right)\sinh\left(\frac{t}{2}\right), \end{aligned} \tag{2.17}$$

$$\begin{aligned} R &\equiv \frac{1}{2}(v' - u') \\ &= \sqrt{r-1}\exp\left(\frac{r}{2}\right)\cosh\left(\frac{t}{2}\right). \end{aligned} \tag{2.18}$$

When $r < r_s$,

$$\begin{aligned} T &\equiv \frac{1}{2}\left(u' + v'\right) \\ &= \sqrt{1-r}\exp\left(\frac{r}{2}\right)\sinh\left(\frac{t}{2}\right), \end{aligned} \tag{2.19}$$

$$\begin{aligned} R &\equiv \frac{1}{2}(v' - u') \\ &= \sqrt{1-r}\exp\left(\frac{r}{2}\right)\cosh\left(\frac{t}{2}\right). \end{aligned} \tag{2.20}$$

Now,

$$\begin{aligned} dT &= \frac{1}{2}\left(du' + dv'\right), \\ dR &= \frac{1}{2}\left(dv' - du'\right), \\ -dT^2 + dR^2 &= -du'dv'. \end{aligned} \tag{2.21}$$

The metric is now,

$$ds^2 = \frac{4}{r}\exp\left(-r\right)\left(-dT^2 + dR^2\right) + r^2 d\Omega^2. \tag{2.22}$$

T, R,θ and ϕ make up the Kruskal-Szekres coordinates. Now, T is always a time-like coordinate, and R is always a spacelike coordinate. Radial null geodesics are straight lines with slope ± 1. The red region below the R axis represents the past interior and the one above represents the future interior. Lines of constant r are hyperbolae in the R-T plane with origin as the center. The pair of straight lines $T = \pm R$ is the horizon of the black hole. From figure 2.1, it is apparent that any radial null geodesic with points inside the future interior cannot escape the horizon.

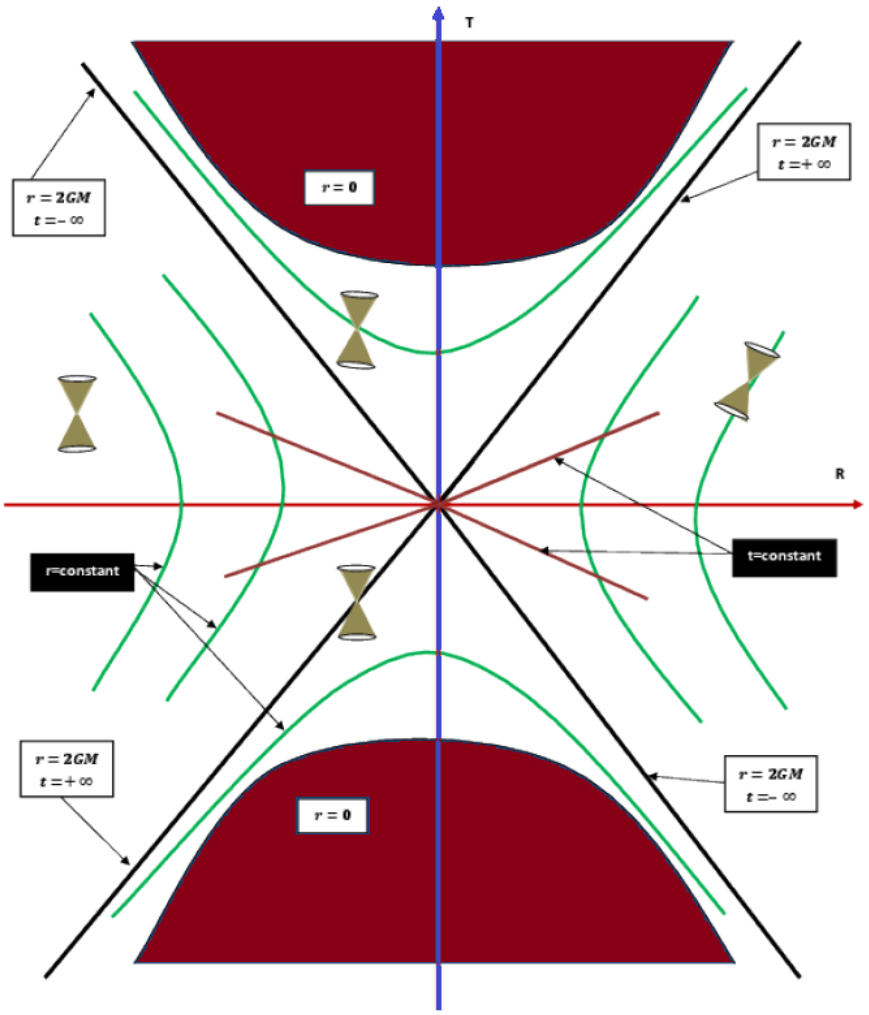

Figure 2.1: Kruskal diagram showing the Schwarzchild solution in R-T plane[32].

2.3 Penrose Diagram

When we are interested in the causal structure of spacetime, we can do a conformal transformation of the metric, which will fit the entire manifold onto a compact region. The two-dimensional diagram that results from the conformal compactification of the coordinates is called the Penrose diagram or simply conformal diagram.

The metric for the Minkowski space is

$$ds^2 = -dt^2 + dr^2 + r^2 d\Omega^2. \tag{2.23}$$

We define coordinates T and R such that

$$\begin{aligned} T + R &\equiv \arctan(t + r), \\ T - R &\equiv \arctan(t - r). \end{aligned} \tag{2.24}$$

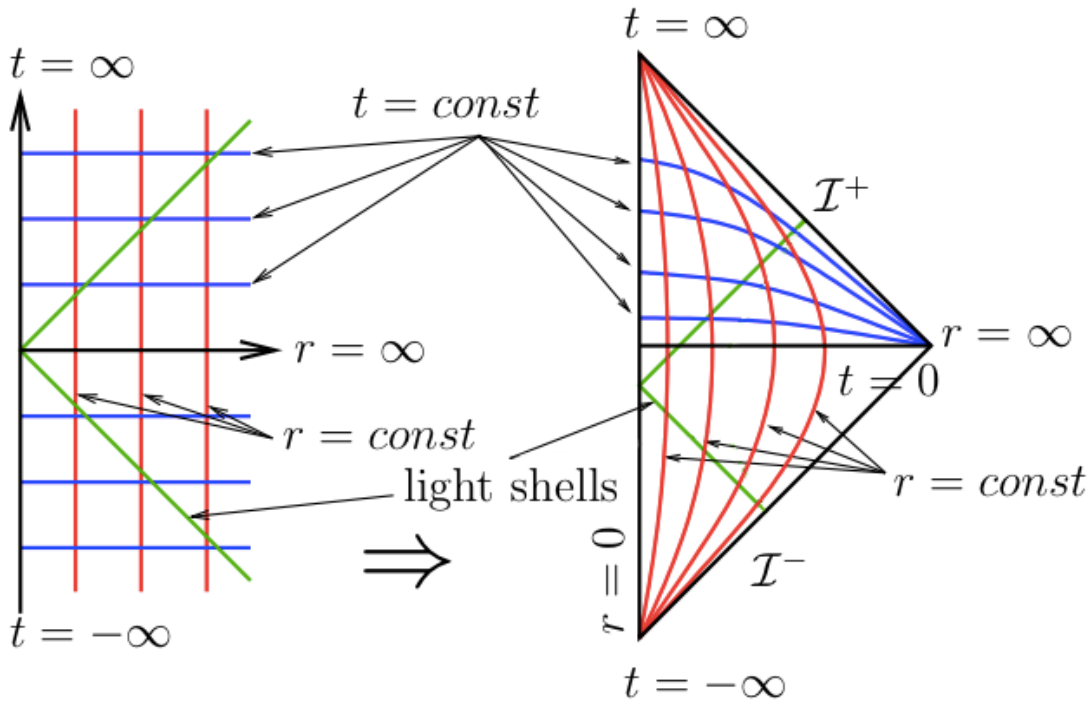

Figure 2.2: Conformal diagram for Minkowski Space; blue lines represent constant time, red lines represent the constant radius, and green lines represent light rays, $\mathcal{I}^-$ and $\mathcal{I}^+$ represent past and future null infinity[31].

This results in a metric conformally equivalent to the Minkowski metric:

$$ds^2 = \left[cos^2\left(T+R\right)cos^2\left(T-R\right)\right]^{-1}\left[-dT^2+dR^2+\left(\frac{\sin\left(2R\right)}{2}\right)^2 d\Omega^2\right]. \quad (2.25)$$

Figure 2.2 shows the spacetime diagram of this transformation.

To find the conformal compactification of the Kruskal-Szekres coordinates, we define

$$\mathcal{V} = \arctan\left(v'\right) \quad and \quad \mathcal{U} = \arctan\left(u'\right). \quad (2.26)$$

The new coordinates map the entire Kruskal-Szekres extention of Schwarzchild spacetime into the range $-\frac{\pi}{2} < \mathcal{U}, \mathcal{V} < \frac{\pi}{2}$. The conformal diagram is given for reference in figure 2.3. Similar to the Kruskal diagram, radial null geodesics are still straight lines with slope ± 1 in the Penrose diagram. Light rays traveling radially outwards from the horizon in the region I, will meet the future null infinity at $\mathcal{I}^+$. On the other hand, light rays from the region I moving radially towards the horizon will be trapped inside region II and approach the future singularity. Likewise, light rays traveling from region III will behave in the same manner. As a consequence, regions I and III causally disconnected. Region IV is the past interior of the black hole.

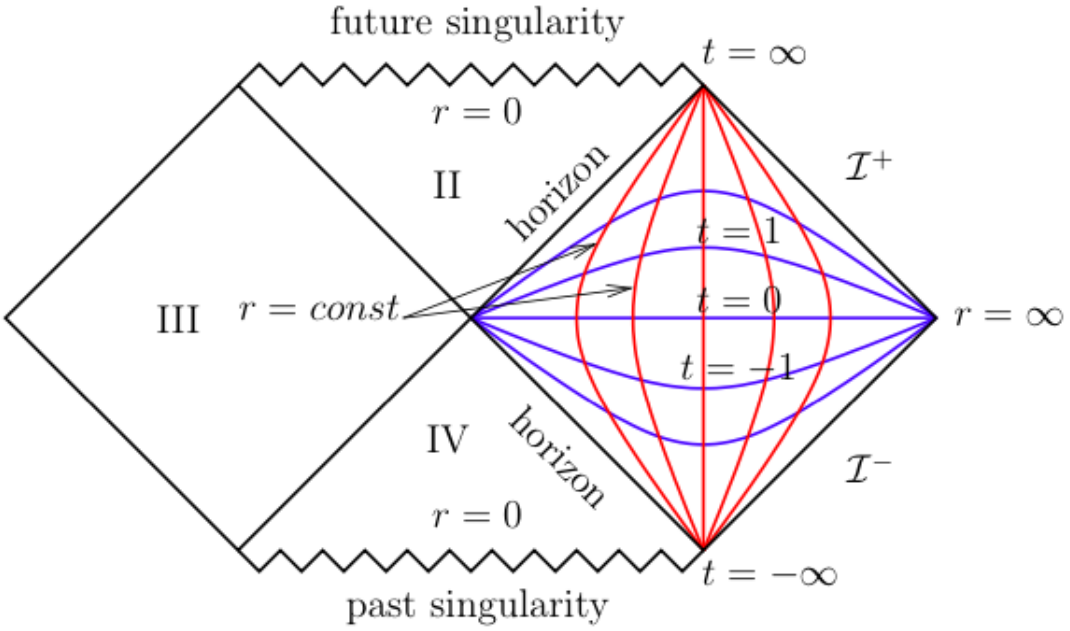

Figure 2.3: Conformal diagram for the Schwarzchild geometry. Regions II and IV represent the future and the past of the interior of the blackhole respectively. Regions I and III are causally disconnected[31].

2.4 Collapse of a Spherical Shell of Photons

Birkhoff's theorem states that the spacetime inside a spherically symmetric shell of matter is flat, whereas outside the spacetime geometry is described by the Schwarzchild metric[31]. Therefore, the full Penrose Diagram for the collapse of a shell of photons can be formed by attaching together two Penrose diagrams: one for Minkowski space and the other describing Schwarzchild space. The left part of figure 2.4 shows the light shell within flat space; Birkhoff's theorem says that the outer portion is incorrect because it is not flat. In contrast, Birkhoff's theorem tells us that the outer portion is Schwarzchild space, as shown in figure 2.5. Finally, the two diagrams are combined in figure 2.5 to produce the entire Penrose diagram of a collapsing shell of photons. A consequence of Birkhoff's theorem is that the horizon extends to a portion within the flat space. Hence, an observer passing through the horizon might not be able to detect anything out of the ordinary. However, the observer must still meet the singularity. Even more surprisingly, an observer can be inside the horizon of a black hole that will form in the future. This depicts the position of the horizon depends on events that have yet to happen; horizons show acausality.

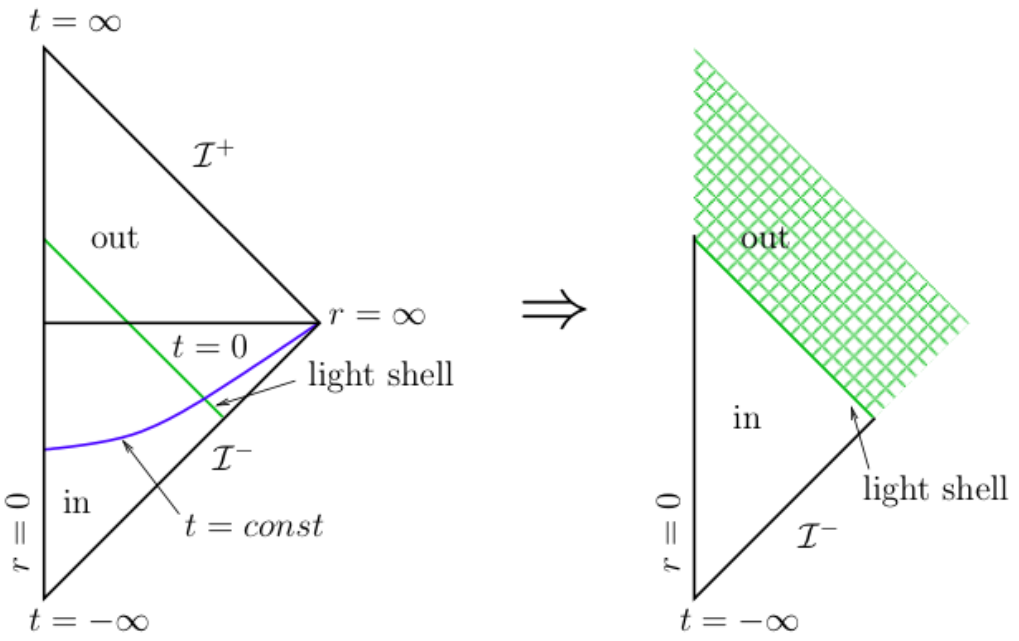

Figure 2.4: The Penrose Diagram inside the light shell is that of the Minkowski space; however, outside the shell, it is not Minkowski space and needs to be discarded[31].

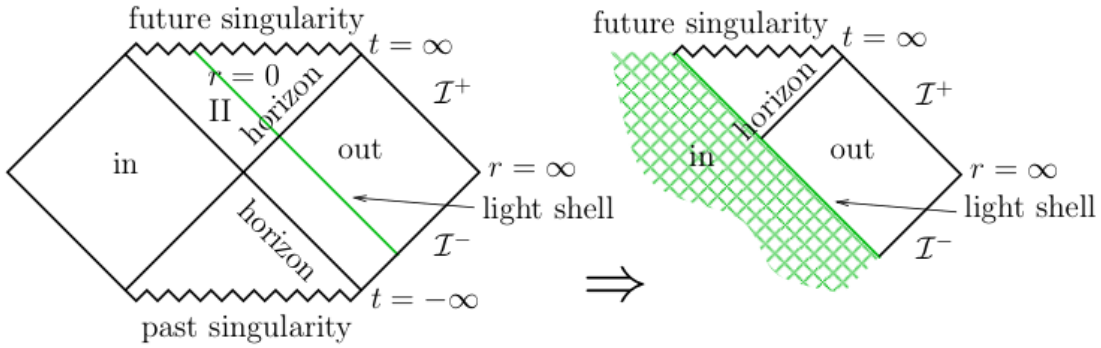

Figure 2.5: The Penrose Diagram outside the shell of photons is that of the Schwarzchild space. Hence, the portion inside needs to be discarded[31].

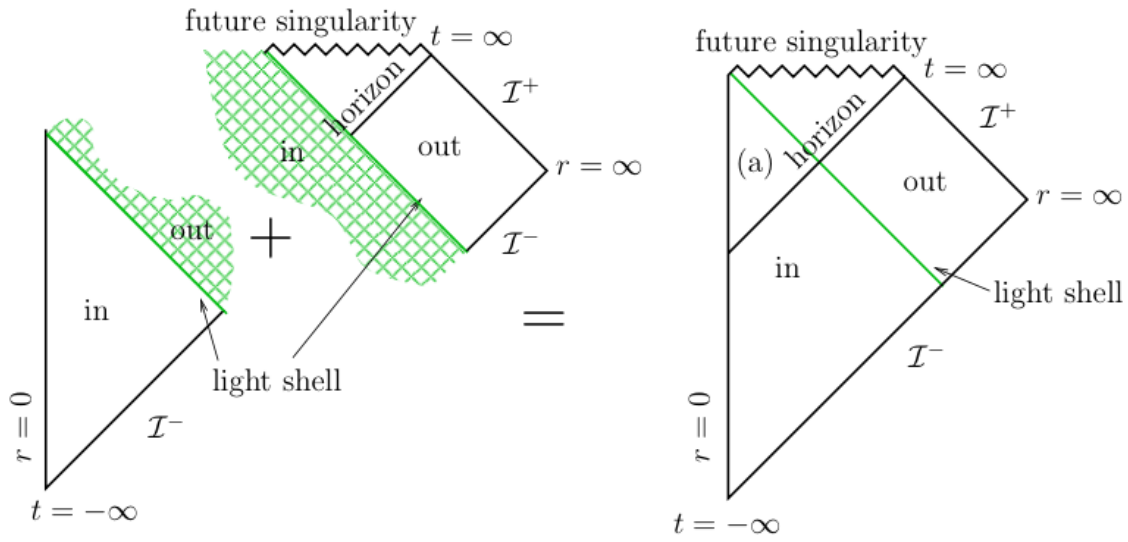

Figure 2.6: The Penrose Diagram for the collapsing shell of photons is the result of sewing the correct pieces of figures 2.4 and 2.5 together[31].

Chapter 3

Quantum Field Theory

3.1 Quantum Field Theory in Flat Spacetime

In flat space the Lagrangian density for a real scalar field is

$$\mathcal{L} = -\frac{1}{2}\eta^{\mu\nu}\partial_\mu\phi\partial_\nu\phi - \frac{1}{2}m^2\phi^2. \tag{3.1}$$

The action is then

$$S = \int d^n x \left(-\frac{1}{2}\eta^{\mu\nu}\partial_\mu\phi\partial_\nu\phi - \frac{1}{2}m^2\phi^2\right), \tag{3.2}$$

where the $\sqrt{-g}$ is not necessary since we are working in Minkowski space with inertial coordinates. This equation is known as the Klein-Gordon equation. The equation of motion from this action is

$$\partial_\mu\partial^\mu\phi - m^2\phi = 0. \tag{3.3}$$

In order to quantize the theory, we find the conjugate momentum

$$\pi = \frac{\partial\mathcal{L}}{\partial(\nabla_0\phi)} = \dot{\phi}. \tag{3.4}$$

The Hamiltonian for the free massive scalar field can be given in terms of the canonical momentum π which is conjugate to the field ϕ [24]:

$$H = \frac{1}{2}\int d^{n-1}x(\pi^2(x) + \nabla^2(x) + m^2\phi^2(x)). \tag{3.5}$$

As an example, we can find plane wave solutions to the Klein-Gordon equation to be

$$\phi(x^\mu) = \phi_0 e^{ik_\mu x^\mu}, \tag{3.6}$$

where $k^\mu = (\omega, \boldsymbol{k})$ and $\omega^2 = \boldsymbol{k}^2 + m^2$ is the dispersion relation that is satisfied. To find the most general set of solutions, we can assume that the solutions to this equation of motion are ϕ_1 and ϕ_2 and we can write an inner product for the solutions for a spacelike hypersurface Σ as

$$(\phi_1, \phi_2) = -i\int_\Sigma \left(\phi_1\partial_\mu\phi_2^* - \phi_2^*\partial_\mu\phi_1\right) d^{n-1}x. \tag{3.7}$$

Using our plane wave solutions, we can compute the inner product to get

$$(e^{ik_1^\mu x_\mu}, e^{ik_2^\mu x_\mu}) = (\omega_2 + \omega_1)e^{-i(\omega_1-\omega_2)t}(2\pi)^{n-1}\delta^{(n-1)}(\boldsymbol{k_1} - \boldsymbol{k_2}), \tag{3.8}$$

where

$$\int e^{(i\boldsymbol{k}_1-\boldsymbol{k}_2)\cdot x} d^{n-1}x = (2\pi)^{n-1}\delta^{(n-1)}(\boldsymbol{k}_1 - \boldsymbol{k}_2).$$

We now have a set of orthonormal solutions:

$$f_k(x^\mu) = \frac{e^{ik_\mu x^\mu}}{[2\omega(2\pi)^{n-1}]^{1/2}}. \tag{3.9}$$

We now have the following relations using our solutions

$$\begin{aligned} (f_{k_1}, f_{k_2}) &= \delta^{(n-1)}(\boldsymbol{k}_1 - \boldsymbol{k}_2), \\ (f_{k_1}, f^*_{k_2}) &= 0, \\ (f^*_{k_1}, f^*_{k_2}) &= -\delta^{(n-1)}(\boldsymbol{k}_1 - \boldsymbol{k}_2). \end{aligned} \tag{3.10}$$

We can finally find a complete orthonormal set of solutions f_k and f_k^* that solve the Klein-Gordon equation where f_k are called positive frequency modes, with and f_k^* are called negative frequency modes.

$$\phi(t,x) = \int d^{n-1}k[\hat{a}_k f_k(t,x) + \hat{a}_k^\dagger f_k^*(t,x)], \tag{3.11}$$

where $\hat{a}_k$ is an annihilation operator and $\hat{a}_k^\dagger$ is a creation operator.

3.2 Quantum Field Theory in Curved Spacetime

In curved spacetime the calculations are analogous to the previous section following a replacement with a covariant form. [7] The Lagrangian density for a real scalar field in curved spacetime is

$$\mathcal{L} = \sqrt{-g}\left(-\frac{1}{2}g^{\mu\nu}\nabla_\mu\phi\nabla_\nu\phi - V(\phi)\right). \tag{3.12}$$

The potential for the scalar field is taken to be quadratic and including another quadratic interaction term containing the Ricci scalar R parametrized by a dimensionless constant ζ for curved spacetime:

$$V(\phi) = \frac{1}{2}m^2\phi^2 + \zeta R\phi^2. \tag{3.13}$$

The action for the scalar field then becomes

$$S = \int d^n x\sqrt{-g}\left(-\frac{1}{2}g^{\mu\nu}\nabla_\mu\phi\nabla_\nu\phi - \frac{1}{2}m^2\phi^2 - \frac{1}{2}\zeta R\phi^2\right). \tag{3.14}$$

There are two interesting choices for the constant ζ. One is to take $\zeta = 0$ which is known as the minimal coupling and it turns off the interaction with the Ricci scalar. Another choice is the conformal coupling where $\zeta = \frac{(n-2)}{4(n-1)}$. When $m^2 = 0$

and the conformal coupling is chosen, the action (3.14) is invariant under conformal transformations

$$\begin{aligned} g_{\mu\nu} &\to \Omega^2(x) g_{\mu\nu}, \\ \phi &\to \Omega^{\frac{2-n}{2}}(x)\phi. \end{aligned} \tag{3.15}$$

In order to quantize the theory, we can find the conjugate momentum (3.12)

$$\pi = \frac{\partial \mathcal{L}}{\partial(\nabla_0 \phi)} = \sqrt{-g}\nabla_0 \phi, \tag{3.16}$$

and impose the canonical commutation relations

$$\begin{aligned} [\phi(t,x), \phi(t,x')] &= 0, \\ [\pi(t,x), \pi(t,x')] &= 0, \\ [\phi(t,x), \pi(t,x')] &= \frac{i}{\sqrt{-g}}\delta^{(n-1)}(x-x'). \end{aligned} \tag{3.17}$$

The equations of motion from the action for the real scalar field is

$$\nabla_\mu \nabla^\mu \phi - m^2\phi - \zeta R\phi = 0. \tag{3.18}$$

Assuming that the solutions to this equation of motion are ϕ_1 and ϕ_2, we can write an inner product for the solutions for a spacelike hypersurface Σ as

$$(\phi_1, \phi_2) = -i \int_\Sigma \left(\phi_1 \nabla_\mu \phi_2^* - \phi_2^* \nabla_\mu \phi_1\right) n^\mu \sqrt{\gamma} d\Sigma, \tag{3.19}$$

where n^μ is the unit vector normal to the hypersurface, γ_{ij} is the metric induced on the hypersurface and $d\Sigma$ is a volume element of the hypersurface. The inner product (3.19) is not dependent on the choice of the hypersurface Σ.

If we have two different disconnected hypersurfaces Σ_1 and Σ_2 and $\mathcal{V}$ is the four dimensional volume bounded by these two hypersurfaces we can use Stokes theorem to get the relation

$$\int_\mathcal{V} \nabla^\mu \left(\phi_1 \nabla_\mu \phi_2^* - \phi_2^* \nabla_\mu \phi_1\right) d\mathcal{V} = i \oint_{\partial\mathcal{V}} \left(\phi_1 \nabla_\mu \phi_2^* - \phi_2^* \nabla_\mu \phi_1\right) d\Sigma^\mu. \tag{3.20}$$

From this relation we can clear see that the left hand side can be simplified using the equation of motion (3.18) to give

$$\begin{aligned} \int_\mathcal{V} \nabla^\mu \left(\phi_1 \nabla_\mu \phi_2^* - \phi_2^* \nabla_\mu \phi_1\right) d\mathcal{V} &= \int_\mathcal{V} \left(\phi_1 \nabla^\mu \nabla_\mu \phi_2^* - \phi_2^* \nabla^\mu \nabla_\mu \phi_1\right) d\mathcal{V} \\ &= i \int_\mathcal{V} \Big(\phi_1 (m^2 + \zeta R)\phi_2^* - \phi_2^* (m^2 + \zeta R)\Big) d\mathcal{V} \\ &= 0. \end{aligned} \tag{3.21}$$

On the right hand side we get

$$i \oint_{\partial\mathcal{V}} \left(\phi_1 \nabla_\mu \phi_2^* - \phi_2^* \nabla_\mu \phi_1\right) d\Sigma^\mu = (\phi_1, \phi_2)_{\Sigma_1} - (\phi_1, \phi_2)_{\Sigma_2}. \tag{3.22}$$

Therefore,

$$(\phi_1, \phi_2)_{\Sigma_1} - (\phi_1, \phi_2)_{\Sigma_2} = 0. \tag{3.23}$$

We can always find an orthonormal set of solutions to the equation of motion for the scalar field. Let us assume these solutions are g_i and g_i^*. These solutions can be thought of as a set of basis modes seen by one observer. These solutions satisfy

$$\begin{aligned} (g_i, g_j) &= \delta_{ij}, \\ (g_i^*, g_j^*) &= -\delta_{ij}, \\ (g_i, g_j^*) &= 0. \end{aligned} \tag{3.24}$$

We can now write the expansion for the field as

$$\phi = \sum_i (\hat{b}_i g_i + \hat{b}_i^\dagger g_i^*). \tag{3.25}$$

The coefficient $\hat{b}_i$ behaves as an annihilation operator and the coefficient $\hat{b}_i^\dagger$ behaves as a creation operator and thus satisfies the commutation relations

$$\begin{aligned} [\hat{b}_i, \hat{b}_j^\dagger] &= \delta_{ij}, \\ [\hat{b}_i, \hat{b}_j] &= [\hat{b}_i^\dagger, \hat{b}_j^\dagger] = 0. \end{aligned} \tag{3.26}$$

If we repeatedly apply the annihilation operator $\hat{b}_i$ on a state, we get the vacuum state which is defined as

$$\hat{b}_i \left|0_u\right\rangle = 0. \tag{3.27}$$

Similarly, we can apply the creation operator $\hat{b}_i^\dagger$ to get a state with n_i excitations

$$\left|n_i\right\rangle = \frac{1}{\sqrt{n_i!}} (\hat{b}_i^\dagger)^{n_i} \left|0_u\right\rangle. \tag{3.28}$$

This is known as the Fock basis for the Hilbert space.

Since the set of solutions g_i and g_i^* are not the only unique solutions to our equation of motion, the vacuum state $|0_u\rangle$ is consequentially also not unique. we can assume another set of orthonormal solutions to the equation of motion as h_i and h_i^*. These solutions can be thought of as a set of basis modes seen by some other observer. Similarly as before we write the expansion as

$$\phi = \sum_i (\hat{c}_i h_i + \hat{c}_i^\dagger h_i^*). \tag{3.29}$$

We similarly have the commutation relations

$$\begin{aligned} [\hat{c}_i, \hat{c}_j^\dagger] &= \delta_{ij}, \\ [\hat{c}_i, \hat{c}_j] &= [\hat{c}_i^\dagger, \hat{c}_j^\dagger] = 0. \end{aligned} \tag{3.30}$$

Likewise we have the annihilation operator $\hat{b}_i$ which can be acted repeatedly to get the vacuum state

$$\hat{c}_i \left|0_v\right\rangle = 0. \tag{3.31}$$

The creation operator $\hat{c}_i^\dagger$ acting repeatedly gives the excited state

$$|n_i\rangle = \frac{1}{\sqrt{n_i!}}(\hat{c}_i^\dagger)^{n_i}\,|0_v\rangle\,. \tag{3.32}$$

We now apply the Bogolubov transformation to transform from the set of solutions $\{g_i, g_i^*\}$ to the solutions $\{h_i, h_i^*\}$ each of which help the respective observers define their notion of particles. With these distinct set of basis modes the observers will disagree on the number of particles that are being observed, as

$$g_i = \sum_j (\alpha_{ij} h_j + \beta_{ij} h_j^*), \tag{3.33}$$

$$h_i = \sum_j (\alpha_{ji}^* g_j - \beta_{ji} h_j^*). \tag{3.34}$$

Here the matrices α_{ij} and β_{ij} can be expressed using the orthonormality conditions to be

$$\alpha_{ij} = (g_i, h_i) \quad and \quad \beta_{ij} = -(g_i, h_i^*). \tag{3.35}$$

These matrices, also known as Bogolubov coefficients, also satisfy the normalization conditions

$$\sum_k (\alpha_{ik}\alpha_{jk} - \beta_{ik}^*\beta_{jk}^*) = \delta_{ij} \quad and \quad \sum_k (\alpha_{ik}\beta_{jk}^* - \beta_{ik}\alpha_{jk}^*) = 0. \tag{3.36}$$

Now we can finally transform between our creation and annihilation operators in these these different modes using the help of our Bogolubov coefficients.

$$\hat{b}_k = \sum_i (\alpha_{ik}\hat{c}_i + \beta_{ik}^*\hat{c}_i^\dagger) \tag{3.37}$$

and

$$\hat{c}_k = \sum_i (\alpha_{ki}^*\hat{b}_i - \beta_{ki}^*\hat{b}_i^\dagger). \tag{3.38}$$

We can define a number operator for each of the u-observer and v-observer

$$\begin{aligned} N_u &= \sum_k \hat{b}_k^\dagger \hat{b}_k, \\ N_v &= \sum_k \hat{c}_k^\dagger \hat{c}_k. \end{aligned} \tag{3.39}$$

With respect to the observer at u, the number operator N_u has the expectation value

$$\langle 0_u|\, N_u\, |0_u\rangle = 0. \tag{3.40}$$

So no particles are observed from their perspective. However, we can also compute the expectation value of the of this number operator with respect to the observer at v

$$\langle 0_u|\, N_v\, |0_u\rangle = \langle 0_u|\, \sum_k \hat{c}_k^\dagger \hat{c}_k\, |0_u\rangle\,. \tag{3.41}$$

Using equation (3.38) we can expand the right hand side

$$\begin{aligned}\langle 0_u|\sum_k \hat{c}_k^\dagger \hat{c}_k\,|0_u\rangle &= \langle 0_u|\sum_{im}(\alpha_{ki}\hat{b}_i^\dagger - \beta_{ki}\hat{b}_i)(\alpha_{km}^*\hat{b}_m - \beta_{km}^*\hat{b}_m^\dagger)\,|0_u\rangle \\ &= \sum_{im}\beta_{ki}\beta_{km}^*\,\langle 0_u|\,(\hat{b}_i\hat{b}_m^\dagger)\,|0_u\rangle \\ &= \sum_{im}\beta_{ki}\beta_{km}^*\,\langle 0_u|\,(\hat{b}_m^\dagger\hat{b}_i + [\hat{b}_i,\hat{b}_m^\dagger])\,|0_u\rangle\,.\end{aligned} \tag{3.42}$$

Using the commutation relation from (3.26),

$$\begin{aligned}\langle 0_u|\sum_k \hat{c}_k^\dagger \hat{c}_k\,|0_u\rangle &= \sum_{im}\beta_{ki}\beta_{km}^*\delta_{im}\,\langle 0_u|0_u\rangle \\ &= \sum_i \beta_{ki}\beta_{ki}^*.\end{aligned} \tag{3.43}$$

So we get

$$\langle 0_u|\,N_v\,|0_u\rangle = tr(\beta\beta^\dagger). \tag{3.44}$$

This is non vanishing which means that the observer at v there is bubbling of particles in the vacuum state $|0_u\rangle$ and thus allows for the possibility of particle creation due to gravitational fields.

3.3 Quantum Field Theory on Black holes

3.3.1 Potential Barriers and S-Matrix

We first look at the wave equation in the Schwarzchild geometry. Using tortoise coordinates this has the form [17]

$$-\frac{\partial^2}{\partial r_*^2}\psi_{\omega,l}(r_*) + V(r_*)\psi_{\omega,l}(r_*) = \omega^2\psi_{\omega,l}(r_*), \tag{3.45}$$

we have solutions of the form

$$f_{rlm} = \sum_{l,m}\frac{1}{r}Y_{lm}(\theta,\phi)e^{-i\omega t}\psi_{\omega,l}(r_*). \tag{3.46}$$

We consider the massless case, $m^2 = 0$ which lets us write a form of the potential which is

$$V(r_*) = \frac{r_* - 1}{{r_*}^3}\left(m^2{r_*}^2 + l(l+1) + \frac{1}{r_*}\right). \tag{3.47}$$

We can see that the potential vanishes at spatial infinity and at the horizon but has a peak:

$$V(r_*) \approx \begin{cases} e^{(r_*/2m)} & r_* \to -\infty, \\ \frac{l(l+1)}{r^2} & r_* \to \infty. \end{cases} \tag{3.48}$$

We can then get solutions in terms of waves being propagated between $r_* \to \infty$ and $r_* \to -\infty$

$$\begin{aligned} r_* \to \infty &: \psi(r_*) = A^+e^{i\omega r_*} + B^+e^{-i\omega r_*}, \\ r_* \to -\infty &: \psi(r_*) = B^-e^{i\omega r_*} + A^-e^{-i\omega r_*}, \end{aligned} \tag{3.49}$$

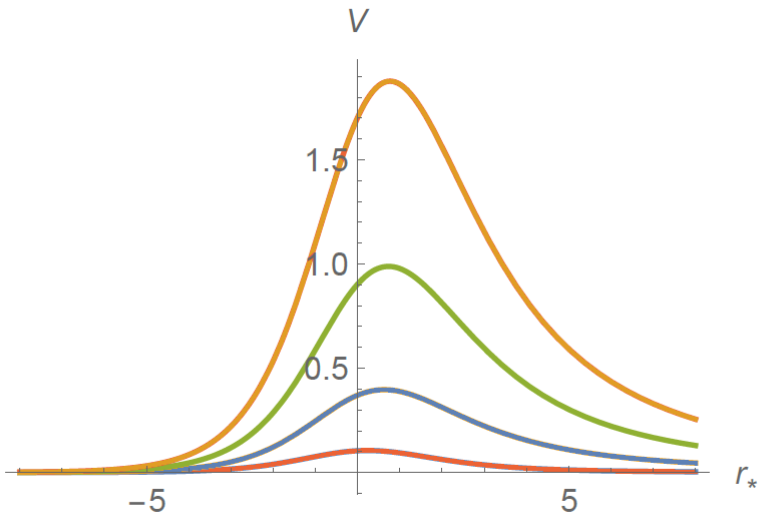

Figure 3.1: Plots for the potential V as a function of r^* for different values of l[11].

where A can be thought of as waves going from the horizon ($r_* \to -\infty$) to the boundary ($r_* \to \infty$) and B as waves coming back from the boundary to the horizon. There should exist a linear relation between them which we can express as

$$\begin{pmatrix} A^+ \\ A^- \end{pmatrix} = S \begin{pmatrix} B^- \\ B^+ \end{pmatrix}. \tag{3.50}$$

where S is a 2×2 matrix known as an S-matrix, such that

$$S = \begin{pmatrix} s_{11} & s_{12} \\ s_{21} & s_{22} \end{pmatrix}. \tag{3.51}$$

The complex conjugate of the solutions are also solutions since they satisfy the Schrodinger equation

$$B^\pm \to A^{\pm *}. \tag{3.52}$$

Thus we can also have the linear relation

$$\begin{pmatrix} A^- \\ A^+ \end{pmatrix} = (S^*)^{-1} \begin{pmatrix} B^- \\ B^+ \end{pmatrix}. \tag{3.53}$$

The S-matrix is unitary, $SS^\dagger = 1$, as

$$\left|B^+\right|^2 + \left|B^-\right|^2 = \left|A^+\right|^2 + \left|A^-\right|^2. \tag{3.54}$$

Using this, we have a relation between the matrix elements as

$$s_{11} = s_{22}. \tag{3.55}$$

For the elements of the S-matrix to be interpreted as reflection and transmission coefficients, at least of the coefficients $B^\pm$, $A^\pm$ must be zero. Taking $B^+ = 0$ and normalizing to give $B^- = 1$, we have the S-matrix elements as

$$S = \begin{pmatrix} t & -\frac{tr*}{t*} \\ r & t \end{pmatrix}, \tag{3.56}$$

where t and r are transmission and reflection coefficients respectively.

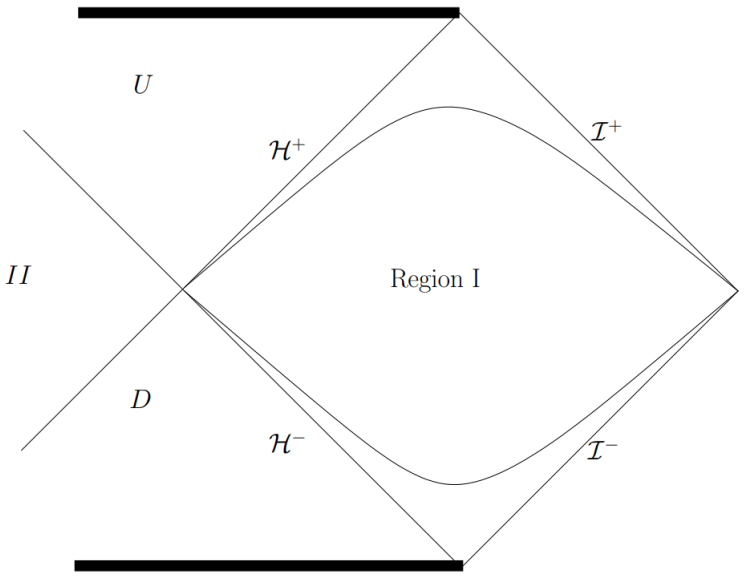

Figure 3.2: Kruskal geometry [17]

3.3.2 Hawking Radiation

It is difficult to study QFT for Black holes formed by gravitational collapse and so it is relevant to study QFT in the Kruskal geometry which has black holes that are eternal[11].

Due to the time dependence in the gravitational collapse of realistic black holes it is difficult to solve the problem using our approach of Bogolubov transformations of the positive frequency modes of the vacuum state before the collapse. However, Hawking was able to find solutions to this problem by realization of the high red-shift of the positive energy modes after a long time has passed since the gravitational collapse. He realized that these modes start off with high energy and so can be thought of as particles travelling along a geodesic.

We can approach the problem in a simpler way as done by Unruh which is to examine the Unruh vacuum of region I in the Kruskal geometry and find the positive energy modes that define this vacuum. We can then Bogolubov analyze these modes.

We can first introduce the modes in the different regions of the Kruskal manifold as

$$u_k^{I,\mathcal{H}^-} \approx \begin{cases} e^{-i\omega_k u} & \text{Region I} \\ 0 & \text{Region II} \end{cases}, \tag{3.57}$$

$$u_k^{II,\mathcal{H}^-} \approx \begin{cases} 0 & \text{Region I} \\ e^{+i\omega_k u} & \text{Region II} \end{cases}, \tag{3.58}$$

where $u_k^{I,\mathcal{H}^-}$ are modes in region I and $u_k^{II,\mathcal{H}^-}$ are modes in region II. For $\mathcal{H}^-$ we have the positive energy modes of order $e^{-i\omega U}$. We can find the Bogolubov

transformations to relate our modes with the U plane as

$$\begin{aligned} U_k^1 &= (1-e^{-8\pi M\omega_k})^{-1/2}\left(u_k^{I,\mathcal{H}^-} + e^{-8\pi M\omega_k/2}u_k^{II,\mathcal{H}^-*}\right), \\ U_k^2 &= (1-e^{-8\pi M\omega_k})^{-1/2}\left(u_k^{II,\mathcal{H}^-} + e^{-8\pi M\omega_k/2}u_k^{I,\mathcal{H}^-*}\right). \end{aligned} \tag{3.59}$$

The modes U_k^1, U_k^2, and the positive energy basis $U_k^{\mathcal{I}^-} \sim e^{-i\omega v}$ are the modes that define the past vacuum. Now, we can define the future vacuum at the null infinity as $V_k^{\mathcal{I}^+} \sim e^{-i\omega u}$ and we arbitrarily choose to trace over $V_k^{\mathcal{H}^-}$ and the region beyond reach of the observer lying asymptotic to the null, $u_k^{II,\mathcal{H}^-}$. We then find a set of Bogolubov transformations that relate the modes $\left(U_k^1, U_k^2, U_k^{\mathcal{I}^-}\right)$ and the modes $\left(V_k^{\mathcal{I}^+}, V_k^{\mathcal{H}^-}, U_k^{II,\mathcal{I}^-}\right)$. Now we can write the modes $u_k^{I,\mathcal{H}^+}, U_k^{\mathcal{I}^-}, V_k^{\mathcal{I}^+}, V_k^{\mathcal{H}^+}$ in terms of each other since they are not independent. They relate via the transmission and reflection coefficients as

$$\begin{aligned} U_k^{I,\mathcal{H}^-} &= t_{\omega_k}V_k^{\mathcal{I}^+} + r_{\omega_k}V_k^{\mathcal{H}^+}, \\ U_k^{\mathcal{I}^-} &= t_{\omega_k}^*V_k^{\mathcal{H}^+} + r_{\omega_k}^*V_k^{\mathcal{I}^+}. \end{aligned} \tag{3.60}$$

Substituting these expressions into our Bogolubov transformations we have

$$\begin{aligned} U_k^1 &= \frac{1}{(1-e^{-8\pi M\omega_k})^{1/2}}\left(t_{\omega_k}V_k^{\mathcal{I}^+} + r_{\omega_k}V_k^{\mathcal{H}^+} + e^{-8\pi M\omega_k/2}u_k^{II,\mathcal{H}^-*}\right), \\ U_k^2 &= \frac{1}{(1-e^{-8\pi M\omega_k})^{1/2}}\left(t_{\omega_k}^*V_k^{\mathcal{I}^+} + r_{\omega_k}^*V_k^{\mathcal{H}^+} + e^{-8\pi M\omega_k/2}(t_{\omega_k}^*V_k^{\mathcal{I}^+*} + r_{\omega_k}^*V_k^{\mathcal{H}^+*})\right), \\ U_k^{\mathcal{I}^-} &= t_{\omega_k}^*V_k^{\mathcal{H}^+} - r_{\omega_k}^*V_k^{\mathcal{I}^+}, \end{aligned} \tag{3.61}$$

and the corresponding complex conjugate expressions $(U_k^{1*}, U_k^{2*}, U_k^{\mathcal{I}^-*})$. Using this we have the S-matrix expression

$$\begin{aligned} |0\rangle_{past} = \prod_{\omega_k}&\left(1-e^{-8\pi M\omega_k}\right)^{\frac{1}{2}} \\ &\exp\left[e^{8\pi M\omega_k/2}a_{\omega_k}^{II,\mathcal{H}^-\dagger}(t_{\omega_k}a_{\omega_k}^{II,\mathcal{H}^+\dagger} + r_{\omega_k}a_{\omega_k}^{\mathcal{H}^+\dagger})\right]|0\rangle_{future}, \end{aligned} \tag{3.62}$$

where we have our creation operators a and annihilation operators $a^\dagger$. Now we can finally arrive at the density matrix for region I by tracing out the $\mathcal{H}^-$ and $\mathcal{H}+$:

$$\rho = \prod_{\omega_k}(1-e^{-8\pi M\omega_k})\sum_n \frac{e^{-8\pi Mn\omega_k|t_{\omega_k}|^{2n}}}{(1-|r_{\omega_k}|^2e^{-8\pi M\omega_k})^{n+1}}|n\rangle\langle n|. \tag{3.63}$$

The $|n\rangle$ are states in the Hilbert space of $\mathcal{I}^+$. When we have $r_{\omega k} = 0$, ρ is equivalent to a canonical ensemble with $\beta = 8\pi M$ having a thermal density matrix that is normalized. Any observer in future will observe the black hole as a thermal bath with $T_H = 1/8\pi M$ as found by Hawking.

Chapter 4

Quantum Information Theory in a Black Hole Background

4.1 Pure versus Mixed States

The density operator associated with a Hilbert space can describe either a pure state or a mixed state. An arbitrary density operator ρ is a linear combination of projection operators $|\psi_i\rangle \langle\psi_i|$,

$$\rho = \sum_i p_i |\psi_i\rangle \langle\psi_i| , \tag{4.1}$$

where the states $|\psi_i\rangle$ are normalized, $p_i \geq 0$ and $\sum_i p_i = 1$. Since $p_i \in \mathbb{R}$, a density operator is always Hermitian, i.e.,

$$\rho^\dagger = \sum_i p_i^* |\psi_i\rangle \langle\psi_i| = \rho. \tag{4.2}$$

The trace of a density operator is

$$\begin{aligned} Tr(\rho) &= \sum_j \langle\psi_j| \rho |\psi_j\rangle \\ &= \sum_j \sum_i p_i \langle\psi_j|\psi_i\rangle \langle\psi_i|\psi_j\rangle \\ &= \sum_j \sum_i p_i \delta_{ij} \\ &= \sum_i p_i \\ &= 1. \end{aligned} \tag{4.3}$$

It is possible to write the density operator as $\rho = A^\dagger A$ with $A = \sum_i \sqrt{p_i} |\psi_i\rangle \langle\psi_i|$; therefore, ρ is positive semidefinite.

$$\rho \geq 0 \tag{4.4}$$

We can construct a density operator with a normalized state vector $|\Psi\rangle$ of the Hilbert space such that [22]

$$\rho = |\Psi\rangle \langle\Psi| . \tag{4.5}$$

Density operators satisfying (4.5) are pure, and they satisfy several properties. They are idempotent:

$$\begin{aligned}\rho^2 &= (|\Psi\rangle\langle\Psi|)(|\Psi\rangle\langle\Psi|) \\ &= |\Psi\rangle\langle\Psi| \\ &= \rho.\end{aligned} \tag{4.6}$$

To quantify a density operator's purity, we will define the purity as $P(\rho) \equiv Tr(\rho^2)$. The purity of a density operator is one if and only if it is pure. When a density operator is associated with a pure state, then it must be idempotent. Tracing (4.6) leads to:

$$Tr\left(\rho^2\right) = Tr(\rho) = 1. \tag{4.7}$$

Since, $\sum_i p_i = 1$ and $p_i \geq 0$, we have $0 \leq p_i \leq 1$. Then we have $\sum_i p_i^2 \leq \sum_i p_i = 1$, and with $Tr\left(p_i^2\right) = \sum_i p_i^2 = 1$,

$$p_i^2 = p_i \implies p_i = 1 \quad or \quad 0. \tag{4.8}$$

Equation (4.7) restricts exactly one p_i to be one and the rest to be zero, which implies that ρ must satisfy (4.5), and therefore, is pure. Hence a density operator associated with a mixed state must satisfy

$$0 < Tr\left(\rho^2\right) < 1 \tag{4.9}$$

A Hilbert space $\mathcal{H}_{AB}$ is bipartite when it can be factorized into two subsystems:

$$\mathcal{H}_{AB} = \mathcal{H}_A \otimes \mathcal{H}_B \tag{4.10}$$

We can write the unentangled states in AB as tensor products of states in A and B

$$|\Psi\rangle = |\phi\rangle_A \otimes |\varphi\rangle_B. \tag{4.11}$$

The density operator associated with seperable mixed states can be written as

$$\rho = \sum_i p_i \rho_i^A \otimes \rho_i^B. \tag{4.12}$$

Let $\psi(a,b)$ represent the degrees of freedom in the total system AB. Then the reduced density operator of subsystem A can be found by integrating the degrees of freedom in subsystem B,

$$\rho_A(a,a') = \int \psi(a,b)\,\psi\left(a',b\right) db. \tag{4.13}$$

(4.13) contains all the statistical information about subsystem A. While the subsystems are mixed, the total system AB is pure. Hence, B is a subsystem that purifies A. If $|A|$ and $|B|$ are used to denote the size of the subsystems and $|A| \leq \frac{1}{2}(|A| + |B|)$, then ρ_A is the Boltzmann distribution in the energy basis,

$$\rho_A = diag\left(e^{-\beta E_1}, e^{-\beta E_2}, ...\right), \tag{4.14}$$

where β is the inverse of temperature.

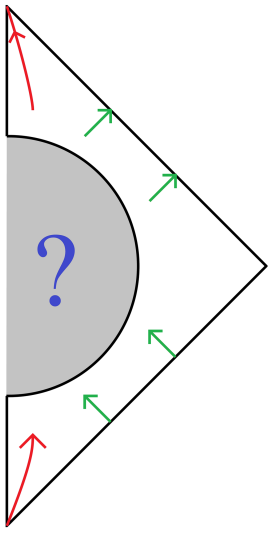

Figure 4.1: The S-matrix is an operator that encodes the transition probabilities of massive particles and massless particles going from past infinity to future infinity[11]. We have used the orange line to denote massive particles and the green line to denote massless particles. The question mark "?" represents a rather complicated interaction between the incoming particles.

4.2 The Unitary S-matrix

We can tell from section 3.2 that the notion of vacuum is dependent on the observer when the gravitational coupling G is non-zero; what may be observed as a vacuum by an observer might be filled with bubbling particles by another. Hence, we need to rely on a quantity other than the correlation functions of local operators. This quantity is known as S-matrix. We expect that the spacetimes which allow the formation and evaporation of black holes to be asymptotically flat. The separation between the incoming and outgoing particles increases with time, which allows us to ignore the particles' gravitational interactions at past and future infinities. Therefore, the Hilbert space, which contains the states at past and future infinity, is identical to a free quantum field theory. Then we can physically interpret the incoming and outgoing states by labeling them with their spins and appropriate boson or fermion statistics.

S-matrix is a linear operator that takes a state from past infinity to future infinity. Suppose that $|\phi\rangle$ is an incoming state and $|\varphi\rangle$ an outstate, then the S-matrix describes the following probability:

$$P\left(\varphi|\psi\right) = \left|\langle\varphi| S |\psi\rangle\right|^2 \tag{4.15}$$

The diagram in 4.1 aids our understanding of (4.15). Consequently, we can compare the S-matrix with the time evolution operator with $t \to \infty$:

$$S = \exp\left(-i\infty H\right). \tag{4.16}$$

The BFSS matrix model is an example of a unitary theory that remains consistent with black hole formation and evaporation[5]. In this model, the unitary S-matrix is an exact observable of an asymptotically flat quantum field theory.

4.3 Recovering Quantum Information from Hawking Radiation and the Page Curve

We will write the Hilbert Space of the early radiation R and late radiation BH of the black hole as

$$\mathcal{H}_{total} = \mathcal{H}_R \otimes \mathcal{H}_{BH} \cong \mathbb{C}^r \otimes \mathbb{C}^b, \tag{4.17}$$

where we denote the dimension of R as r and BH as b. A quantum state $|\psi\rangle$ which belongs to $\mathcal{H}_{total}$ is of the form

$$|\psi\rangle = \sum_{i,j} c_{ij} |i\rangle_R |j\rangle_{BH}. \tag{4.18}$$

We will assume that $|\psi\rangle$ is a gaussian vector, which means c_{ij} is a symmetric complex gaussian random variable:

$$c_{ij} \sim N_{\mathbb{C}} \left(0, \frac{1}{d}\right). \tag{4.19}$$

The real part and the imaginary part are independent random variables and are also normally distributed:

$$\mathrm{Re}\left(c_{ij}\right) \sim N_{\mathbb{R}} \left(0, \frac{1}{2d}\right) \quad \textit{and} \quad \mathrm{Im}\left(c_{ij}\right) \sim N_{\mathbb{R}} \left(0, \frac{1}{2d}\right). \tag{4.20}$$

The following are expectations of the some even powers of $\left|c_{ij}\right|$, the odd powers have an expectation value of zero,

$$\begin{aligned}
\mathbb{E}\left(\left|c_{ij}\right|^2\right) &= \mathbb{E}\left[\left(\mathrm{Re}\left(c_{ij}\right)^2 + \mathrm{Im}\left(c_{ij}\right)^2\right)\right] \\
&= \frac{1}{2d} + \frac{1}{2d} \\
&= \frac{1}{d}, \\
\mathbb{E}\left(\left|c_{ij}\right|^4\right) &= \mathbb{E}\left[\left(\mathrm{Re}\left(c_{ij}\right)^4 + 2\,\mathrm{Re}\left(c_{ij}\right)^2 \mathrm{Im}\left(c_{ij}\right)^2 + \mathrm{Im}\left(c_{ij}\right)^4\right)\right] \\
&= \frac{3}{4d^2} + \frac{1}{2d^2} + \frac{3}{4d^2} \\
&= \frac{2}{d^2}.
\end{aligned} \tag{4.21}$$

Now, we can evalute the expectation of the inner product of the quantum state,

$$\begin{aligned}
\mathbb{E}\left(\langle\psi|\psi\rangle\right) &= \sum_{ij} \mathbb{E}\left(\left|c_{ij}\right|^2\right) \\
&= d\left(\frac{1}{d}\right) \\
&= 1.
\end{aligned} \tag{4.22}$$

Similarly, we can calculate the variance of the inner product of the quantum state,

$$\begin{aligned}
\mathrm{Var}\left(\langle\psi|\psi\rangle\right) &= \mathbb{E}\left[\left(\langle\psi|\psi\rangle - \mathbb{E}\left(\langle\psi|\psi\rangle\right)\right)^2\right] \\
&= \mathbb{E}\left(\langle\psi|\psi\rangle - 1\right)^2 \\
&= \mathbb{E}\left[\left(\sum_{ij}|c_{ij}|^2 - 1\right)\left(\sum_{kl}|c_{kl}|^2 - 1\right)\right] \\
&= \sum_{i,j,k,l}\mathbb{E}\left(|c_{ij}|^2|c_{kl}|^2\right) - \sum_{ij}\mathbb{E}\left(|c_{ij}|^2\right) - \sum_{kl}\mathbb{E}\left(|c_{kl}|^2\right) + 1 \\
&= \sum_{i,j,k,l}\mathbb{E}\left(|c_{ij}|^2|c_{kl}|^2\right) - 1 \\
&= \sum_{(i,j)\neq(k,l)}\mathbb{E}\left(|c_{ij}|^2\right)\mathbb{E}\left(|c_{kl}|^2\right) + \sum_{i,j}\mathbb{E}\left(|c_{i,j}|^2\right) - 1 \\
&= \left(d^2 - d\right)\frac{1}{d^2} + d\left(\frac{2}{d}\right) - 1 \\
&= \frac{1}{d}.
\end{aligned} \tag{4.23}$$

The reduced density operator on R is

$$\begin{aligned}
\rho_R &= Tr_{BH}\left|\psi\right\rangle\left\langle\psi\right| \\
&= Tr_{BH}\sum_{i,j,i',j'} c_{i,j}c^*_{i',j'}\left|i\right\rangle_R\left|j\right\rangle_{BH}\left\langle i'\right|_R\left\langle j'\right|_{BH} \\
&= Tr_{BH}\sum_{i,j,i',j'} c_{i,j}c^*_{i',j'}\left|i\right\rangle_R\left\langle i'\right|_R\left|j\right\rangle_{BH}\left\langle j'\right|_{BH} \\
&= \sum_{i,j,i'} c_{i,j}c^*_{i',j}\left|i\right\rangle_R\left\langle i'\right|_R.
\end{aligned} \tag{4.24}$$

We can calculated the purity of the reduced density operator on$R$,

$$\begin{aligned}
P\left(\rho_R\right) &= Tr\left(\rho^2\right) \\
&= Tr\left(\sum_{i,j,i'} c_{i,j}c^*_{i',j}\left|i\right\rangle_R\left\langle i'\right|_R\sum_{k,l,k'} c_{k,l}c^*_{k',l}\left|k\right\rangle_R\left\langle k'\right|_R\right) \\
&= \sum_{i,j,k,l} c_{i,j}c^*_{k,j}c_{k,l}c^*_{i,l}.
\end{aligned} \tag{4.25}$$

Now, we are at a position to calculate the expection value of the purity of ρ_R,

$$\begin{aligned}
\mathbb{E}\left[P\left(\rho_R\right)\right] &= \sum_{i,j,k,l}\mathbb{E}\left(c_{i,j}c^*_{k,j}c_{k,l}c^*_{i,l}\right) \\
&= \sum_{i,j}\mathbb{E}\left(|c_{ij}|^4\right) + \sum_{i,j\neq l}\mathbb{E}\left(|c_{i,j}|^2|c_{i,l}|^2\right) + \sum_{i\neq k,j}\mathbb{E}\left(|c_{i,j}|^2|c_{k,j}|^2\right) \\
&= rb\left[\frac{2}{(rb)^2}\right] + \left(r^2 - r\right)b\left[\frac{1}{(rb)^2}\right] + \left(b^2 - b\right)r\left[\frac{1}{(rb)^2}\right] \\
&= \frac{1}{r} + \frac{1}{b}.
\end{aligned} \tag{4.26}$$

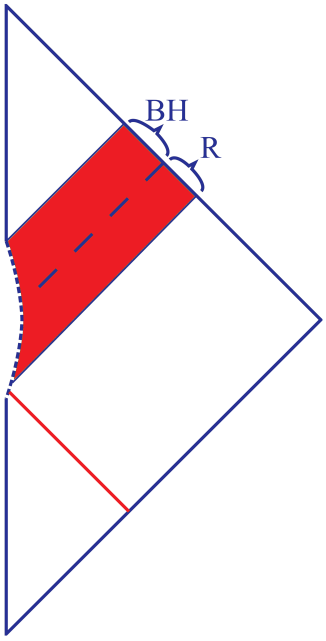

Figure 4.2: The straight undashed red line at the bottom indicates a black hole formation from a shell of photons. The dashed curve to the left denotes the horizon, and the black dashed straight line indicates the split of the early and late parts of Hawking radiation. This is also the S-matrix for the black hole[11].

In this chapter, we refer to the von Neumann entropy as the entanglement entropy. The Rényi entropy is of ρ_R is given as

$$S_\alpha(\rho_R) = \frac{1}{1-\alpha} \log Tr(\rho_R^\alpha), \tag{4.27}$$

where $\alpha \geq 0$ and $\alpha \neq 1$. When we take the limit $\alpha \to 1$ we get the entanglement entropy:

$$S(\rho_R) = S_1(\rho_R) = -Tr(\rho_R log \rho_R). \tag{4.28}$$

The Rényi entropy is non-increasing in α because its derivative is non positive,i.e. $\frac{dS_\alpha}{d\alpha} \leq 0$. Therefore, the entanglement entropy satisfies the inequality:

$$\begin{aligned} S(\rho) &\geq S_2(\rho_R) \\ &= -\log P(\rho_R). \end{aligned} \tag{4.29}$$

Furthermore, the expectation value of the entanglement entropy also satisfies the inequality:

$$\begin{aligned} \mathbb{E}[S(\rho_R)] &\geq \mathbb{E}[S_2(\rho_R)] \\ &= -\log \mathbb{E}[P(\rho_R)] \end{aligned} \tag{4.30}$$

Hence, the entanglement entropy satisfies,

$$\mathbb{E}[S(\rho_R)] \geq -\log\left(\frac{1}{r} + \frac{1}{b}\right) \tag{4.31}$$

The Rényi entropy for $\alpha = 2$ and the entanglement entropy are almost equal, which allows us to approximate

$$\mathbb{E}[S(\rho_R)] \approx \begin{cases} \log b - \frac{b}{r} & \text{if } b \ll r \\ \log r - \frac{r}{b} & \text{if } r \ll b \end{cases}. \tag{4.32}$$

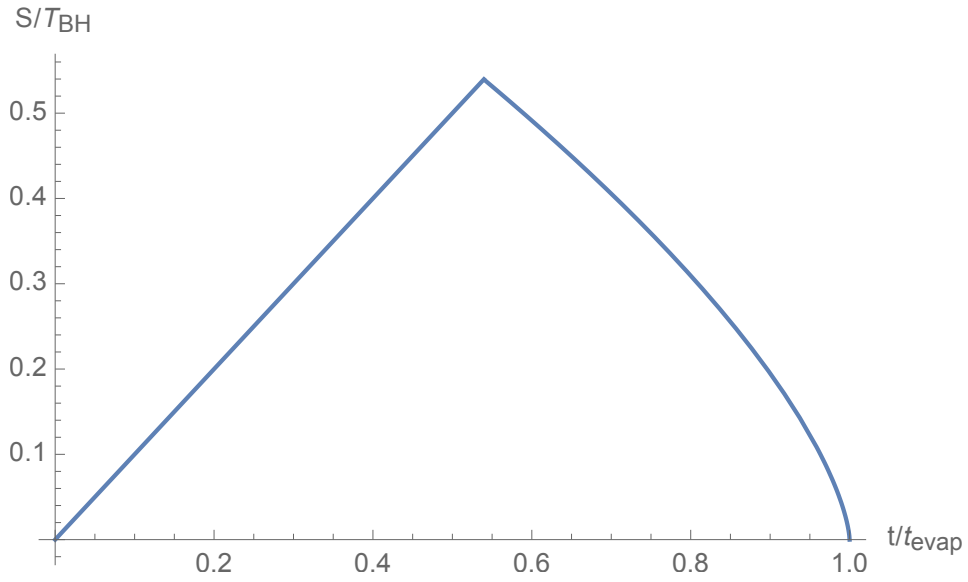

Figure 4.3: The Page curve shows that the entanglement entropy, for a black hole in a pure state, initially increases linearly and then starts decreasing from Page time $t_{Page} \approx 0.54 t_{evap}$ and $S \approx 0.6 S_0$ [23]. Information starts to come out of the black hole afterward.

Equation (4.32) tells us that information starts to come out after the entanglement entropy reaches its maximum value when the black hole has emitted roughly half of its course-grained Bekenstein-Hawking entropy, S_0. This particular time is called the page time, t_{page}. The entanglement entropy increases linearly with time, $S = tT_{BH}$, as it would for purely thermal radiation. If a black hole's age is less than its page time, then the black hole is young; otherwise, it is an 'old' black hole.

The rate of change of mass of a black hole is

$$\frac{dM}{dt} \propto -r_h^2 T_{BH}^4, \tag{4.33}$$

where r_h is the horizon radius and T_{BH} is the temperature of the black hole. The solution of the differential equation in (4.33) is

$$M(t) = \left(M_0^3 - 3At\right)^{\frac{1}{3}} \tag{4.34}$$

Hence, the Bekenstein-Hawking entropy is now

$$S(t) = S_0 \left(1 - \frac{t}{t_{evap}}\right)^{\frac{2}{3}}. \tag{4.35}$$

We have plotted the entanglement entropy S against time t with the help of Mathematica in figure 4.3.

4.4 Page's Theorem

If we have the have a bipartite Hilbert space,

$$\mathcal{H}_{AB} = \mathcal{H}_A \otimes \mathcal{H}_B, \tag{4.36}$$

where, without any loss of generality $|A| \leq |B|$. Then Page's theorem tells us that A and B are nearly maximally entangled whenever $\frac{|A|}{|B|} \ll 1$. In order to state the theorem precisely, we need two different types of trace norms and integration over the Haar Measure. One way to measure the difference between states is to rely on the L_1 and L_2 norm:

$$\|M\|_1 \equiv Tr\sqrt{M^\dagger M} \quad and \quad \|M\|_2 \equiv \sqrt{Tr\left(M^\dagger M\right)}. \tag{4.37}$$

L_1 and L_2 norms satisfy the following inequality:

$$\|M\|_2 \leq \|M\|_1 \leq \sqrt{N}\|M\|_2. \tag{4.38}$$

where N is the dimensionality of the Hilbert space. Let U be a random unitary matrix over the Haar measure, which will randomize a quantum state $|\psi\rangle$ such that,

$$|\psi\left(U\right)\rangle \equiv U\left|\psi_0\right\rangle. \tag{4.39}$$

Then a specific version of Page's theorem is

$$\int dU \|\rho_A(U) - \frac{I_A}{|A|}\|_1 \leq \sqrt{\frac{|A|^2 - 1}{|A||B| + 1}}. \tag{4.40}$$

In order to prove this theorem, we will need to use the following integrals:

$$\begin{aligned}
\int dU &= 1, \\
\int dU U_{ij} U^\dagger_{kl} &= \frac{1}{N}\delta_{il}\delta_{jk}, \\
\int dU U_{ij} U_{kl} U^\dagger_{mn} U^\dagger_{op} &= \frac{1}{N^2-1}\left(\delta_{in}\delta_{kp}\delta_{jm}\delta_{lo} + \delta_{ip}\delta_{kn}\delta_{jo}\delta_{lm}\right) \\
&\quad - \frac{1}{N\left(N^2-1\right)}\left(\delta_{in}\delta_{kp}\delta_{jo}\delta_{lm} + \delta_{in}\delta_{kn}\delta_{jm}\delta_{lo}\right).
\end{aligned} \tag{4.41}$$

$$\begin{aligned}
\left(\int dU \|\rho_A - \frac{I_A}{|A|}\|_1\right)^2 &\leq \int dU \left(\|\rho_A(U) - \frac{I_A}{|A|}\|_1\right)^2 \text{(Jensen's inequality)} \\
&\leq |A| \int dU \left(\|\rho_A(U) - \frac{I_A}{|A|}\|_2\right)^2 \text{(from (4.38))} \\
&\leq |A| \int dU \left[Tr\left(\rho_A(U)^2\right) - \frac{1}{|A|}\right] \\
&\leq \frac{|A|^2 - 1}{|A||B| + 1}
\end{aligned} \tag{4.42}$$

Therefore,

$$\int dU \|\rho_A(U) - \frac{I_A}{|A|}\|_1 \leq \sqrt{\frac{|A|^2 - 1}{|A||B| + 1}}. \tag{4.43}$$

We can also arrive at Page's theorem using the entanglement entropy S_A. Let us define

$$\Delta\rho_A \equiv \rho_A - \frac{I_A}{|A|}. \tag{4.44}$$

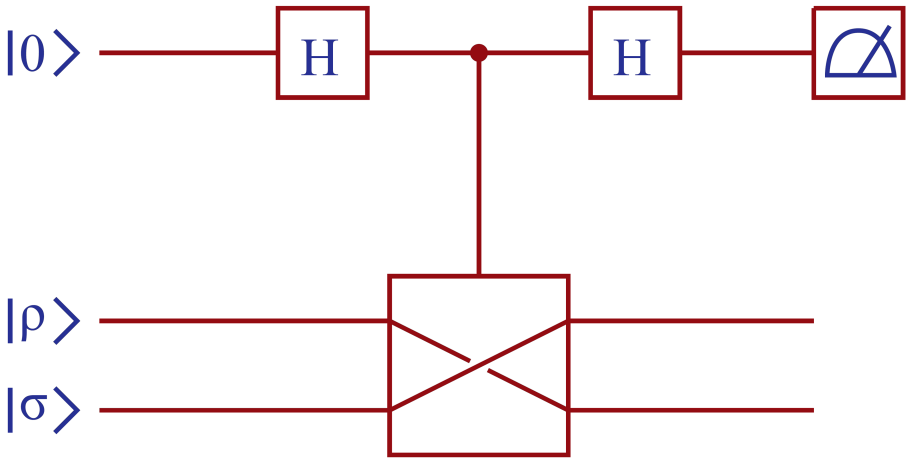

Figure 4.4: To check for unitarity, we can use the swap test, which swaps the operator $\rho \otimes \sigma$ to $\sigma \otimes \rho$ if the swap gate measures the superposition from Hadamard gate as $|1\rangle$ and remains unchanged otherwise. The expected outcome in the Z basis for the qubit passing through the Hadamard gate on the right is $Tr\,(\rho\sigma)$[11].

Now, we can evaluate the following integral, taking the limit, $\frac{|A|}{|B|} \ll 1$,

$$\begin{aligned}\int dUS_A &= -\int dUTr\,(\rho_A \log \rho_A) \\ &= Tr\left[\left(\frac{I_A}{|A|} + \Delta\rho_A\right)\left(\log|A| - |A|\Delta\rho_A + \frac{1}{2}|A|^2\Delta\rho^2 + \cdots\right)\right] \\ &= \log|A| - \frac{|A|}{2}\int dUTr\Delta\rho_A^2 + \cdots \\ &= \log|A| - \frac{1}{2}\frac{A}{B}\cdots\end{aligned} \tag{4.45}$$

Both versions of Page's theorem can explain the Page curve with a similar argument, as shown with the Gaussian random complex variable in section 4.3.

4.5 Quantum Circuit to Test Unitarity

We can prepare two identical black holes and record the entire radiation as quantum states with a quantum computer. Then we implement the circuit in 4.4, which measures the swap operator with the outcomes ± 1. The expectation value of this experiment is $Tr\,(\rho\sigma)$, with the quantity being generally very close to zero. However, when the states are pure and equal:

$$Tr\,(\rho\sigma) = Tr\left(\rho^2\right) = 1. \tag{4.46}$$

Preskill and Hayden[12] suggested that if black hole evaporation is unitary, this test could distinguish in O(1) number of tries that the states are pure and equal to very high certainty. There will be a certain degree of error in practice while experimenting; hence, we will have to rely on quantum error correction.

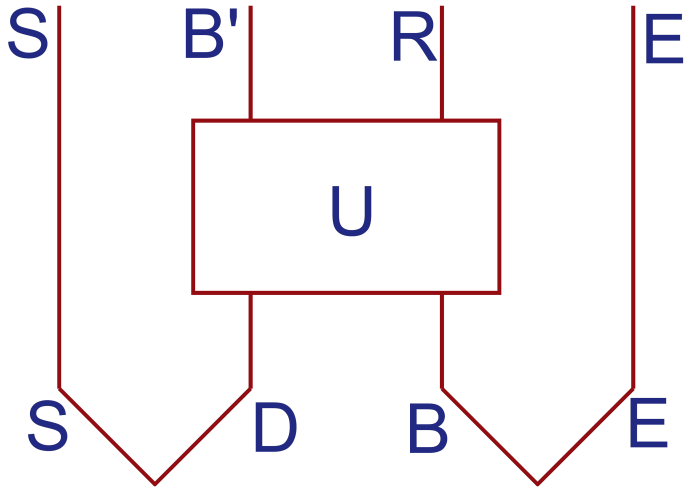

Figure 4.5: An old black hole whose late radiation E is maximally entangled with the early radiation B. The quantum memory D, which is maximally entangled with S is dumped into the black hole. The black hole applies a thoroughly mixing unitary transformation U, after which radiation R is emitted and radiation B' is still inside the black hole. Hence, we want to find when the subsystem S is close to being maximally entangled with ER[11].

4.6 Extracting Quantum Information from Hawking Radiation

Suppose we have a system of n qubits with residing in a Hilbert space of dimension 2^n, such that

$$|\psi\rangle = \sum_i c_i |i\rangle . \tag{4.47}$$

The no-cloning theorem prevents us from copying a quantum state $|\psi\rangle$ from system A to a blank state $|0\rangle$ in system B, the following operation violates unitarity in quantum mechanics:

$$|\psi\rangle_A |0\rangle_B \to |\psi\rangle_A |\psi\rangle_B . \tag{4.48}$$

Instead we have to rely on transferring of quantum information:

$$|\psi\rangle_A |0\rangle_B \to |0\rangle_A |\psi\rangle_B . \tag{4.49}$$

Transferring quantum information is still successful if system B has $U_B |\psi\rangle_B$ as $U_B^\dagger$ can act to get $|\psi\rangle_B$ back,

$$|\psi\rangle_A |0\rangle_B \to |0\rangle_A U_B |\psi\rangle_B , \tag{4.50}$$

where U_B is unitary. Let us prepare a system C which is maximally entangled with system A, then

$$\frac{1}{\sqrt{|A|}} |i\rangle_A |0\rangle_B |i\rangle_C \to |0\rangle_A \frac{1}{\sqrt{|a|}} U_B |i\rangle_B |i\rangle_C . \tag{4.51}$$

If C purifies A, then the density states ρ_{AC} must be very close to $\rho_A \otimes \rho_B$. Now, if the quantum system D is dumped into the black hole as shown in figure 4.5. To recover D we have to wait till B' purifies S, that is

$$\|\rho_{SB'} - \rho_S \otimes \rho_{B'}\| \ll 1. \tag{4.52}$$

From the Page Curve we know that black hole which starts from a pure state, emits no information till Page time. We can rely on integral on the Haar measure (4.41) and that $|B'||R| = |E||D|$ to find what happens for an old black hole whose internal radiation is already entangled with E,

$$\begin{aligned} \int dU \|\rho_{SB'} - \rho_S \otimes \rho_{B'}\|_1 &\leq \sqrt{\frac{\left(|D|^2 - 1\right)\left(|B'|^2 - 1\right)}{|D|^2|E|^2 - 1}} \\ &\approx \frac{|D|}{|R|}. \end{aligned} \tag{4.53}$$

If k more bits than the contents of D have been radiated after the unitary mixing, then $\frac{|D|}{|R|} = 2^{-k}$. Hence, information comes out exponentially fast as the right-hand side of (4.53) becomes extremely small with increasing k. Therefore, as Preskill and Hayden stated, old black holes are equivalent to information mirrors.

Chapter 5

AdS/CFT and Holography

5.1 Introduction

AdS/CFT of the holographic principle provided compelling evidence in support of the unitarity of black hole evaporation. AdS/CFT is a vast topic and we explore parts of it for our relevant discussion in this section. We end this section with a discussion of the Holographic Entanglement Entropy.

5.2 Holographic Principle

Several developments in theory led to the idea of the Holographic principle. First, we look at the *Bekenstein bound* on the universal upper limit of the entropy for any object,

$$S \leq 2\pi RE, \tag{5.1}$$

where R is the maximal radius and E is the total energy of the object.

This bound was derived from the condition that black holes must obey the second law of thermodynamics when any object containing some entropy is dropped into a Schwarzchild black hole without any radial motion near its horizon.

Susskind later suggested a bound that contains the Planck scale explicitly. This bound is known as the *holographic entropy bound* [11][33],

$$S \leq \frac{A}{4l_p^2}, \tag{5.2}$$

where $l_p^2 = \hbar G/c^3$. This gives the idea that the maximum entropy in a region of spacetime is bounded by the area of the boundary of the region.

This area scaling of entropy led to the idea that a quantum gravity theory can be related to a theory in one fewer dimension and became known as the *holographic principle* as promoted by Susskind.

5.3 AdS/CFT Correspondence

The Anti- de Sitter/ Conformal Field Theory correspondence emerged initially from low energy limits in string theory and is the most successful realization of the holographic principle. Maldacena's paper from 1997 initiated the study of this duality between a 'bulk' theory relating to a 'boundary' theory.

The statement of AdS/CFT, also known as the Maldacena Conjecture, goes as follows:

Type IIB String Theory on $AdS_5 \times S^5$ which is a gravitational theory is dual to to $\mathcal{N}$=4, SU(N) Super Yang-Mills theory which is a gauge theory and is conformally invariant. [4]

Instead of going into the details leading to this statement, we present the AdS/ CFT correspondence as a self-consistent framework. In simpler terms, the correspondence establishes a relationship between a strongly coupled gauge theory to a gravitational theory in one higher dimensional AdS spacetime. At finite temperature, this strongly coupled gauge theory is equivalent to a gravitational theory in AdS Black hole. [20]

The free parameters on the AdS side are the string coupling g_s and the ratio L^2/α' which is dimensionless and where L is the radius of curvature and $\alpha' = l_s^2$ and l_s is the string length. The parameters on the CFT side are the gauge group N and the coupling constant g_{YM}^2. The correspondence is established by the following relations: [4]

$$g_{YM}^2 = 2\pi g_s \quad and \quad 2g_{YM}^2 N = L^4/\alpha'^2. \tag{5.3}$$

In the second equation $\lambda = g_{YM}^2 N$ is the 't Hooft coupling.

5.4 AdS Spacetime

Anti-de Sitter spacetime is a solution of Einstein's equations if the vacuum energy $\Lambda < 0$,

$$R_{\mu\nu} - \frac{1}{2} g_{\mu\nu} R = \Lambda g_{\mu\nu}. \tag{5.4}$$

AdS Spacetime is the maximally symmetric solution to this equation. In $d+1$ spacetime dimensions this has the metric:

$$ds^2 = -\left(1 + (\frac{r}{R_{ads}})^2\right) dt^2 + \left(\frac{1}{1 + (\frac{r}{R_{ads}})^2}\right) dr^2 + r^2 d\Omega_{d-1}^2. \tag{5.5}$$

We can use 'global coordinates' to describe AdS space by taking $r = R_{ads} \tan\rho$: [16]

$$ds^2 = \frac{R_{ads}^2}{\cos^2\rho} \left(-dt^2 + d\rho^2 + \sin^2\rho d\Omega_{d-1}^2\right). \tag{5.6}$$

In the above equation R_{ads} is the AdS Radius. We will take $R_{ads} = 1$ in this section. This has the property that when $r << 1$ it resembles Minkowski space in sperical coordinates. The parameter t takes values in the interval $(-\infty, +\infty)$ and r has the interval $[0, \infty)$. We have also used $d+1$ dimensions for the AdS space

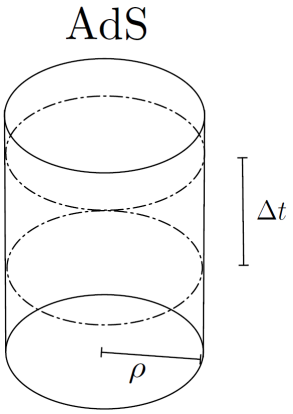

Figure 5.1: AdS in Global Coordinates[9]

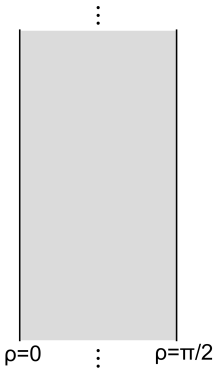

Figure 5.2: The spatially finite Penrose diagram for AdS space [11]. Here $\rho \in [0, \pi/2)$ and $t \in (-\infty, +\infty)$. Light rays move at 45 degree angles in the plane t-ρ. The left hand side is the origin of the cylindrical coordinates at $\rho = 0$ and the right hand side is the boundary of the cylinder at $\rho = \pi/2$.

since the dual CFT has one lower dimension and is so it taken to have d spacetime dimensions.

It is necessary to choose a certain distance and curvature scale for an AdS spacetime. We use $\rho \in [0, \pi/2)$ as the radial coordinate and $t \in (-\infty, +\infty)$. The angular coordinate Ω covers a $d-1$ dimensional sphere. If $d = 3$ this has the familiar form:

$$d\Omega^2 = d\theta^2 + \sin^2\theta d\phi^2. \tag{5.7}$$

In equation (5.6), we can carry out a conformal rescaling. The diverging prefactor is $1/\cos^2\rho$ which can be simply dropped or multiplied by a Weyl factor of $\cos^2\rho$ to get

$$ds^2 = -dt^2 + d\rho^2 + \sin^2\rho d\Omega_{d-1}^2. \tag{5.8}$$

This is the same metric as the Einstein Static Universe. The only difference is that ρ takes values between $[0, \pi/2)$ which has the same boundary structure as one-half of the Einstein Static Universe where $\rho \in [0, \pi)$. We call such a spacetime *Asymtotically AdS*. This is particularly useful since the boundary of AdS is important in the study of AdS/CFT.

We can now also visualize a spatially finite Penrose diagram. The boundary of AdS is the cylinder $R \times S^{d-1}$ which we get by taking the limiting value at spatial infinity as $\rho \to \pi/2$. If we consider looking at $(n+1)$ dimensional AdS_{n+1} space which can be embedded onto a $(n+2)$ dimensional Minkowski spacetime, where $(y^0, y^1, ..., y^n, y^{n+1}) \in \mathbb{R}^{n,2}$ we have the interval

$$ds^2 = -(dy^0)^2 + (dy^1)^2 + ... + (dy^n)^2 - (dy^{n+1})^2, \tag{5.9}$$

$$ds^2 = \eta_{MN} dy^M dy^N, \tag{5.10}$$

where $\eta = \text{diag}(-, +, +, ..., +, -)$ and $M, N \in \{0, ..., n+1\}$. AdS_{n+1} can be represented by a hypersurface in $\mathbb{R}^{n,2}$:

$$\eta_{MN} y^M y^N = -(y^0) + \sum_{i=1}^{n} (y^i)^2 - (y^{n+1})^2. \tag{5.11}$$

This hypersurface is invariant under the isometry group $SO(n,2)$. The dimension of this group is $\frac{1}{2}(n+1)(n+2)$ which is the same as the dimension of the group $SO(n+2)$ which is for a flat space of same dimensionality that is invariant under the Poincarè group where translations give $n+1$ dimensions and Lorentz transformations give the remaining $\frac{1}{2}n(n+1)$ dimensions.

5.5 Conformal Field Theory

A Conformal Field Theory is a quantum field theory that is invariant under the conformal group. The conformal group is the group of transformations that preserve angles but not necessarily lengths. The Conformal Group is generated by Poincarè transformations, dilations, and special conformal transformations.

The usual Poincarè transformations are transformations of the form:

$$x^\mu \to \Lambda^\mu_\nu x^\nu + a^\mu, \tag{5.12}$$

which includes spacetime translations: $x^\mu \to x^\mu + \alpha^\mu$ and (Lorentz) rotations: $x^\mu \to x^\mu + \omega^\mu_\nu x^\nu$.

If we consider n-dimensional Euclidean Space E^n, we know that the Poincareé group has n translation generators and $\frac{1}{2}n(n-1)$ rotation generators.

$$\dim \text{Poincaré}(E^n) = \frac{1}{2}n(n+1) \tag{5.13}$$

The Conformal group is $SO(1, n+1)$ which has: [25]

$$\dim SO(1, n+1) = \frac{1}{2}(n+2)(n+1). \tag{5.14}$$

The $SO(1, n+1)$ group has $n+1$ more generators than the Poincaré group in n dimensions. These additional generators arise from the dilations and special conformal transformations.

Dilations are scale transformations:

$$x'^{\mu} \to \lambda x^{\mu}, \tag{5.15}$$

where $\lambda \in \mathbb{R}$. This gives one generator.

We can also use discrete transformations known as inversions which have the form

$$x^{\mu} \to \frac{x^{\mu}}{x^2}. \tag{5.16}$$

The inversion of x follow by a translation by α can be represented as

$$\frac{x'^{\mu}}{x'^2} = \frac{x^{\mu}}{x^2} + \alpha^{\mu}. \tag{5.17}$$

We can now think of another inversion in the form

$$x'^2 = \frac{x^2}{1 + 2\alpha_{\mu}x^{\mu} + \alpha^2 x^2}. \tag{5.18}$$

Using this we can write:

$$x'^{\mu} = \frac{x^{\mu} + \alpha^{\mu}x^2}{1 + 2\alpha_{\mu}x^{\mu} + \alpha^2 x^2}. \tag{5.19}$$

which are Special Conformal Transformations (SCT). Here α^{μ} has n parameters as $\mu = 1, ..., n$ which gives the remaining n generators. The isometry group $SO(1, n+1)$ in Euclidean signature is the same as the $SO(2, n)$ group in the Minkowski case. So we see that the conformal group is identical to the isometry group on AdS_{n+1}.

5.5.1 The Conformal Algebra

Since the conformal group is a continuous group we can have a Lie algebra of the conformal group. We can do the representation in terms of scalar fields $\phi(x)$ with x^{μ} which has a Cartesian coordinate where $\mu = 1, ..., n$. The infinitesimal generators of the conformal group are:

$$\begin{aligned}
\text{Translations: } P_{\mu} &= i\partial_{\mu}, \\
\text{Rotations: } L_{\mu\nu} &= i(x_{\mu}\partial_{\nu} - x_{\nu}\partial_{\mu}) \\
&= -(x_{\mu}P_{\nu} - x_{\nu}P_{\mu}), \\
\text{Dilations: } D &= -ix^{\mu}\partial_{\mu}, \\
\text{SCT: } K_{\mu} &= i(2x_{\mu}x \cdot \partial - x^2\partial_{\mu}) \\
&= -2x_{\mu}D + x^2 P_{\mu}.
\end{aligned} \tag{5.20}$$

Using these generators we can work out the Lie Algebra of this group

$$\begin{aligned}
\left[D, P_{\mu}\right] &= +iP_{\mu}, \\
\left[D, K_{\mu}\right] &= -iK_{\mu}, \\
\left[P_{\mu}, K_{\nu}\right] &= 2i(g_{\mu\nu}D + L_{\mu\nu}), \\
\left[L_{\mu\nu}, P_{\rho}\right] &= i(g_{\nu\rho}P_{\rho} - g_{\mu\rho}P_{\mu}), \\
\left[L_{\mu\nu}, L_{\rho\tau}\right] &= i(g_{\mu\tau}L_{\nu\rho} + g_{\nu\rho}L_{\mu\tau} - g_{\mu\rho}L_{\nu\tau} - g_{\nu\tau}L_{\mu\rho}), \\
\left[L_{\mu\nu}, K_{\rho}\right] &= i(g_{\nu\rho}K_{\mu} - g_{\mu\rho}K_{\nu}).
\end{aligned} \tag{5.21}$$

5.5.2 Properties of Conformal Field Theories

Primary Operators

Primary operators are a special set of local operators that can transform under conformal transformations. The scaling dimensions of these operators, Δ, is real and non negative in a unitary CFT, i.e $\Delta \geq 0$. Using the commutation relations in (5.20), we find

$$DK_\mu \mathcal{O}(x) = \big([D, K_\mu] + K_\mu D\big)\, \mathcal{O}(0) = i(\Delta - 1) K_\mu \mathcal{O}(x). \tag{5.22}$$

Similarly,

$$DP_\mu \mathcal{O}(x) = \big([D, P_\mu] + P_\mu D\big)\, \mathcal{O}(x) = i(\Delta + 1) P_\mu \mathcal{O}(x), \tag{5.23}$$

where $\mathcal{O}(x)$ is an operator that transforms irreducibly under dilations and so is an eigen-operator of D which means $[D, \mathcal{O}(x)] = \Delta \mathcal{O}(x)$.

This means that the operator P_μ raises the scaling dimension and K_μ lowers it. Hence, if we apply K_μ repeatedly on an operator $\mathcal{O}$ we obtain $K_{\mu_1} ... K_{\mu_N} \mathcal{O}$ but since the allowed dimensions must be positive, we will have a special set of operators such that

$$[K_\mu, \mathcal{O}(x)] = 0. \tag{5.24}$$

Operators that satisfy this condition are knows as primary operators or primary fields. Under dilations the primary operators transform as

$$\mathcal{O}'(x') = \lambda^{-\Delta} \mathcal{O}(x). \tag{5.25}$$

The P_μ generators give derivatives of primary operators which are called descendants. We apply these generators an infinite number of times $P_{\mu_1} ... P_{\mu_N} \mathcal{O}(0)$ which would give a conformal dimension of $\Delta + n$. Under dilations they would rescale as $\lambda^{-\Delta - n}$ but they are not primary anymore. Primary operators are of interest since they have simple correlation functions. As an example we can consider the time ordered two point function of a scalar primary operator $\mathcal{O}$ with conformal dimension Δ, [11]

$$\langle \Omega |\, T\mathcal{O}(x,t)\mathcal{O}(0,0)\, | \Omega \rangle = \frac{1}{(|x|^2 - t^2 + i\epsilon)^\Delta}. \tag{5.26}$$

The State-operator correspondence

In CFTs the state-operator correspondence is a powerful tool. This correspondence states that a special set of local operators known as primary operators on $\mathbb{R}^d$ can be related to a state on $\mathbb{S}^{d-1}$. This is possible due to a conformal transformation from $\mathbb{R}^d$ to $\mathbb{R} \times \mathbb{S}^{d-1}$.

In Euclidean plane $\mathbb{R}^d$ we can write the metric in spherical coordinates as

$$ds^2 = d\rho^2 + \rho^2 d\Omega_{d-1}^2; \tag{5.27}$$

this is conformally equivalent to $\mathbb{R} \times \mathbb{S}^{d-1}$ for which if we do the coordinate change $\rho = e^{t_E}$ and remove the conformal factor $\Omega^2 = e^{2t_E}$ we get the form

$$ds^2 = e^{2t_E} \left(dt_E^2 + d\Omega_{d-1} \right). \tag{5.28}$$

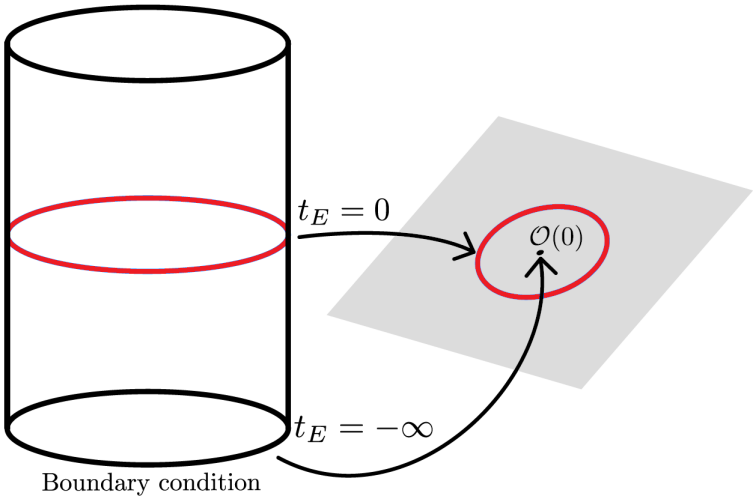

Figure 5.3: The state-operator correspondence[6].

We see that the dilations ρ have become time translations of t_E. In 5.3, we see that we have a state at $t_E = 0$ in the $\mathbb{R} \times \mathbb{S}^{d-1}$ cylinder with boundary conditions at $t_E = -\infty$ which is being exponentially mapped onto the Euclidean plane $\mathbb{R}^d$ where the state is on the sphere at $\rho = 1$. The boundary condition at $t_E = -\infty$ gets exponentially mapped to a local condition at $\rho = 0$.

Using the state-operator correspondence we can see that a condition at $\rho = 0$ is equivalent to the insertion of a local operator in the CFT. The Euclidean path integral on the sphere $\rho < 1$ in $\mathbb{R}^d$ results in a quantum state at $t_E = 0$ on the cylinder $\mathbb{R} \times \mathbb{S}^{d-1}$. If the local operator has a dimension of Δ at $\rho = 0$ then the quantum state has an energy Δ at $t_E = 0$. This means that there is a bijective map and an path integral over a compact manifold which are two fundamental properties of the state-operator correspondence.

5.6 The dictionary

We can review the statement of AdS/CFT as the following:

> Any CFT on $\mathbb{R} \times \mathbb{S}^{d-1}$ is equivalent to a quantum gravity theory in asymptotically $AdS_{n+1} \times M$ spacetime where M is a compact manifold.

The mapping of the observables between the theories is known as the dictionary. We have previously shown that the isometry group $SO(2, n)$ is both the conformal group and the asymptotic symmetry group of AdS_{n+1}. The dictionary states that the duality arises due to an isomorphism between the AdS_{n+1} Hilbert space $\mathcal{H}_{AdS}$ and the CFT Hilbert space $\mathcal{H}_{CFT}$. The dictionary establishes the idea that extrapolating a bulk scalar field to the boundary gives a primary operator of dimension Δ in the CFT. This means for a CFT there is always a semiclassical dual near the vacuum:[1]

$$\mathcal{O}(t, \Omega) = \lim_{r \to \infty} r^{\Delta} \phi(t, r, \Omega). \tag{5.29}$$

As an example, can consider that the time-ordered two point function for a free massive scalar field in AdS with the two points on $\mathbb{S}^{d-1}$. The application of the

dictionary results in obtaining the two-point function in the CFT on $\mathbb{R} \times \mathbb{S}^{d-1}$ for a scalar of dimension Δ,

$$\lim_{r\to\infty} \langle 0| \phi(t', \Omega')\phi(t, \Omega) |0\rangle = \langle 0| \mathcal{O}(t', \Omega')\mathcal{O}(t, \Omega) |0\rangle . \tag{5.30}$$

To reproduce everything we know about the bulk quantum gravity another condition must be satisfied. We must look at which particular cases of the CFT give a good semiclassical definition: where the Planck length l_p is much smaller than the AdS Radius, R_{ads}. A semiclassical dual can exist if the induced metric on the boundary is arbitrary and has a Euclidean geometry as allowed by asymptotically-AdS boundary conditions in addition to the existence of the dual near the vacuum.

5.7 AdS Black Holes

Black holes have thermodynamic properties quantum mechanically. Considering this quantum effect of matter we know a black hole emits Hawking radiation. For a Schwarzchild black hole this temperature is given by

$$k_B T = \frac{\hbar c^3}{8\pi G M}. \tag{5.31}$$

Comparing the first law of black holes with the first law of thermodynamics $dE = TdS$ we get

$$S = \frac{A}{4G\hbar} k_B c^3 = \frac{A}{4{l_p}^2}, \tag{5.32}$$

which is the exact bound as discussed earlier in equation 5.2.

In AdS, the Hawking Radiation from black holes bounces back from the boundary in finite time. Small black holes evaporate fully before their radiation reaches the boundary so are unstable and large black holes are eternal and stable. For black holes with their Schwarzchild radius approaching the AdS radius, the reflection and the radiation rates become equal.

The transition between the stability and instability for AdS_4 was estimated by statistical arguments to be

$$ER_{ads} = \left(\frac{R_{ads}}{l_p}\right)^2 \left(\frac{R_{ads}}{l_p}\right)^{-2/5}. \tag{5.33}$$

Here the E is an energy state in the CFT for a black hole whose Schwarzchild radius is of the order of the AdS radius. This equation shows that the transition happens when for the black hole the $\frac{R_{ads}}{l_p}$ is parametrically smaller than the AdS radius. In AdS_{d+1} the scaling has the order of $-\frac{(d-1)(d-2)}{2d-1}$ instead of being parametric for the transition. This means that the transition expression turns out to be

$$ER_{ads} = \left(\frac{R_{ads}}{l_p}\right)^{d-1} \left(\frac{R_{ads}}{l_p}\right)^{-\frac{(d-1)(d-2)}{2d-1}}, \tag{5.34}$$

or

$$ER_{ads} = \left(\frac{R_{ads}}{l_p}\right)^{\frac{d^2-1}{2d-1}}. \tag{5.35}$$

5.7.1 Schwarzchild Black Hole in AdS

In $d+1$ dimensional asymptotically AdS spacetime the static Schwarzchild black hole has the metric:

$$ds^2 = -f(r)dt^2 + f(r)^{-1}dr^2 + r^2 d\Omega_{d-1}^2, \tag{5.36}$$

Here

$$f(r) = 1 + \frac{r^2}{R_{ads}^2} - \frac{\alpha}{r^{d-2}}, \tag{5.37}$$

where α is the mass of the black hole multiplied with the Newton's constant in $d+1$ dimensions

$$\alpha = \frac{8\Gamma(\frac{d}{2})GM}{(d-1)\pi^{(d-2)/2}}. \tag{5.38}$$

Taking the positive root of f at the horizon $r = r_s$ where we approach the coordinate singularity,

$$1 + \frac{r_s^2}{R_{ads}^2} - \frac{\alpha}{r_s^{d-2}} = 0. \tag{5.39}$$

Furthermore, assuming that the Euclidean version of the geometry is smooth we get the Hawking temperature

$$T = \frac{(d-2)R_{ads}^2 + dr_s^2}{4\pi r_s R_{ads}^2}. \tag{5.40}$$

For the small black hole mass limit ($\alpha \ll R_{ads}^{d-2}$) we get

$$T \approx \frac{d-2}{4\pi r_s}. \tag{5.41}$$

For the large black hole mass limit ($\alpha \gg R_{ads}^{d-2}$) we get

$$T \approx \frac{dr_s}{4\pi R_{ads}^2}. \tag{5.42}$$

We can also calculate the evaporation rate of a small black hole in AdS using the Stefan-Boltzmann law

$$\frac{d\alpha}{dt} \sim \alpha^{-2/(d-2)}. \tag{5.43}$$

This gives the lifetime growing as an order of the mass of the black hole

$$\tau \sim \alpha^{d/(d-2)}. \tag{5.44}$$

For large black holes we get can calculate the evaporation rate to be

$$\frac{d\alpha}{dt} \sim \alpha^2, \tag{5.45}$$

which gives the lifetime

$$\tau_0 - \tau \sim \mu^{-1}, \tag{5.46}$$

where τ_0 is the upper bound for which the mass of the black hole is infinite and τ is the time until the black hole evaporates to the Schwarzchild radius of order of the AdS radius. [19]

5.7.2 BTZ Black Hole

The BTZ black hole is a special case for $d = 2$ dimensions. In this case the metric in equation 5.36 for the Schwarzchild black hole is replaced by the metric

$$ds^2 = (\frac{r^2}{R_{ads}^2} - m)dt^2 - (\frac{r^2}{R_{ads}^2} - m)^{-1}dr^2 - r^2 d\phi^2. \tag{5.47}$$

To relate the m with the mass of this BTZ black hole, if the geometry of the resulting 3 dimensional AdS spacetime AdS_3 is defined to have zero mass we get

$$m = 8GM_{ads} - 1. \tag{5.48}$$

In this case the BTZ black hole does not have a minimum mass that is zero. Instead, if we take m=0 for our metric in equation 5.47 we get the relation

$$m = 8GM_{BTZ}. \tag{5.49}$$

This case is more relevant to us as it gives us the Schwarzchild radius, $r_s = \sqrt{m}R_{ads}$ which means that as $m \to 0$, $r_s \to 0$.

The Hawking temperature of the BTZ black hole is calculated to be

$$T = \frac{\sqrt{m}}{2\pi R_{ads}}, \tag{5.50}$$

and its entropy is

$$S = \frac{\pi\sqrt{m}R_{ads}}{2G}. \tag{5.51}$$

In 5.50 we can see that the hawking temperature of these black holes decrease as their mass decreases so their lifetime is infinite. These small black holes are therefore unstable.

5.8 The information paradox resolved in AdS/CFT

Hawking imagined the formation of a black hole through gravitational collapse and its evaporation into AdS/CFT by emitting Hawking radiation. The black hole of our concern must be sufficiently big to be semiclassical and small to evaporate completely leaving behind only the hawking radiation. Using our case for AdS_{d+1} in (5.35) this has the range

$$\left(\frac{R_{ads}}{l_p}\right) \ll ER_{ads} \ll \left(\frac{R_{ads}}{l_p}\right)^{\frac{d^2-1}{2d-1}}. \tag{5.52}$$

The infalling matter onto the black hole must somehow be correlated to the outgoing Hawking radiation. So if the infalling matter has a pure state configuration then the final state should also be a pure state. This is only possible if the evolution is unitary. AdS/CFT allows this possibility since the CFT is a supersymmetric gauge theory on the boundary which is manifestly unitary. Some issues arise in the AdS spacetime interpretation due its global structure. This arises

since the boundary of the cylindrical structure can be heuristically interpreted to be at infinity, any spacelike slice can allow lightlike signals to propagate from the boundary to the region inside the structure in an affine parameter that is finite. Thus, even in the absence of black holes it is difficult to define any evolution in the AdS space to have a quantum mechanical evolution. By imposing boundary conditions at infinity and studying special black holes which have a short lifetime we can bypass this issue leading to the evolution obeying unitarity. This is how the conjecture shows that the information is preserved in the quantum mechanical black hole evolution. In the following chapter 6, we will look at how the principle of holographic duality relates to the Bekenstein-Hawking entropy of a black hole.

5.9 Holographic Entanglement Entropy

The holographic description of the entanglement entropy is one of the most interesting proposals derived by Ryu and Takayanagi [28] using the AdS/CFT correspondence.

The proposed formula using the $\mathrm{AdS}_{d+2}/\mathrm{CFT}_{d+1}$ correspondence for the Entanglement entropy for a subsystem A which has a boundary in $d-1$ dimension ∂A in S^d in a CFT on $\mathbb{R} \times S^d$ is

$$S_A = \frac{\text{Area of } \gamma_A}{4G_N^{(d+2)}}, \tag{5.53}$$

where γ_A is the minimal d dimensional surface area in AdS_{d+2} which has the boundary ∂A and $4G_N^{(d+2)}$ is the Newton constant in $d+2$ dimensions.

A heuristic derivation has been shown in the following way: [21]
The Ricci Scalar is comparable with the delta function under the assumption that the n-sheeted AdS_{d+2} describes the backreacted geometry S_n,

$$R = 4\pi (1-n)\, \delta(\gamma_A) + R^{(0)}. \tag{5.54}$$

In the equation above (5.54), we have the boundary conditions that

$$\delta(\gamma_A) = \begin{cases} \infty & x \in \gamma_A \\ 0 & otherwise \end{cases}, \tag{5.55}$$

and R^0 is that of the pure AdS_{d+2}. Now, we will substitute R into the supergravity action ,

$$S_{AdS} = -\frac{1}{16\pi G_N^{(d+2)}} \int_M dx^{d+2} \sqrt{g}\, (R + \Lambda) + \cdots . \tag{5.56}$$

We have written only the bulk Einstein-Hilbert action because the other terms are proportional to n, which leads to them being cancelled in the following ratio:

$$\begin{aligned} Tr\,(\rho_A^n) &= (Z_1)^{-n} \int_{(t_E,x)\in\mathcal{R}_n} D\phi e^{-S(\phi)} \\ &\equiv \frac{Z_n}{(Z_1)^n}. \end{aligned} \tag{5.57}$$

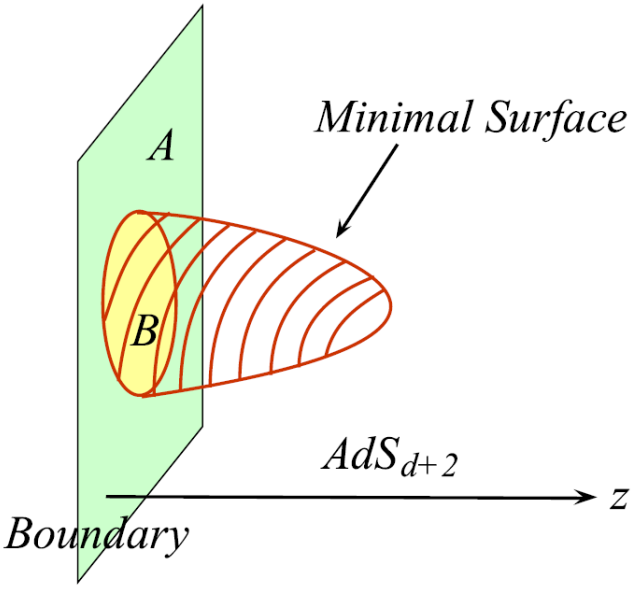

Figure 5.4: Calculation of the holographic entanglement entropy using a minimal surface from AdS/CFT[28].

Hence, we can use the equivalence of the partition functions of CFT and AdS gravity

$$Z_{CFT} = Z_{AdS \quad Gravity}, \tag{5.58}$$

to calculate the holographic entanglement entropy:

$$\begin{aligned} S_A &= -\frac{\partial}{\partial n} \log Tr\rho_A^n|_{n=1} \\ &= -\frac{\partial}{\partial n}\left[\frac{(1-n)\,\text{Area}\,(\gamma_A)}{4G_N^{d+2}}\right]_{n=1} \\ &= \frac{\text{Area}\,(\gamma_A)}{4G_N^{d+2}}. \end{aligned} \tag{5.59}$$

Therefore, we have derived the formula for holographic entanglement entropy in (5.53) [10]. It can be seen that the formula satisfies the basic properties of the entanglement entropy [28] which include (i) $S_A = S_B$ where B is the complement of A and (ii) $S_{A_1} + S_{A_2} \leq S_{A_1 \cup A_2}$ which is the strong-subadditivity condition which will be discussed again in the next section (6.2).

The computations of Holographic Entanglement Entropy in AdS_3/CFT_2, in higher dimensions and for Yang-Mills at Finite Temperature all have been explicitly shown by Ryu and Takayanagi [28]. Furthermore, the assumption that we used on the Ricci Scalar in (5.54) is satisfied in 3-dimensional pure gravity with certainty.

Interestingly, the holographic entanglement entropy formula (5.53) scales as the area. This is analogous to the Area law for entropy of harmonic oscillators [30] and the holographic entropy bound as shown in equation 5.2.

Chapter 6

Entanglement Entropy Between Subsystems of Harmonic Oscillators

6.1 Entanglement Entropy within Flat Space

Assume that there is a massless, scalar quantum field represented by a bipartite Hilbert space $\mathcal{H}$. Since the space is bipartite, we can write it as a tensor product of two Hilbert spaces $\mathcal{H}_{in}$ and H_{out}, i.e $\mathcal{H} = \mathcal{H}_{in} \otimes \mathcal{H}_{out}$. We can choose the non-degenerate ground state on H to be represented by $|\psi_0\rangle$. This state is associated with the pure state density operator $\rho_0 = |\psi_0\rangle \langle\psi_0|$. Imagine that there is a sphere in the flat space with an arbitrary radius R, which has degrees of freedom residing inside of it and can be associated with $\mathcal{H}_{in}$. The degrees of freedom lying outside the sphere can be associated with $\mathcal{H}_{out}$ The von Neumann entropy (also referred to as entanglement entropy) associated with the outer sphere is $S = -Tr\rho_{out} \ln \rho_{out}$ [14] which also represents the tracing of all the internal degrees of freedom lying inside the sphere. We will investigate the relationship between S and R.
Now let us define $S' = Tr\rho_{in} \ln \rho_{in}$ which has the same eigenvalues as S. As any entanglement entropy S''' in terms of eigenvalues is $S''' = \sum_n p_n \ln p_n$, S and S' must be equal as they share the same set of eigenvalues. Hence, both entropies S and S' must depend on a common property, which is the area of the sphere. Since the area is dimensional and S is dimensionless, we need a dimensionful parameter to relate it with the area A. Furthermore, the interior of the sphere is independent of the infrared cutoff, which leaves only one dimensionful parameter, the ultraviolet cutoff M. Therefore, S must be a function of M^2A(which is dimensionless).

6.2 Characteristics of entanglement entropy

The density matrix for finite-dimensional Hilbert Space is

$$\rho = \sum_{\alpha} p_\alpha |\psi_\alpha\rangle \langle\psi_\alpha| \tag{6.1}$$

where α is used to represent a vector from a particular quantum system.

The density operator have the following properties[29][14]:
The expectation value of an operator A with respect to a subset of ensemble with the state ψ_α is

$$\begin{aligned}\langle A\rangle &= \sum_\alpha p_\alpha \langle\psi_\alpha| A |\psi_\alpha\rangle \\ &= \sum_\alpha p_\alpha Tr\, |\psi_\alpha\rangle \langle\psi_\alpha| A \\ &= Tr\rho A.\end{aligned} \tag{6.2}$$

The density matrix is Hermitian, positive semidefinite with a trace of 1. The proof of these properties are in 4.1.

$$\begin{aligned}\rho^\dagger &= \rho \\ \rho &\geq 0 \\ Tr\rho &= 1\end{aligned} \tag{6.3}$$

The density matrix is pure, whenever it can be expressed as

$$\rho = |\psi\rangle \langle\psi| . \tag{6.4}$$

Eq.(5.3) implies that ρ is diagonalizable and has eigenvalues p_a. The associated Shannon entropy is the von Neumann entropy:

$$S(\rho) = -Tr\rho \ln\rho = \langle -\ln\rho\rangle_\rho. \tag{6.5}$$

Since the trace is cyclic, the entanglement entropy is invariant under unitary transformations of the form

$$S(U\rho U^\dagger) = S(\rho). \tag{6.6}$$

Let us consider a bipartite Hilbert space $\mathcal{H}_{AB}$ such that

$$\mathcal{H}_{AB} = \mathcal{H}_A \otimes \mathcal{H}_B. \tag{6.7}$$

The reduced density matrix ρ_A which can give the expectation values of operators of the form $\mathcal{O}_A \otimes I_B$ is the partial trace of ρ_{AB}

$$\rho_A := Tr_B \rho_{AB}. \tag{6.8}$$

For a pure state, ρ_{AB} is a tensor product $\rho_{AB} = \rho_A \otimes \rho_B$, the correlation functions of operators on A and B vanish:

$$\langle \mathcal{O}_A \otimes \mathcal{O}_B\rangle_{\rho_{AB}} - \langle \mathcal{O}_A\rangle_{\rho_A} \langle \mathcal{O}_B\rangle_{\rho_B} = 0. \tag{6.9}$$

The von Neumann entropy is extensive and subadditive:

$$\begin{aligned}\rho_{AB} = \rho_A \otimes \rho_B &\iff S(AB) = S(A) + S(B), \\ \rho_{AB} \neq \rho_A \otimes \rho_B &\iff S(AB) < S(A) + S(B).\end{aligned} \tag{6.10}$$

The mutual information is defined as

$$I(A:B) := S(A) + S(B) - S(AB). \tag{6.11}$$

The mutual information also bounds correlators

$$\frac{1}{2}\left(\frac{\langle \mathcal{O}_A \otimes \mathcal{O}_B\rangle - \langle \mathcal{O}_A\rangle\langle \mathcal{O}_B\rangle}{\|\mathcal{O}_A\|\|\mathcal{O}_B\|}\right)^2 \leq I(A:B). \tag{6.12}$$

The mutual information does not decrease upon adjoining systems, i.e.,

$$I(A:BC) \geq I(A:B). \tag{6.13}$$

The entropy satisfies three inequalities, strong subadditivity, Araki-Lieb inequality, and the second form of strong subadditivity, respectively, by adjoining a system C:

$$\begin{aligned} S(AB) + S(BC) &\geq S(B) + S(ABC), \\ S(AB) + S(BC) &\geq S(A) + S(C), \\ S(AB) &\geq |S(A) - S(B)|. \end{aligned} \tag{6.14}$$

When AB is pure,

$$S(A) = S(B). \tag{6.15}$$

ρ_A is a Gibbs state in terms of modular Hamiltonian H_A,

$$\rho_A = \frac{1}{Z} e^{-H_A}. \tag{6.16}$$

Eq.(5.5) also implies

$$S(A) = \langle H_A\rangle + \ln Z. \tag{6.17}$$

Eq.(5.16) tell us that we can think of any state as being in a canonical ensemble which will allow us to use statistical physics. The spectrum of H_A is also called the entanglement spectrum.

6.3 Entropy of two coupled harmonic oscillators

Let $|\psi\rangle$ be an arbitrary state of the composite system; we will expand it in terms of basis vectors $|x_{in}\rangle$ in H_{in} and $|x_{out}\rangle$ in H_{out}. Here, $|x_{in}\rangle$ represents the position basis in a single harmonic oscillator in H_{in} and $|x_{out}\rangle$ represents a position basis for a single harmonic oscillator in H_{out}.
The normal coordinates are defined as follows:

$$\begin{aligned} x\pm &= \frac{1}{\sqrt{2}}\left(x_{in} \pm x_{out}\right), \\ \omega_+ &= \sqrt{k_0}, \\ \omega_- &= \sqrt{k_0 + 2k_1}, \\ p\pm &= \frac{1}{\sqrt{2}}\left(p_{in} + p_{out}\right). \end{aligned} \tag{6.18}$$

The Hamiltonian for a coupled harmonic oscillator is

$$H = \frac{1}{2}\left[p_{in}^2 + p_{out}^2 + k_0\left(x_{in}^2 + x_{out}^2\right) + k_1\left(x_{in} - x_{out}^2\right)\right]. \tag{6.19}$$

Under coordinate transformation, the Hamiltonian becomes:

$$H = \frac{1}{2}\left(p_+^2 + p_-^2 + \omega_+^2 x +^2 \omega_-^2 x_-^2\right). \tag{6.20}$$

The normalized ground state wave function for entangled coupled oscillators of the composite system are given by[8]

$$\psi_0\left(x_{in}, x_{out}\right) = \pi^{-\frac{1}{2}}\left(\omega_-\omega_+\right)^{1/4} \exp\left(-\frac{\omega_+ x_+^2 + \omega_- x_-^2}{2}\right). \tag{6.21}$$

$$|\psi\rangle = \int dx_{in} \int dx_{out} \psi\left(x_{in}, x_{out}\right) |x_{in}\rangle \, |x_{out}\rangle \tag{6.22}$$

Here, $\psi\left(x_{in}, x_{out}\right)$ wave function in position space. Similarly, we can write the ground state as

$$|\psi_0\rangle = \int dx_{in} \int dx_{out} \psi_0\left(x_{in}, x_{out}\right) |x_{in}\rangle \, |x_{out}\rangle \, . \tag{6.23}$$

Hence,

$$\rho_0 = |\psi_0\rangle \langle\psi_0| \tag{6.24}$$

$$= \int dx_{in} \int dx_{out} \int dx'_{in} \int dx'_{out} \psi_0\left(x_{in}, x_{out}\right) \psi_0^*\left(x'_{in}, x'_{out}\right) |x_{in}\rangle \, |x_{out}\rangle \left\langle x'_{in}\right| \left\langle x'_{out}\right| .$$

Since, an operator $O = O_{in} \otimes O_{out}$ is a tensor product of subsystems [27],

$$\begin{aligned} Tr_{in}(O) &= O_{out} Tr\left(O_{in}\right) \\ Tr_{in}\left(|x_{in}\rangle \, |x_{out}\rangle \left\langle x'_{in}\right| \left\langle x'_{out}\right|\right) &= Tr_{in}\left(|x_{in}\rangle \left\langle x'_{in}\right| \otimes |x_{out}\rangle \left\langle x'_{out}\right|\right) \\ &= |x_{out}\rangle \left\langle x'_{out}\right| Tr\left(|x_{in}\rangle \left\langle x'_{in}\right|\right) \\ &= |x_{out}\rangle \left\langle x'_{out}\right| \delta\left(x_{in} - x'_{in}\right), \end{aligned} \tag{6.25}$$

and

$$\rho_{out} = Tr_{in}\left(\rho_0\right)$$

$$= \int dx_{in} \int dx_{out} \int dx'_{in} \int dx'_{out} \psi_0\left(x_{in}, x_{out}\right) \psi_0^*\left(x'_{in}, x'_{out}\right) |x_{out}\rangle \left\langle x'_{out}\right| \delta\left(x_{in} - x'_{in}\right)$$

$$= \int dx_{in} \int dx_{out} \int dx'_{out} \psi_0\left(x_{in}, x_{out}\right) \psi_0^*\left(x'_{in}, x'_{out}\right) |x_{out}\rangle \left\langle x'_{out}\right| . \tag{6.26}$$

The matrix elements are $\rho_{out}\left(x_{out}, x'_{out}\right) = \langle x_{out}| \rho_0 \left|x'_{out}\right\rangle$, which kills the 'out' integrals of(5.7). Writing the integral with limits:

$$\begin{aligned} \rho_{out}\left(x_{out}, x'_{out}\right) &= \int_{-\infty}^{+\infty} dx_{in} \psi_0\left(x_{in}, x_{out}\right) \psi_0^*\left(x_{in}, x'_{out}\right) \\ &= \int_{-\infty}^{+\infty} dx_{in} \frac{\sqrt{\omega_+\omega_-}}{\pi} \exp\left[\frac{w_+ + w_-}{2} x_{in}^2 + \right. \\ &\left(\frac{\omega_- x_{out}}{2} - \frac{\omega_+ x_{out}}{2} + \frac{\omega_- x'_{out}}{2} - \frac{\omega_+ x_{out}}{2}\right) x_{in} \\ &\left. - \frac{\omega_+ + \omega_-}{4} x_{out}'^2\right], \end{aligned} \tag{6.27}$$

where we used the Gaussian integral from (A.1). Defining constants β and γ such that:

$$\begin{aligned} \beta &= \frac{1}{4}\frac{(\omega_+ - \omega_-)^2}{\omega_+ + \omega_-}, \\ \gamma - \beta &= \frac{2\omega_+\omega_-}{\omega_+ + \omega_-}. \end{aligned} \tag{6.28}$$

The matrix elements become

$$\rho_{out}(x_{out}, x'_{out}) = \sqrt{\frac{\gamma-\beta}{\pi}} \exp\left[-\frac{\gamma}{2}\left(x^2_{out} + x'^2_{out}\right) + \beta x_{out} x'_{out}\right]. \tag{6.29}$$

Since, entropy can be described in terms of eigenvalues, p_n of ρ_{out}, we want to solve the eigenvalue equation

$$\int_{-\infty}^{+\infty} dx' \rho_{out}(x, x) f_n(x') = p_n f_n(x). \tag{6.30}$$

The solution to the equation is quite easily found by guessing[30]:

$$\begin{aligned} p_n &= (1-\xi)\xi^n, \\ f_n(x) &= H_n(\sqrt{\alpha}x) \exp\left(-\frac{\alpha x^2}{2}\right), \end{aligned} \tag{6.31}$$

where H_n is a Hermite polynomial of nth degree, and

$$\begin{aligned} \alpha &= \sqrt{\gamma^2 - \beta^2} = \sqrt{\omega_+\omega_-}, \\ \xi &= \frac{\beta}{\gamma + \alpha}. \end{aligned} \tag{6.32}$$

It can be inferred that ρ_{out} is equivalent to a thermal density matrix for a simple harmonic oscillator with a frequency of α and a temperature of $T = -\frac{\alpha}{\ln(\xi)}$ with the help equation(5.16).
The entanglement entropy can be expressed in terms of eigenvalues of ρ_{out}

$$\begin{aligned} S &= \sum_{n=0}^{\infty} p_n \ln p_n \\ &= -\frac{\xi \ln \xi + (1-\xi)\ln(1-\xi)}{1-\xi} \\ &= -\left[\frac{\xi}{1-\xi}\ln\xi + \ln(1-\xi)\right] \end{aligned} \tag{6.33}$$

It should be noted that since ξ is a function of K_1/k_0, so is the entanglement entropy.

6.4 Generalization to N-coupled harmonic oscillators

The Hamiltonian for the oscillator is

$$H = \frac{1}{2}\sum_{i=1}^{N} p_i^2 + \frac{1}{2}\sum_{i,j}^{N} x_i K_{ij} x_j, \tag{6.34}$$

where K is a real $N \times N$ symmetric positive matrix; hence, it is Hermitian with positive eigenvalues. If K_D is a diagonal matrix and U is orthoginal, then K can be expressed as $K = U^T K_D U$. Therefore, the square root of K is $\Omega = U^T K_D^{\frac{1}{2}} U$. The normalised ground state wave function for N-coupled oscillators:

$$\psi_0 (x_1, ..., x_n) = \pi^{-\frac{N}{4}} (det\Omega)^{\frac{1}{4}} \exp\left(-\frac{x \cdot \Omega \cdot x}{2}\right). \tag{6.35}$$

Tracing over the first n, which is analogous to the "inside" case for 2-coupled oscillators, yields ρ_{out}:

$$\begin{aligned} &\rho_{out} \left(x_{n+1}, x_{n+2}, ..., x_N; x'_{n+1}, x'_{n+2}, ..., x'_N x\right) = \\ &\int \prod_{i=1}^{n} dx_i \psi_0 \left(x_1, ..., x_n, x_{n+1}, .., x_N\right) \psi_0^* \left(x_1, ..., x_n, x'_{n+1}, ..., x'_N\right). \end{aligned} \tag{6.36}$$

We can write Ω in terms of matrices A, B and C, where A is $n \times n$, B and C are $(N-n) \times (N-n)$.

$$\Omega = \begin{pmatrix} A & B \\ B^T & C \end{pmatrix} \tag{6.37}$$

The integral is now evaluated with higher dimensional Gaussian Integral (A.3); hence, ρ_{out} is

$$\rho_{out}(x, x') \sim \exp\left(-\frac{x^T \cdot \gamma \cdot x + x'^T \cdot \gamma \cdot x'}{2} + x^T \cdot \beta \cdot x'\right). \tag{6.38}$$

Now x has $N - n$ components and $\beta = \frac{1}{2} B^T A^{-1} B$. Since, β and γ do not commute, equation(5.23) does not represent a thermal density matrix for a system of oscillators. The generalization of Eq. (5.14) implies that $(detG)\rho_{out}(Gx, Gx')$ and $\rho_{out}(x, x')$ share the same eigenvalues as $\rho_{out}(x, x')$, when G is a non-singular matrix. Let $x = \gamma^{-\frac{1}{2}} y$ and $\beta' = \gamma^{-\frac{1}{2}} \beta \gamma^{-\frac{1}{2}}$. This leads to

$$\rho_{out}(y, y') \sim \exp\left[-\frac{y.y + y'.y'}{2} + y \cdot \beta' \cdot y'\right]. \tag{6.39}$$

Let $y = Wz$, where W is orthogonal with $W^T \beta' W$ diagonal and β_i is the eigenvalue of β, then

$$\rho_{out}\left(z, z'\right) \sim \prod_{i=n+1}^{N} \exp\left(-\frac{z_i^2 + z_i'^2}{2} + \beta'_i z_i z'_i\right). \tag{6.40}$$

This is the same equation as Eq.(5.13) if $\gamma \to 1$ and $\beta \to \beta'_i$. Hence, the entropy is found by adding individual entropies associated with β_i the help of Eq. (5.17) with $\xi_i = \frac{\beta'_i}{1+\left(1-\beta_i'^2\right)^{\frac{1}{2}}}$,

$$S = \sum_i S\left(\xi_i\right). \tag{6.41}$$

6.5 Generalization for a Quantum Field

This result can be generalized for the Hamiltonian of a quantum field.

$$H = \frac{1}{2}\int dx^3 \left(\pi^2(\vec{x}) + |\boldsymbol{\nabla}\cdot\varphi(\vec{x})|^2\right). \tag{6.42}$$

If $x = |\vec{x}|$ and Z_{lm} are real spherical harmonics: $Z_{l0} = Y_{l0}$, $Z_{lm} = \sqrt{2}ReY_{lm}$ for $m > 0$, and $Z_{lm} = \sqrt{2}ImY_{lm}$ for $m < 0$. The wave partial wave components are

$$\begin{aligned}\varphi_{lm}(x) &= x\int d\Omega Z_{lm}(\theta,\phi)\phi(\vec{x})\\ \pi_{lm}(x) &= x\int d\Omega, Z_{lm}(\theta,\phi)\,\pi(\vec{x}).\end{aligned} \tag{6.43}$$

These operators are Hermitian and obey the canonical commutation relations in natural units,

$$[\varphi_{lm}(x), \pi_{l'm'}(x)] = i\delta_{ll'}\delta_{mm'}\delta(x - x'). \tag{6.44}$$

We can define H_{lm} such that $H = \sum_{lm} H_{lm}$:

$$H_{lm} = \frac{1}{2}\int_0^\infty dx\{\pi_{lm}^2(x) + x^2\left[\frac{\partial}{\partial x}\left(\frac{\varphi(x)}{x}\right)\right]^2 + \frac{l(l+1)}{x^2}\varphi^2(x)\}. \tag{6.45}$$

Now, we impose the constraints due to ultraviolet and infrared cutoff. Transforming from the radial coordinate x to the lattice coordinate where each point has a separation length of a, which is the inverse ultraviolet cutoff. This implies $M = a^{-1}$. Let $L = (N+1)a$, where N is a large integer such that $\varphi_{lm}(x)$ vanishes when $x \geq L$ which implies that L^{-1} is the infrared cutoff so that

$$H_{lm} = \frac{1}{2a}\sum_{j=1}^{N}\left[\pi_{lm,j}^2 + \left(j+\frac{1}{2}\right)^2\left(\frac{\varphi_{lm,j}}{j} - \frac{\varphi_{lm,j+1}}{j+1}\right)^2 + \frac{l(l+1)}{j^2}\varphi_{lm,j}^2\right]. \tag{6.46}$$

Here, $\varphi lm, N+1 = 0$,$\phi_{lm,j}$ and $\pi lm, j$ are hermitian and dimensionless. They also satisfy the commutation relationship

$$\left[\varphi_{lm,j}, \pi_{l'm',j'}\right] = i\delta_{ll'}\delta_{mm'}\delta_{jj'}. \tag{6.47}$$

H_{lm} has the same form of Eq.(5.35). Therefore, we can numerically compute the entropy $S_{lm}(n,N)$ by tracing over the ground state of H_{lm}. Hence, the total entropy is $S = \sum_{lm} S_{lm}(n,N)$. Eq.(5.35) also implies that H_{lm} is independent of l, so $S_l(n,N) = S_{lm}(n,N)$. Summing over all values of m is $2l+1$, which gives the total entropy as $S = \sum_l (2l+1)S_l(n,N)$. When $l >> N$, $S_l(n,N)$ is computed perturbatively as follows:

$$\begin{aligned}S_l(n,N) &= \xi_l(n)\left[-\ln\xi_l(n) + 1\right],\\ \xi_(n) &= \frac{n(n+1)(2n+1)^2}{64l^2(l+1)^2} + O\left(l^{-6}\right).\end{aligned} \tag{6.48}$$

The graph in 6.1 demonstrate the situation where the $R = (n+\frac{1}{2})a$ and $S(n,N)$ as a function of R^2 are calculated for $1 \leq n \leq 30$ and $N = 60$. The points fit equation of a straight line $S = 0.3M^2R^2$.

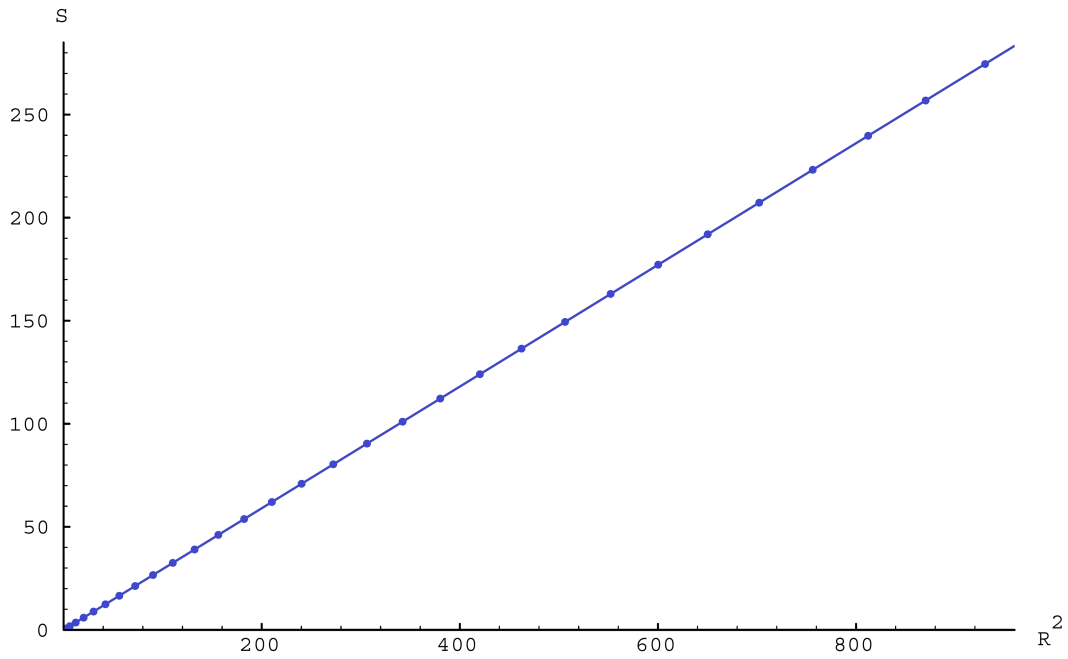

Figure 6.1: The entropy S found by tracing the degrees of freedom inside a sphere of radius R. The graph connecting the points is a straight line[30].

6.6 Connection with the Entropy of a Black Hole

The above calculations show that the entropy is independent of the information contained inside the sphere. Generalization of this calculation is that for any black hole which resides in a 3-dimensional space, it must have entropy, which depends on a quantity of one lower dimension, i.e., the area. This interpretation agrees very well with the formula for the intrinsic entropy of a black hole, $S_{BH} = \frac{1}{4} M_{Pl}^2 A$, where M_{Pl} is the Planck Mass, and A is the surface area of the black hole.

Chapter 7

Entanglement Entropy of the Quenched Double Oscillator

7.1 The Quenched Hamiltonian

In this section we review the calculation as done by Ali and Moynihan on the entanglement entropy of the quenched double oscillator [3] which we plan to generalize to the N oscillator case in the next chapter (8) for our calculation. We briefly review the setup, calculations and the results from this paper below.

In the double oscillator case the non-interacting hamiltonian is

$$H_1 = \frac{1}{2}(p_x^2 + p_y^2) + \frac{\omega^2}{2}(x^2 + y^2). \tag{7.1}$$

The ground state of this hamiltonian in the position basis is

$$\psi_o(x, y) = \sqrt{\frac{\omega}{\pi}} \exp\Big[-\frac{\omega}{2}(x^2 + y^2)\Big]. \tag{7.2}$$

When the double oscillator is quenched at $t = 0$, it has an interaction term and the new hamiltonian is

$$H_2 = \frac{1}{2}(p_x^2 + p_y^2) + \frac{\omega^2}{2}(x^2 + y^2) + \lambda xy. \tag{7.3}$$

Due to the interaction term being quadratic, the ground state is found by switching to normal coordinates using the position and momentum operators $z_\pm = \frac{1}{\sqrt{2}}(x \pm y)$ and $p_\pm = \frac{1}{\sqrt{2}}(p_x + p_y)$ respectively. This gives us the hamiltonian H_2 in the new coordinates

$$H_2 = \frac{1}{2}(p_+^2 + p_-^2)^2 + \frac{\omega_+^2 z_+^2}{2} + \frac{\omega_-^2 z_-^2}{2}, \tag{7.4}$$

where $\omega_\pm = \sqrt{\omega^2 \pm \lambda}$ The ground state oh H_1 which is $\psi_0(x, y)$ in the normal coordinates is now

$$\psi_0(z_+, z_-) = \sqrt{\frac{\omega}{\pi}} \exp\Big\{[-\frac{\omega}{2}(z_+^2 + z_-^2)]\Big\}. \tag{7.5}$$

7.2 The State After a Quench

We can time evolve this ground state

$$|\psi_1(t)\rangle = e^{-iH_2 t}\,|\psi_0\rangle\,. \tag{7.6}$$

This gives us

$$\begin{aligned}\psi_1(z_+,z_-,t) &= \langle z_+,z_-|\,e^{-iH_2 t}\,|\psi_0\rangle \\ &= \int dz'_+dz'_-K(z_+,z_-;z'_+,z'_-;z'_+,z'_-;t)\psi_0(z'_+,z'_-),\end{aligned} \tag{7.7}$$

where $K(z_+,z_-;z'_+,z'_-;z'_+,z'_-;t)$ is the propagator for the double oscillator. In normal coordinates this propagator can be written as a product of propagators of two single free oscillators:

$$K(z_+,z_-;z'_+,z'_-;z'_+,z'_-;t) = K(z_+,t;z'_+,,0)K(z_-,t;z'_-,0). \tag{7.8}$$

Where the propagator

$$K(z_+,t;z'_+,0) = \sqrt{\frac{\omega_+}{2\pi i\sin\omega_+ t}}\exp\left[\frac{i\omega_+}{2\sin\omega_+ t}\{(z_+^2+z_+'^2)\cos\omega_+ t - 2z_+z'_+\}\right], \tag{7.9}$$

and similarly

$$K(z_-,t;z'_-,0) = \sqrt{\frac{\omega_-}{2\pi i\sin\omega_- t}}\exp\left[\frac{i\omega_-}{2\sin\omega_- t}\{(z_-^2+z_-'^2)\cos\omega_- t - 2z_-z'_-\}\right]. \tag{7.10}$$

Substituting these expressions into (7.7) and carrying out Gaussian integrals for the z'_+ and z'_- using (A.1) we obtain

$$\psi_1 = \mathcal{N}\exp\left\{\frac{(x^2+y^2)}{2}(\alpha_+ + \alpha_-) + xy(\alpha_+ - \alpha_-)\right\}, \tag{7.11}$$

where $\mathcal{N}$ is a time dependent constant that we have defined as

$$\mathcal{N} = \sqrt{\frac{\omega}{\pi}}\sqrt{\frac{-\omega_+\omega_-}{\sin\omega_+ t\sin\omega_- t}}\frac{1}{\sqrt{(\omega - i\omega_+\cot\omega_+ t)(\omega - i\omega_-\cot\omega_- t)}} \tag{7.12}$$

and

$$\alpha_\pm = \frac{1}{2}\left\{i\omega_\pm\cot\omega_\pm t - \frac{\omega_\pm^2}{\omega\sin^2\omega_\pm t - i\omega_\pm\cos\omega_\pm\cos\omega_\pm t\sin\omega_\pm t}\right\}. \tag{7.13}$$

7.3 The Density Operator

For this pure state, ψ_1, we have the density operator

$$\begin{aligned}\rho(x,y;x',y') &= \psi_1(x,y)\psi_1^*(x',y') \\ &= |\mathcal{N}|\exp\left\{\frac{x^2+y^2}{2}(\alpha_+ + \alpha_-) + xy(\alpha_+ - \alpha_-)\right\} \\ &\quad\times\exp\left\{\frac{x'^2+y'^2}{2}(\alpha_+^* + \alpha_-^*) + x'y'(\alpha_+^* - \alpha_-^*)\right\}.\end{aligned} \tag{7.14}$$

7.4 The Reduced Density Operator

We can now find the reduced density operator with position x by setting $y = y'$ and integrating with respect to y. This gives

$$\begin{aligned}\rho_{out}(x,x') &= \int dy \rho(x,y;x',y) \\ &= \overline{\mathcal{N}} \exp\{\Lambda x^2 - \Lambda^* x'^2 + \Gamma x x'\},\end{aligned} \tag{7.15}$$

where we have defined

$$\begin{aligned}\Lambda &= -\frac{1}{2}(\alpha_+ + \alpha_-) + \frac{1}{4}\frac{(\alpha_+ - \alpha_-)^2}{\mathrm{Re}(\alpha_+ + \alpha_-)}, \\ \Lambda^* &= -\frac{1}{2}(\alpha_+^* + \alpha_-^*) + \frac{1}{4}\frac{(\alpha_+^* - \alpha_-^*)^2}{\mathrm{Re}(\alpha_+^* + \alpha_-^*)}, \\ \Gamma &= -\frac{1}{2}\frac{|\alpha_+ + \alpha_-|^2}{\mathrm{Re}(\alpha_+ + \alpha_-)}, \\ \overline{\mathcal{N}} &= i|\mathcal{N}|^2\sqrt{\frac{\pi}{\mathrm{Re}(\alpha_+ + \alpha_-)}}.\end{aligned} \tag{7.16}$$

7.5 The Eigenvalue Problem

In the eigenbasis of ρ_{out}

$$\rho_{out}\left|m\right\rangle = \lambda_m \left|m\right\rangle, \tag{7.17}$$

$$\overline{\rho}_{out} = \frac{\rho_{out}}{Tr\rho_{out}}, \tag{7.18}$$

$$\begin{aligned}Tr\rho_{out} &= \sum_{i=0}^{\infty} \left\langle m\right| \rho_{out} \left|m\right\rangle \\ &= \sum_{i=0}^{\infty} \lambda_m \left\langle m|m\right\rangle \\ &= \sum_{i=0}^{\infty} \lambda_m.\end{aligned} \tag{7.19}$$

We want to find the eigenvalues of the normalized reduced density operator,

$$\begin{aligned}\overline{\rho}_{out}\left|m\right\rangle &= \frac{\rho_{out}}{\sum_{i=0}^{\infty}\lambda_m}\left|m\right\rangle \\ &= \frac{\lambda_m}{\sum_{i=0}^{\infty}\lambda_m}\left|m\right\rangle \\ &= p_m \left|l\right\rangle.\end{aligned} \tag{7.20}$$

Here,

$$p_m = \frac{\lambda_m}{\sum_{i=0}^{\infty}\lambda_m} \quad and \quad \sum_{i=0}^{\infty} p_m = 1. \tag{7.21}$$

7.6 The Eigenvalues and the Eigenfunctions

We will adopt Srednicki's eigenfunction ansatz

$$f_m(x) = C_m H_m\left(\sqrt{a}x\right) \exp\left(-\frac{b}{2}x^2\right), \tag{7.22}$$

where C_m are the normalization constants and H_m are the Hermite polynomiads of degree m. Furthermore, we will use the contour-integral representation of Hermite polynomials,

$$H_m\left(\sqrt{a}x'\right) = \frac{m!}{2\pi i}\oint_C \frac{\exp\left(2t\sqrt{a}x' - t^2\right)}{t^{n+1}}dt. \tag{7.23}$$

After doing the integral in x', we have

$$\frac{\overline{\mathcal{N}}C_m m!}{2\pi i}\sqrt{\frac{\pi}{\Lambda^* + b/2}}\oint_C dt \exp\left[\frac{\left(\Gamma x + 2t\sqrt{a}\right)^2}{4\left(\Lambda^* + \frac{b}{2}\right)}\right]\frac{\exp\left(-t^2\right)}{t^{n+1}}, \tag{7.24}$$

which must be proportional to $\exp\left(-\frac{b}{2}x^2\right)$:

$$-\Gamma + \frac{\Gamma^2}{4\left(\Lambda^* + \frac{b}{2}\right)} = -\frac{b}{2}. \tag{7.25}$$

This is a quadratic equation in terms b, for which we will take the positive square root to ensure that entanglement entropy is non-negative,

$$b = (\Lambda - \Lambda^*) + \sqrt{(\Lambda^* + \Lambda)^2 - \Gamma^2}. \tag{7.26}$$

Now, let us define the remaining parts of equation (7.24), which has to be proportional to $H_m\left(\sqrt{a}x'\right)$

$$\mathcal{X}_m = \frac{m!}{2\pi i}\oint_C dt \frac{\exp\left(-t^2\right)}{t^{n+1}}\exp\left(\frac{4t^2 a + 4t\sqrt{a}\Gamma x}{4\Lambda^* + 2b}\right). \tag{7.27}$$

We will do a variable transformation such that

$$\tau = \frac{t\Gamma}{2\Lambda^* + b}. \tag{7.28}$$

Using (7.28) we have,

$$\mathcal{X}_m = \left(\frac{\Gamma}{2\Lambda^* + b}\right)^m \frac{m!}{2\pi i}\oint_C d\tau \frac{\exp\left(2\tau\sqrt{a}x - \tau^2\right)}{\tau^{n+1}}. \tag{7.29}$$

Hence, to ensure proportionality, we have the following equation,

$$\left(\frac{2\Lambda^* + b}{\Gamma}\right)^2\left[\frac{4\Lambda^* + 2b - 4a}{4\Lambda^* + 2b}\right] = 1. \tag{7.30}$$

The solution of equation (7.30) is

$$a = \frac{(2\Lambda^* + b)}{2}\left[1 - \left(\frac{\Gamma}{2\Lambda^* + b}\right)^2\right]. \tag{7.31}$$

Now, we have solved the eigenvalue equation:

$$\int dx' \rho_{out}\left(x, x'\right) f_m\left(x'\right) = \overline{\mathcal{N}}\left(\frac{\Gamma}{2\Lambda^* + b}\right)^m f_m\left(x\right). \tag{7.32}$$

Therefore, the unnormalized eigenvalues are

$$\lambda_m = \frac{\overline{\mathcal{N}}\Gamma^n}{(2\Lambda^* + b)^n}. \tag{7.33}$$

To get the normalized eigenvalues, we use equation (7.21),

$$p_m = \beta^m\left(1 - \beta\right). \tag{7.34}$$

where β is

$$\begin{aligned} \beta &= \frac{\Gamma}{2\Lambda^* + b} \\ &= \frac{\Gamma}{\Lambda + \Lambda^* + \sqrt{(\Lambda^* + \Lambda) - \Gamma^2}}. \end{aligned} \tag{7.35}$$

In order to carry out the infinite sum to get (7.34), we have to impose the following constraint:

$$\Lambda + \Lambda^* > \Gamma, \tag{7.36}$$

so that $|\beta| < 1$.

7.7 The Entanglement Entropy

The entanglement entropy is now given in terms of β,

$$\begin{aligned} S_{EE} &= -\sum_{m=0}^{\infty} p_m \ln\left(p_m\right) \\ &= -\frac{\beta\ln\left(\beta\right) + \left(1-\beta\right)\ln\left(1-\beta\right)}{1-\beta}. \end{aligned} \tag{7.37}$$

In the following section 7.8, we will show how the entanglement entropy can be represented graphically due to its time-dependence. We used the source code for producing the result from Ali and Moynihan.

7.8 Graphical Representation for the Quenched Double Oscillator

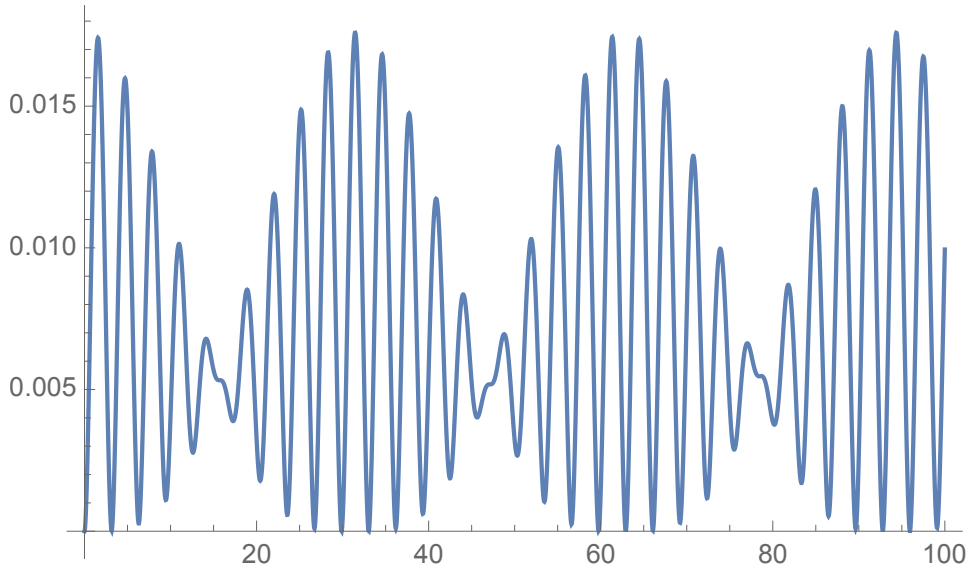

Figure 7.1: The entanglement entropy when $N = 2$, $\omega = 1$ and $\lambda = 0.1$[3].

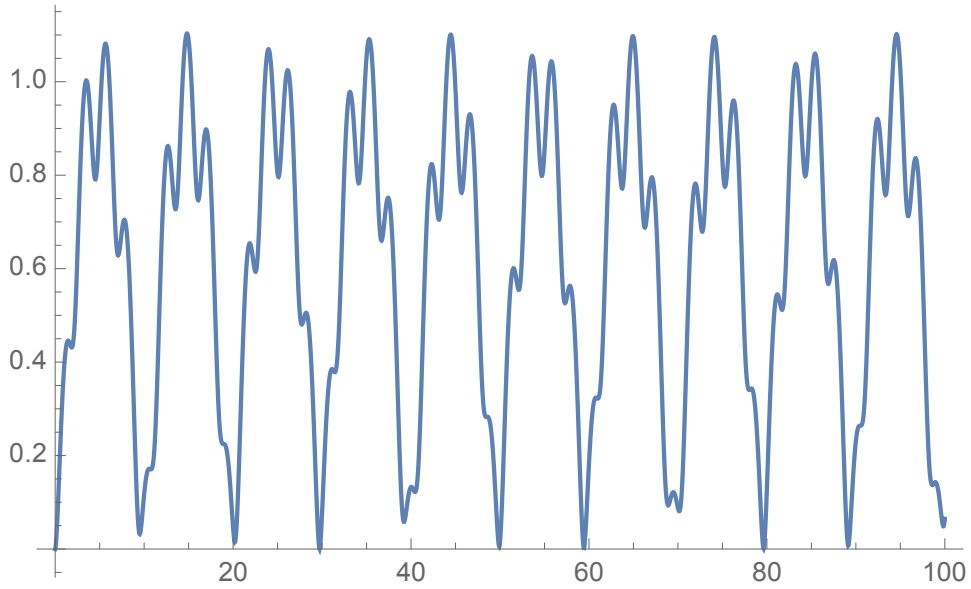

Figure 7.2: The entanglement entropy when $N = 2$, $\omega = 1$ and $\lambda = 0.9$[3].

Chapter 8

Calculation of Entropy of Quenched N-Oscillators

8.1 Time Evolution of a Sudden Quench

We will start with the Hamiltonian for non-interacting N harmonic oscillators, whose Hamiltonian is given by,

$$H_1 = \frac{1}{2}\sum_{a=0}^{N-1}\left(p_a^2 + \omega^2 x_a^2\right). \tag{8.1}$$

The Hamiltonian for a free field theory on a discretized circular lattice is [2]

$$H_2 = \frac{1}{2}\sum_{a=0}^{N-1}\left(p_a^2 + \omega^2 x_a^2 + \Omega^2 x_a x_{a+1}\right), \tag{8.2}$$

where we define the boundary conditions that $x_a = x_{a+N}$. We will decouple the Hamiltonian in terms of normal modes obtained by a discrete Fourier transform [15],

$$\tilde{x}_k = \frac{1}{\sqrt{N}}\sum_{a=0}^{N-1}\exp\left(-\frac{2\pi i k}{N}a\right)x_a \quad \tilde{p}_k = \frac{1}{\sqrt{N}}\sum_{a=0}^{N-1}\exp\left(\frac{2\pi i k}{N}a\right)p_a, \tag{8.3}$$

and

$$\tilde{\omega}_k^2 = \omega^2 + \Omega^2\cos\frac{2\pi k}{N}. \tag{8.4}$$

The reason for choosing the opposite signs in (8.3) is to produce the conventional canonical commutation relationships $[\tilde{x}_k, \tilde{p}_{k'}] = i\delta_{k,k'}$ and $[\tilde{x}_k, \tilde{x}_{k'}] = [\tilde{p}_k, \tilde{p}_{k'}] = 0$. The Fourier transformation results in the following normal mode Hamiltonian,

$$H_2 = \frac{1}{2}\sum_{k=0}^{N-1}\left(|\tilde{p}_k|^2 + \tilde{\omega}_k^2|\tilde{x}_k|^2\right). \tag{8.5}$$

The ground state wave function for H_1 (8.1) above is

$$\psi_0(x_0, ..., x_{N-1}) = \prod_{a=0}^{N-1}\left(\frac{\omega}{\pi}\right)^{\frac{1}{4}}\exp\left(-\frac{1}{2}\omega x_a^2\right). \tag{8.6}$$

We will define the vectors x and $\tilde{x}$

$$\begin{aligned} x &= (x_0, x_1, \ldots, x_{n-1})^T, \\ \tilde{x} &= (\tilde{x}_0, \tilde{x}_1, \ldots, \tilde{x}_{n-1})^T. \end{aligned} \tag{8.7}$$

The Fourier transformation in (8.3) is now described by the unitary matrix Λ, such that $\tilde{x} = \Lambda x$ and $\tilde{x}^\dagger = x^T \Lambda^\dagger$, where Λ is defined by its elements, which is indexed from 0 to $N-1$, denoted by a and b

$$(\Lambda)_{ab} \equiv \frac{1}{\sqrt{N}} \exp\left(-\frac{2\pi i a b}{N}\right). \tag{8.8}$$

If we define column vectors of Λ as $|u_b\rangle$, then the row vectors of $\Lambda^\dagger$ is $\langle u_a|$. In order to prove that Λ is unitary, it is sufficient to show that $\langle u_a|u_b\rangle = \delta_{a,b}$.

$$\langle u_a|u_b\rangle = \frac{1}{N} \sum_{k=0}^{N-1} \exp\left(-\frac{2\pi i\,(a-b)}{N} k\right) \tag{8.9}$$

When $a = b$, $\langle u_a|u_b\rangle = 1$ and when $a \neq b$,

$$\begin{aligned} \langle u_a|u_b\rangle &= \frac{1}{N} \sum_{k=0}^{N-1} \exp\left(-\frac{2\pi i\,(a-b)}{N} k\right) \\ &= \frac{1}{N} \frac{1 - \exp\left[-2\pi i\,(a-b)\right]}{1 - \exp\left(-\frac{2\pi i (a-b)}{N}\right)} \\ &= 0 \end{aligned} \tag{8.10}$$

Hence, $\langle u_a|u_b\rangle = \delta_{a,b}$. Now, we can write the ground state wavefunction as

$$\begin{aligned} \psi_0 &= \left(\frac{\omega}{\pi}\right)^{\frac{N}{4}} \exp\left(-\frac{1}{2}\omega \sum_{a=0}^{N-1} x_a^2\right) \\ &= \left(\frac{\omega}{\pi}\right)^{\frac{N}{4}} \exp\left(-\frac{1}{2}\omega x^T x\right) \\ &= \left(\frac{\omega}{\pi}\right)^{\frac{N}{4}} \exp\left(-\frac{1}{2}\omega \tilde{x}^\dagger \Lambda \Lambda^\dagger \tilde{x}\right) \\ &= \prod_{a=0}^{N-1} \left(\frac{\omega}{\pi}\right)^{\frac{1}{4}} \exp\left(-\frac{1}{2}\omega |\tilde{x}_k|^2\right). \end{aligned} \tag{8.11}$$

To interpret the wave function consistently in both normal and position coordinates, we define the normalization scheme in normal coordinates.

$$\int \frac{d\tilde{x}_k^* d\tilde{x}_k}{-2\mu_k i} \psi_0\left(\tilde{x}_k\right)^* \psi_0\left(\tilde{x}_k\right) = 1, \tag{8.12}$$

where

$$\mu_k = \sqrt{\int \frac{d\tilde{x}_k^* d\tilde{x}_k}{-2i} \psi_0\left(\tilde{x}_k\right)^* \psi_0\left(\tilde{x}_k\right)}. \tag{8.13}$$

Now we are in a position to time evolve ψ_0 for the quenched Hamiltonian H_2. Our idea is to find the state's wavefunction after $t > 0$ from when there are interactions between the oscillators. The term "sudden quench" highlights the change from the non-interacting behaviors to interacting behaviors.

$$\begin{aligned}\Psi_1 &= \langle \tilde{x}_0, ..., \tilde{x}_{N-1}| \exp\left(-iH_2 t\right) |\psi_0\rangle \\ &= \int d\tilde{x} d\tilde{x}^\dagger K\left(\tilde{x}_0, .., \tilde{x}_{N-1}; \tilde{x}'_0, ..., \tilde{x}'_{N-1}\right) \psi_0,\end{aligned} \tag{8.14}$$

where the propagator K is the product of propagators of N free oscillators

$$K\left(\tilde{x}_0, .., \tilde{x}_{N-1}; \tilde{x}'_0, ..., \tilde{x}'_{N-1}\right) = \prod_{k=0}^{N-1} K\left(\tilde{x}_k, t; \tilde{x}'_k, 0\right), \tag{8.15}$$

where

$$\begin{aligned}K\left(\tilde{x}_k, t; \tilde{x}'_k, 0\right) = \sqrt{\frac{\tilde{\omega}_k}{2\pi i \sin\tilde{\omega}_k t}} \exp\Bigg[\frac{i\tilde{\omega}_k}{2\sin\tilde{\omega}_k t}\Big\{\left(|\tilde{x}_k|^2 + |\tilde{x}_k|'^2\right)\cos\tilde{\omega}_k t \\ - \tilde{x}_k \tilde{x}'^*_k - \tilde{x}^*_k \tilde{x}'_k\Big\}\Bigg],\end{aligned} \tag{8.16}$$

and

$$d\tilde{x} d\tilde{x}^\dagger = \prod_{i=0}^{N-1} \frac{d\tilde{x}_k d\tilde{x}^*_k}{-2\mu i}. \tag{8.17}$$

So we have the quenched state by solving the integral in equation (8.14) using (A.2) from appendix A:

$$\begin{aligned}\Psi_1 &= \mathcal{N} \prod_{k=0}^{N-1} \exp\left(\frac{i\tilde{\omega}_k |\tilde{x}_k|^2}{2}\cot\tilde{\omega}_k t - \frac{\omega_k^2 |\tilde{x}_k|^2}{2\left(\omega \sin^2\tilde{\omega}_k t - i\tilde{\omega}_k \cos\tilde{\omega}_k t \sin\tilde{\omega}_k t\right)}\right) \\ &= \mathcal{N} \prod_{k=0}^{N-1} \exp\left(-\frac{1}{2}\mathcal{Z}_k |\tilde{x}_k|^2\right),\end{aligned} \tag{8.18}$$

where $\mathcal{N}$ is a time-dependent constant which we have defined

$$\mathcal{N} = \prod_{k=0}^{N-1} \left(\frac{\tilde{\omega}_k}{\pi}\right)^{\frac{1}{4}} \sqrt{\frac{\tilde{\omega}_k}{2\pi i \sin\tilde{\omega}_k t}} \left(\omega - i\omega_k cot\omega_k t\right)^{-\frac{1}{2}} \tag{8.19}$$

and

$$\mathcal{Z}_k = -i\tilde{\omega}_k \cot\tilde{\omega}_k t + \frac{\omega_k^2}{\omega \sin^2\tilde{\omega}_k t - i\tilde{\omega}_k \cos\tilde{\omega}_k t \sin\tilde{\omega}_k t} \tag{8.20}$$

The real part of $\mathcal{Z}_k$ is positive as required by Ψ_1 to be square-integrable:

$$\mathrm{Re}\left(\mathcal{Z}_k\right) = \frac{\omega\tilde{\omega}_k^2}{\cos^2\left(\tilde{\omega}_k t\right) + \omega^2 \sin^2\left(\tilde{\omega}_k t\right)}. \tag{8.21}$$

Therefore, our quenched ground state is

$$\begin{aligned}\Psi_1 &= \mathcal{N}\prod_{k=0}^{N-1}\exp\left(-\frac{1}{2}\mathcal{Z}_k|\tilde{x}_k|^2\right)\\ &= \mathcal{N}\exp\left(-\frac{1}{2}\sum_{k=0}^{N-1}\mathcal{Z}_k|\tilde{x}_k|^2\right)\\ &= \mathcal{N}\exp\left(-\frac{1}{2}\tilde{x}^\dagger\mathcal{Z}_d\tilde{x}\right)\\ &= \mathcal{N}\exp\left(-\frac{1}{2}x^T\Lambda^\dagger\mathcal{Z}_d\Lambda x\right),\end{aligned} \tag{8.22}$$

where $\mathcal{Z}_d \equiv diag\left(\mathcal{Z}_0, \mathcal{Z}_1, ..., \mathcal{Z}_{N-1}\right)$. Now, we will define $\mathcal{Z} \equiv \Lambda^\dagger\mathcal{Z}_d\Lambda$ so that,

$$\Psi_1 = \mathcal{N}\exp\left(-\frac{1}{2}x^T\mathcal{Z}x\right). \tag{8.23}$$

Only the symmetric part of $\mathcal{Z}$ contributes to the quadratic term $x^T\mathcal{Z}x$ as $x^T\mathcal{Z}x = x^T\left[\frac{1}{2}\left(\mathcal{Z}+\mathcal{Z}^T\right)\right]x$. Hence, we will redefine $\mathcal{Z}$ as its symmetric part, i.e,

$$\mathcal{Z} \equiv \frac{1}{2}\left(\mathcal{Z}+\mathcal{Z}^T\right). \tag{8.24}$$

8.2 The Pure Density Operator and the Reduced Density Operators

The density operator associated with the pure state is

$$\begin{aligned}\rho\left(x,x'\right) &= \Psi_1\left(x\right)\Psi_1\left(x'\right)^*\\ &= |\mathcal{N}|^2\exp\left(-\frac{1}{2}x^T\mathcal{Z}x\right)\exp\left(-\frac{1}{2}x'^T\mathcal{Z}^*x'\right).\end{aligned} \tag{8.25}$$

The density operator can be thought of as an infinite dimensional matrix with indices x and x' with elements described by (8.25). It is Hermitian, as swapping x and x' and then performing a conjugation will keep it invariant:

$$\rho\left(x,x'\right) = \rho\left(x',x\right)^*. \tag{8.26}$$

Letting $x_i = x'_i$ where $i \in \{0, 1\ldots, n-1\}$ and $x' = (x_0, x_1\ldots, x_{n-1}, x'_m, \ldots x'_{N-1})$,

$$x = \begin{pmatrix}y & z\end{pmatrix}^T \quad and \quad x' = \begin{pmatrix}y & z'\end{pmatrix}^T. \tag{8.27}$$

As $\mathcal{Z}$ is symmetric,

$$\mathcal{Z} = \begin{pmatrix}A & C\\ C^T & B\end{pmatrix}, \tag{8.28}$$

$$\begin{aligned}x^T\mathcal{Z}x &= y^TAy + z^TC^Ty + y^TCz + z^TBz\\ &= y^TAy + 2z^TC^Ty + z^TBz,\\ x'^T\mathcal{Z}^*x' &= y^TA^*y + z'^TC^\dagger y + y^TC^*z' + z'^TB^*z'\\ &= y^TA^*y + 2z'^TC^\dagger y + z'^TB^*z'.\end{aligned} \tag{8.29}$$

To find the elements of the reduced density operator,

$$\begin{aligned}\rho_{out}(z,z') &= \int |\mathcal{N}|^2 \exp\left(-\frac{1}{2}y^T\left(A+A^*\right)y + \mathcal{J}^T y - \frac{1}{2}z^T B z - \frac{1}{2}z'^T B^* z'\right) dy \\ &= |\mathcal{N}|^2 \sqrt{\frac{(\pi)^n}{det\left(\mathrm{Re}\left(A\right)\right)}} \exp\left(\frac{1}{2}\mathcal{J}^T\alpha^{-1}\mathcal{J} - \frac{1}{2}z^T B z - \frac{1}{2}z'^T B^* z'\right) \\ &= \overline{\mathcal{N}} \exp\left(-\frac{1}{2}z^T\mathcal{A}z - \frac{1}{2}z'^T\mathcal{A}^* z' + z^T\Gamma z'\right),\end{aligned} \tag{8.30}$$

where

$$\begin{aligned}\alpha &= 2\,\mathrm{Re}\left(A\right), \\ \mathcal{J} &= -Cz - C^\dagger z', \\ \mathcal{A} &= B - C^T\alpha^{-1}C \\ \Gamma &= C^T\alpha^{-1}C^*, \\ \overline{\mathcal{N}} &= |\mathcal{N}|^2\sqrt{\frac{(2\pi)^n}{det\left(\alpha\right)}},\end{aligned} \tag{8.31}$$

and we used the Gaussian integral (A.3).

To show that the reduced density operator is Hermitian, we swap the indices and use the fact that Γ is Hermitian, $\Gamma^T = \Gamma^*$ and note that the expression remains the same:

$$\begin{aligned}z^T\Gamma z' &= \frac{1}{2}\left(z^T\Gamma z' + z'^T\Gamma^T z\right) \\ &= \frac{1}{2}\left(z^T\Gamma z' + z'^T\Gamma^* z\right).\end{aligned} \tag{8.32}$$

8.3 An Attempt to Diagonalize the Matrices in Reduced Density Operator

The first line of attack would be to diagonalize the matrices inside density operator. Diagonalization would have been possible had we, not time evolved, in which case $\mathcal{A} = \mathcal{A}^*$, and the operator would be identical to Srednicki's one [30]. Then it would be possible to diagonalize the operator in two steps. First we would do the basis transformation $z = \mathcal{A}^{-\frac{1}{2}}z_1$ and this would free up the first two quadratic terms, then an orthogonal transformation $z_1 = Oz_2$ such that $O^T\mathcal{A}^{-\frac{1}{2}}\Gamma\mathcal{A}^{-\frac{1}{2}}O$ is diagonal. However, as $\mathcal{A}$ has an imaginary component, with the transfromation $z = \mathcal{A}^{-\frac{1}{2}}z_1$, we will end up with

$$\rho_{out}\left(z_1, z_1'\right) = \overline{\mathcal{N}} \exp\left(-\frac{1}{2}z_1^T z_1 - \frac{1}{2}z_1'^T\mathcal{A}^{-\frac{1}{2}}\mathcal{A}^*\mathcal{A}^{-\frac{1}{2}}z_1' + z_1^T\mathcal{A}^{-\frac{1}{2}}\Gamma\mathcal{A}^{-\frac{1}{2}}z'\right). \tag{8.33}$$

We can diagonalize (8.33) if and only if $\mathcal{A}^{-\frac{1}{2}}\mathcal{A}^*\mathcal{A}^{-\frac{1}{2}}$ commutes with $\mathcal{A}^{-\frac{1}{2}}\Gamma\mathcal{A}^{-\frac{1}{2}}$. Since, they will not commute in general, we cannot proceed with this approach.

8.4 The Eigenvalue Problem

In the eigenbasis of ρ_{out}

$$\rho_{out} |m\rangle = \lambda_m |m\rangle , \tag{8.34}$$

$$\overline{\rho}_{out} = \frac{\rho_{out}}{Tr\rho_{out}}, \tag{8.35}$$

$$\begin{aligned} Tr\rho_{out} &= \sum_{i=0}^{\infty} \langle m| \rho_{out} |m\rangle \\ &= \sum_{i=0}^{\infty} \lambda_m \langle m|m\rangle \\ &= \sum_{i=0}^{\infty} \lambda_m. \end{aligned} \tag{8.36}$$

We want to find the eigenvalues of the normalized reduced density operator,

$$\begin{aligned} \overline{\rho}_{out} |m\rangle &= \frac{\rho_{out}}{\sum_{i=0}^{\infty} \lambda_m} |m\rangle \\ &= \frac{\lambda_m}{\sum_{i=0}^{\infty} \lambda_m} |m\rangle \\ &= p_m |l\rangle . \end{aligned} \tag{8.37}$$

Here,

$$p_m = \frac{\lambda_m}{\sum_{i=0}^{\infty} \lambda_m} \quad and \quad \sum_{i=0}^{\infty} p_m \quad = 1. \tag{8.38}$$

8.5 The Eigenfunctions and Eigenvalues

We attempt to solve the following integral equation, with the ansatz $f(z)_m$ we discovered,

$$\begin{gathered} \int \rho_{out} f(z')_m dz' = \lambda_m f(z)_m, \\ \overline{\mathcal{N}} \exp\left(-\frac{1}{2} z^T \mathcal{A} z\right) \int \exp\left(-\frac{1}{2} z'^T \mathcal{A}^* z' + z^T \Gamma z'\right) f(z')_m dz' = \lambda_m f(z)_m. \end{gathered} \tag{8.39}$$

In the following, $\mathcal{B}$, M and M' are time-dependent constant complex matrices.

$$\begin{aligned} f(z)_m &= C_m H_m (Mz) \exp\left[-\frac{1}{2} z^T (\mathcal{B} - \mathcal{A}^*) z\right] \\ V &= (v_m, v_{n+1}, ..., v_{N-1})^T \\ k &= N - n \\ \langle V \rangle &= \prod_{i=n}^{N-1} v_i^{m+1} \\ H(Mz)_m &\equiv \left(\frac{m!}{2\pi i}\right)^k \oint_C \frac{e^{2V^T Mz + V^T RV}}{\langle V \rangle} dV \\ \Lambda(V, z) &= \Gamma^T z + 2M^T V \end{aligned} \tag{8.40}$$

We will assume that $\mathcal{B}$ is a symmetric and positive definite matrix so that the following Gaussian integral is convergent, which is solved as follows:

$$\begin{aligned}&\oint_C \frac{e^{V^T R V}}{\langle V \rangle} \int \exp\left(-\frac{1}{2} z'^T \mathcal{B} z' + \left(\Gamma^T z + 2M^T V\right)^T z'\right) dz' dV \\ &= \sqrt{\frac{(2\pi)^k}{det\,(\mathcal{B})}} \oint_C \frac{e^{V^T R V}}{\langle V \rangle} \exp\left(\frac{1}{2} \Lambda^T (V,z)\, \mathcal{B}^{-1} \Lambda (V,z)\right) dV\end{aligned} \tag{8.41}$$

The term inside the exponential of equation (8.41)

$$\begin{aligned}\frac{1}{2}\Lambda^T (V,z)\, \mathcal{B}^{-1} \Lambda (V,z) &= \frac{1}{2}\left(\Gamma^T z + 2M^T V\right)^T \mathcal{B}^{-1} \left(\Gamma^T z + 2M^T V\right) \\ &= \frac{1}{2} z^T \Gamma \mathcal{B}^{-1} \Gamma^T z + z^T \Gamma \mathcal{B}^{-1} M^T V \\ &+ V^T M \mathcal{B}^{-1} \Gamma^T z + 2V^T M \mathcal{B}^{-1} M^T V\end{aligned} \tag{8.42}$$

Equating the coefficient matrices in the quadratic form to solve for $\mathcal{B}$:

$$\mathcal{A} + \mathcal{A}^* - \Gamma \mathcal{B}^{-1} \Gamma^T = \mathcal{B} \tag{8.43}$$

In general, equation (8.43) cannot be solved analytically and requires numerical treatment. However, we have an approximate analytical solution when we assume that the symmetric part of Γ contributes to the product $\Gamma \mathcal{B}^{-1} \Gamma^T$, which leads to $\Gamma \mathcal{B}^{-1} \Gamma^T = \Gamma_{sym} \mathcal{B}^{-1} \Gamma_{sym}$. There is strong numerical evidence that this approximation has an extremely high degree of precision.

$$\mathcal{A} + \mathcal{A}^* - \Gamma_{sym} \mathcal{B}^{-1} \Gamma_{sym} = \mathcal{B}, \tag{8.44}$$

which has a solution when Γ is not singular with $\mathcal{C} = \Gamma_{sym}^{-\frac{1}{2}} (\mathcal{A} + \mathcal{A}^*) \Gamma_{sym}^{-\frac{1}{2}}$, as we sandwich both sides by $\Gamma_{sym}^{-\frac{1}{2}}$

$$\begin{aligned}\mathcal{C} - \Gamma_{sym}^{\frac{1}{2}} \mathcal{B}^{-1} \Gamma_{sym}^{\frac{1}{2}} &= \Gamma_{sym}^{-\frac{1}{2}} \mathcal{B} \Gamma_{sym}^{-\frac{1}{2}} \\ X^2 - \mathcal{C} X + I &= 0,\end{aligned} \tag{8.45}$$

where $X = \Gamma_{sym}^{-\frac{1}{2}} \mathcal{B} \Gamma_{sym}^{-\frac{1}{2}}$. The analytical solution to the matrix quadratic equation (8.43) exists only because $\mathcal{C}$ commutes with I. In terms of $\mathcal{B}$, then the solution becomes

$$\begin{aligned}\mathcal{B} &= \frac{1}{2} \Gamma_{sym}^{\frac{1}{2}} \left(\mathcal{C} + \sqrt{\mathcal{C}^2 - 4I}\right) \Gamma_{sym}^{\frac{1}{2}} \\ &= \frac{1}{2}\left(\mathcal{A} + \mathcal{A}^* + \sqrt{\Gamma_{sym}^{\frac{1}{2}} (\mathcal{A} + \mathcal{A}^*) \Gamma_{sym}^{-1} (\mathcal{A} + \mathcal{A}^*) \Gamma_{sym}^{\frac{1}{2}} - 4\Gamma_{sym}^2}\right).\end{aligned} \tag{8.46}$$

Now, let us define

$$\begin{aligned}\mathcal{X}_m \equiv \left(\frac{m!}{2\pi i}\right)^k \oint_C \frac{e^{V^T R V}}{\langle V \rangle} \exp\Big(z^T \Gamma \mathcal{B}^{-1} M^T V + \\ V^T M \mathcal{B}^{-1} \Gamma^T z + 2V^T M \mathcal{B}^{-1} M^T V\Big) dV.\end{aligned} \tag{8.47}$$

$\mathcal{X}_m$ is proportional to $H_m\left(MV\right)$

$$z^T\Gamma\mathcal{B}^{-1}M^TV + V^TM\mathcal{B}^{-1}\Gamma^Tz = 2W^TMz, \tag{8.48}$$

where,

$$W^T = V^TM\mathcal{B}^{-1}\Gamma^TM^{-1}. \tag{8.49}$$

We will construct M as a matrix which diagonalizes $\mathcal{B}^{-1}\Gamma^T$, such that $\mathcal{D} = M\mathcal{B}^{-1}\Gamma^TM^{-1}$ will be diagonal. This is always possible because product of a positive definite symmetric matrix with a Hermitian matrix is diagonalizable. Hence, we can write the following,

$$W = \mathcal{D}V \quad and \quad W^T = V^T\mathcal{D}. \tag{8.50}$$

$$\begin{aligned} &2V^TM\mathcal{B}^{-1}M^TV + V^TRV \\ &\quad = 2W^T\mathcal{D}^{-1}M\mathcal{B}^{-1}M^T\mathcal{D}^{-1}W + W^T\mathcal{D}^{-1}R\mathcal{D}^{-1}W \\ &\quad = W^T\left(2\mathcal{D}^{-1}M\mathcal{B}^{-1}M^T\mathcal{D}^{-1} + \mathcal{D}^{-1}R\mathcal{D}^{-1}\right)W \end{aligned} \tag{8.51}$$

Equating (7.50) with the coefficients of $\mathcal{X}_m$ with $\overline{\mathcal{H}}$ to solve for R,

$$2\mathcal{D}^{-1}M\mathcal{B}^{-1}M^T + \mathcal{D}^{-1}R\mathcal{D}^{-1} = R. \tag{8.52}$$

Equation (7.45) is a linear equation of the form $K_1 + K_2RK_2 = R$ with a unique solution of R, where $k_1 = 2\mathcal{D}M\mathcal{B}^{-1}M^T$, $K_2 = \mathcal{D}^{-1}$.We will proceed with the "vec" trick, which is formed from a matrix R by stacking its element into a column matrix which is denoted by $vec(R)$. The Kronecker product is denoted by "$\otimes$".The following equation

$$K_1 + K_2RK_2 = R, \tag{8.53}$$

is equivalent to

$$\begin{aligned} vec\left(K_1\right) + \left(K_2^T \otimes K_2\right) vec\left(R\right) &= vec\left(R\right) \\ \left(I - K_2^T \otimes K_2\right) vec\left(R\right) &= vec\left(K_1\right) \\ vec\left(R\right) &= \left(I - K_2^T \otimes K_2\right)^{-1} vec\left(K_1\right). \end{aligned} \tag{8.54}$$

Hence,

$$vec\left(R\right) = \left(I - \mathcal{D}^{-1} \otimes \mathcal{D}^{-1}\right)^{-1} vec\left(\mathcal{D}^{-1}M\mathcal{B}^{-1}M^T\right). \tag{8.55}$$

Since $V = \mathcal{D}^{-1}W$, the Jacobian of the transfromation from dV to dW is

$$dV = det\left(\mathcal{D}^{-1}\right) dW. \tag{8.56}$$

Since $\mathcal{D}$ is a diagonal matrix,

$$\langle V\rangle = det\left(\mathcal{D}^{-1}\right)^{m+1} \langle W\rangle \tag{8.57}$$

$\mathcal{X}_m$ now becomes

$$\begin{aligned}\mathcal{X}_m &= det\left(\mathcal{D}^{-1}\right)^{-m}\left(\frac{m!}{2\pi i}\right)^k \oint\limits_C \frac{e^{2W^T Mz+W^T RW}}{\langle W\rangle}dW \\ &= det\left(\mathcal{D}\right)^m\left(\frac{m!}{2\pi i}\right)^k \oint\limits_C \frac{e^{2W^T Mz+W^T RW}}{\langle W\rangle}dW.\end{aligned} \tag{8.58}$$

Hence,

$$\begin{aligned}\int \rho_{out} f_m(z')dz' &= \overline{\mathcal{N}}' det\left(\mathcal{D}\right)^m f_m\left(z\right) \\ &= \overline{\mathcal{N}}' det\left(M\mathcal{B}^{-1}\Gamma^T M^{-1}\right)^m f_m(z) \\ &= \overline{\mathcal{N}}' det\left(\mathcal{B}^{-1}\Gamma\right)^m f_m\left(z\right)\end{aligned} \tag{8.59}$$

where $\overline{\mathcal{N}}'$ is the m independent constant. Therefore, the eigenvalues which are yet to be normalized are

$$\lambda_m = \overline{\mathcal{N}}' det\left(\mathcal{D}\right)^m \tag{8.60}$$

$\overline{\mathcal{N}}'$ is cancelled during normalization.

$$\begin{aligned}p_m &= \frac{\overline{\mathcal{N}}' det\left(\mathcal{D}\right)^m}{\sum_{l=0}^{\infty}\overline{\mathcal{N}}' det\left(\mathcal{D}\right)^l} \\ &= \frac{\beta^m}{\sum_{l=0}^{\infty}\beta^l} \\ &= \beta^m\left(1-\beta\right)\end{aligned} \tag{8.61}$$

Here, β is defined as

$$\beta \equiv det\left(\mathcal{B}^{-1}\Gamma\right). \tag{8.62}$$

We must impose the constraint that $\beta < 1$, which leads to

$$\begin{aligned}det\left(\mathcal{B}^{-1}\Gamma\right) &< 1 \\ det\left(\Gamma\right) &< det\left(\mathcal{B}\right).\end{aligned} \tag{8.63}$$

8.6 The Entanglement Entropy

The entanglement entropy is now given in terms of β,

$$\begin{aligned}S_{EE} &= -\sum_{m=0}^{\infty} p_m \ln\left(p_m\right) \\ &= -\frac{\beta\ln\left(\beta\right)+\left(1-\beta\right)\ln\left(1-\beta\right)}{1-\beta},\end{aligned} \tag{8.64}$$

where β is

$$\beta = \frac{det\left(\Gamma\right)}{det\left(\mathcal{B}\right)}. \tag{8.65}$$

8.7 Limiting Cases of the Eigenvalues

The solution to (8.44) does not exist using our formalism when the determinant of Γ is a time-independent constant of zero, which happens whenever $k > N/2$, as it no longer allows multiplying both sides of (8.44) by $\Gamma_{sym}^{-\frac{1}{2}}$ as Γ_{sym} simultaneously becomes singular. The limit $det\,(\Gamma) \to 0$ does not make sense as a constant cannot approach anything. Instead, we must apply our cyclic boundary condition and that (8.25) describes a pure density state. Let ρ be the density operator of the pure state, ρ_{in} be one of the subsystems that result after tracing out, and ρ_{out} be the remaining subsystem. As ρ is pure, the Araki-Lieb equality can be applied,

$$S\left(\rho_{out}\right) = S\left(\rho_{in}\right). \tag{8.66}$$

Without loss of generality, let us assume that ρ_{out} describes the system with $k = min\,(n, N-n)$ oscillators. Then $det\,(\Gamma)$ is time-varying, and limits can be applied, and our formalism will work. Since we can calculate the entanglement entropy using either of the reduced density operator, ρ_{out}, or ρ_{in}, we choose to work only with ρ_{out}. We are now at a position to apply the limit $\det\left(\Gamma\right) \to 0$. First, we can approximate that the diagonal elements of $\mathcal{C}^2$ are much larger than 4. This makes sense because as $\det\left(\Gamma_{sym}\right)$ keeps getting smaller so does $\det\left(\Gamma_{sym}^{1/2}\right)$, the elements of $\Gamma_{sym}^{-\frac{1}{2}}$ will keep getting larger, which results in the elements of $\mathcal{C}$ getting larger. Therefore, using the fact that $(\mathcal{A} + \mathcal{A}^*)$ is symmetric, real, and positive definite,

$$\begin{aligned}
\lim_{det(\Gamma)\to 0} det\left(\mathcal{B}\right) &= \lim_{det(\Gamma)\to 0} \det\left(\frac{1}{2}\Gamma_{sym}^{\frac{1}{2}}\left(\mathcal{C} + \sqrt{\mathcal{C}^2 - 4I}\right)\Gamma_{sym}^{\frac{1}{2}}\right) \\
&= \lim_{det(\Gamma)\to 0} \det\left(\frac{1}{2}\Gamma_{sym}^{\frac{1}{2}}\left(\mathcal{C} + \sqrt{\mathcal{C}^2}\right)\Gamma_{sym}^{\frac{1}{2}}\right) \\
&= \lim_{det(\Gamma)\to 0} \det\left(\mathcal{A} + \mathcal{A}^*\right) \\
&> 0.
\end{aligned} \tag{8.67}$$

Now,

$$\begin{aligned}
\beta &= \lim_{det(\Gamma)\to 0} \frac{det\left(\Gamma\right)}{det\left(\beta\right)} \\
&= 0.
\end{aligned} \tag{8.68}$$

Hence,

$$S_{EE} = 0. \tag{8.69}$$

8.8 Validation of Approximation

Since we are working with the non-analytical equation (8.43), in this section, the exact solution refers to being exact with a certain degree of precision. To compare the solution of (8.44) with (8.43), we will first show that Γ has a high degree of symmetry so that the required exact solution of (8.43) is close enough to the solution of (8.44) that we can feed the solution of (8.44) as the initial guess to any numerical root-finding method for a set of non-linear equations. One such method is Newton's method. In this section, we will look at the symmetry of Γ,

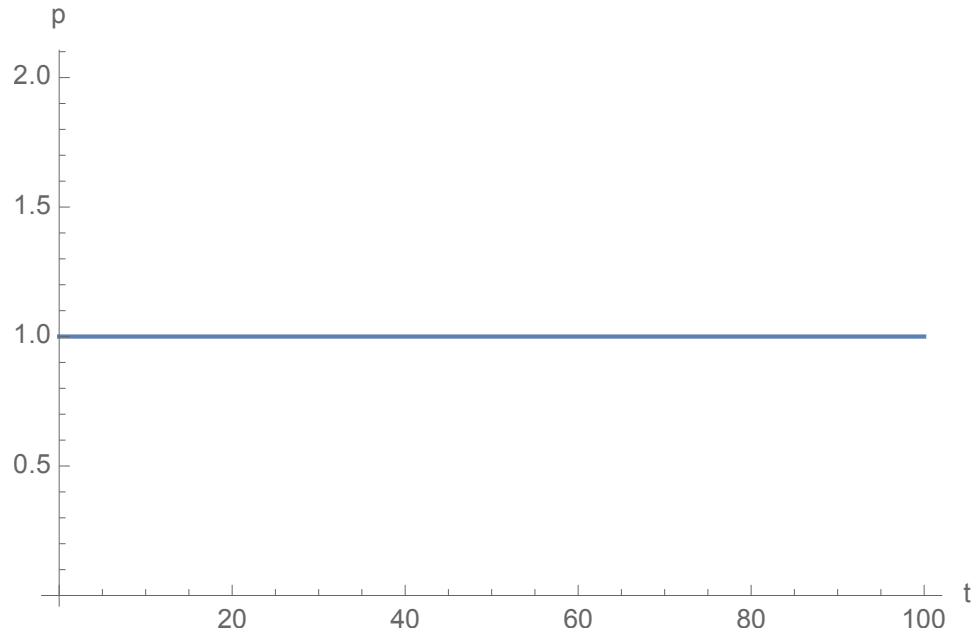

Figure 8.1: Symmetry p when $N = 5$, $k = 2$, $\omega^2 = 1$ and $\Omega^2 = 0.1$

and the entanglement entropy obtained using our approximation contrasted with the same obtained by using the "FindRoot" method in Mathematica, and the corresponding absolute difference. The symmetric part and the antisymmetric part of Γ are defined as

$$\Gamma_{sym} \equiv \frac{1}{2}\left(\Gamma + \Gamma^T\right) \quad and \quad \Gamma_{asm} \equiv \frac{1}{2}\left(\Gamma - \Gamma^T\right). \tag{8.70}$$

The Frobenius norm of the symmetric and antisymmetric part of Γ are defined as

$$\|\Gamma_{sym}\| \equiv \sqrt{Tr\left(\Gamma_{sym}\Gamma_{sym}^{\dagger}\right)} \quad and \quad \|\Gamma_{asm}\| \equiv \sqrt{Tr\left(\Gamma_{asm}\Gamma_{asm}^{\dagger}\right)}, \tag{8.71}$$

where $\|.\|$ is used to denote the Frobenius norm of the respective matrix. The amount of symmetry of a matrix can be measured by using the Frobenius norm of its symmetric and antisymmetric part. We can define the metric to measure the symmetry of Γ as

$$p \equiv \frac{\|\Gamma_{sym}\| - \|\Gamma_{asm}\|}{\|\Gamma_{sym}\| + \|\Gamma_{asm}\|}. \tag{8.72}$$

From (8.72), we can see that when Gamma is perfectly symmetric $p = 1$ as $\|\Gamma_{asm}\| = 0$; similarly, when Gamma is perfectly antisymmetric $p = -1$ as $\|\Gamma_{sym}\| = 0$, and when the symmetric and the antisymmetric part are comparable $p = 0$. Moreover, anything in between describes Γ being more symmetric than antisymmetric, i.e., when $0 < p < 1$, or Γ being more antisymmetric than symmetric, i.e., when $-1 < p < 0$.

When $k = 1$, Γ is simply a number, which is symmetric in terms of matrix symmetry. When $K = 2$, Γ is real and symmetric; figure 8.1 shows the variation of symmetry with time. When $k = 3$, Γ is Hermitian, and has antisymmetric imaginary part. Figure 8.2 shows one such case. We can compute the time average of

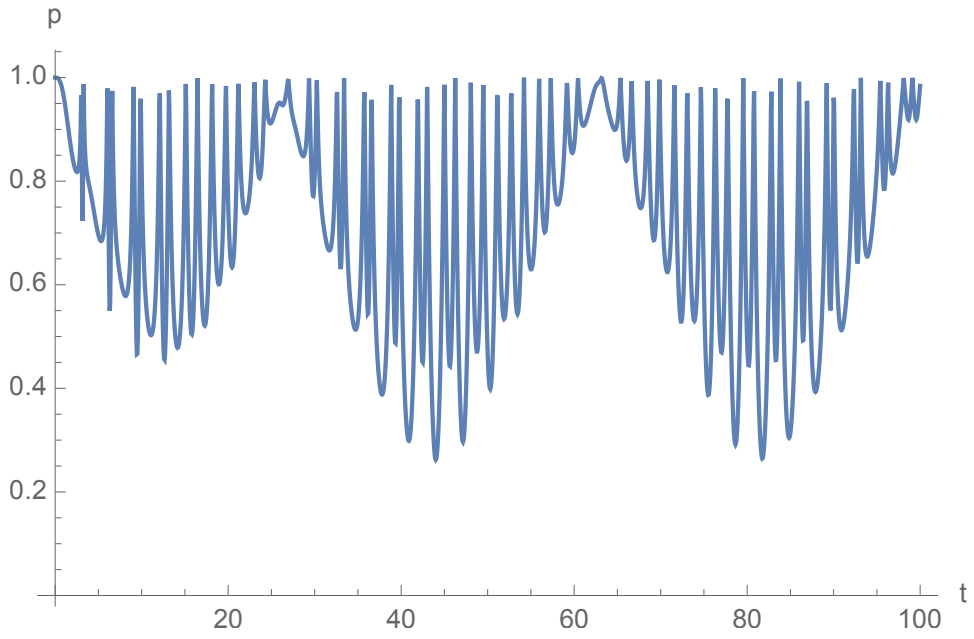

Figure 8.2: Symmetry p when $N = 6$, $k = 3$, $\omega^2 = 1$ and $\Omega^2 = 0.1$

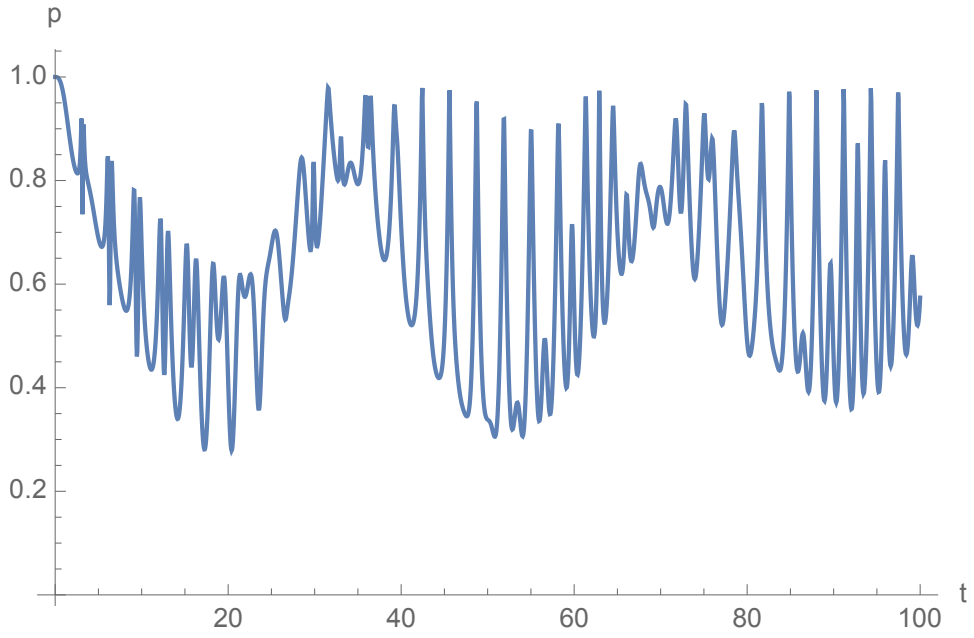

Figure 8.3: Symmetry p when $N = 8$, $k = 4$, $\omega^2 = 1$ and $\Omega^2 = 0.1$

any function f, with Δt as the time interval,

$$\langle f \rangle = \frac{1}{\Delta t} \int_0^{\Delta t} f(t)\, dt. \tag{8.73}$$

The average symmetry for figure 8.2 is 0.72, indicating a significant amount of symmetry in Γ. As we increase N and k in figure 8.3, the average symmetry becomes 0.63. Although the symmetry seems to have decreased with k, we will find evidence that the antisymmetric part contributes insignificantly to the product $\Gamma^T \mathcal{B}^{-1} \Gamma$. Since Gamma is always more symmetric than antisymmetric, we can

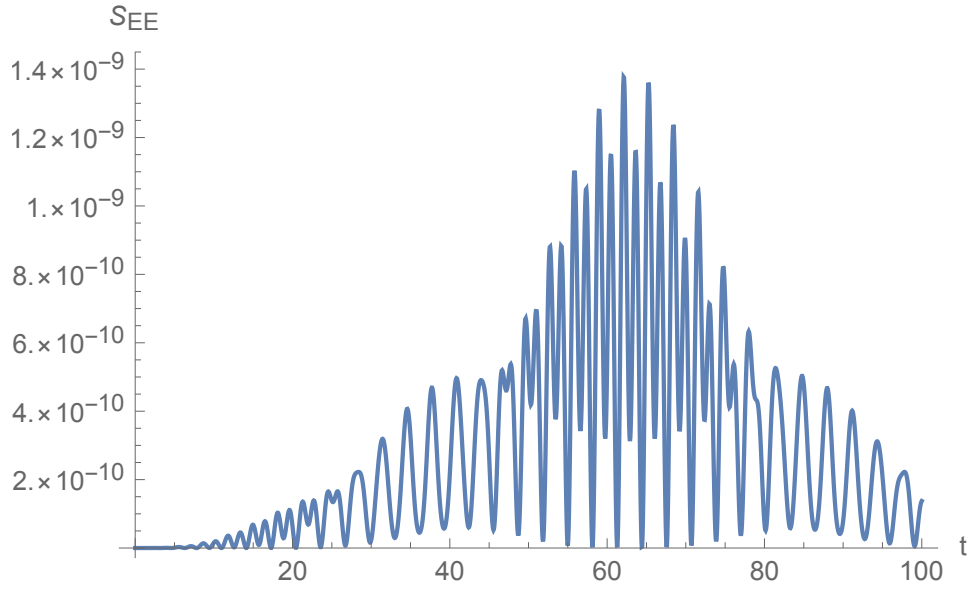

Figure 8.4: The entanglement entropy approximated with $N = 6$, $k = 3$, $\omega^2 = 1$, $\Omega^2 = 0.1$, and it has a time average of 2.85×10^{-10}.

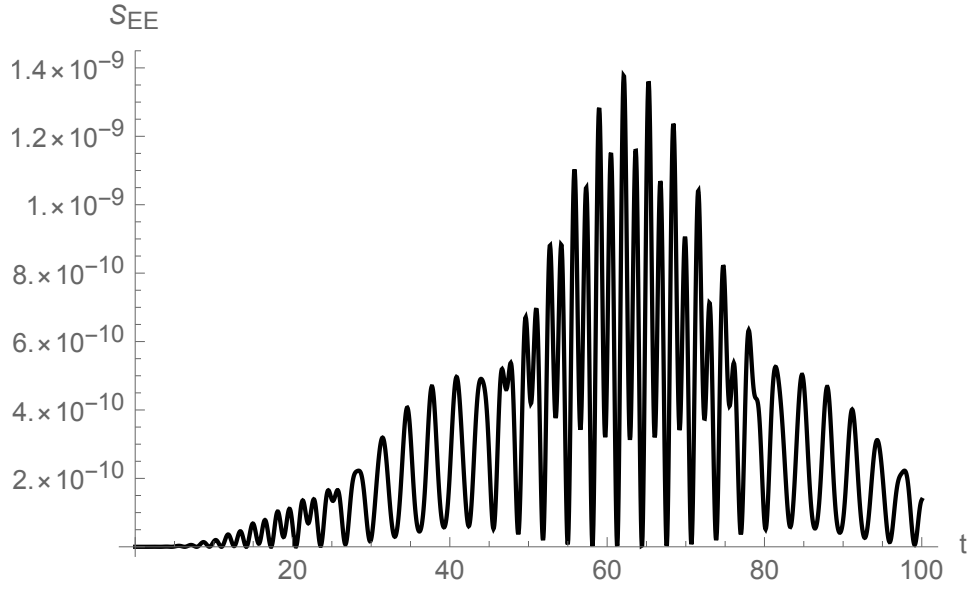

Figure 8.5: The exact entanglement entropy when $N = 6, k = 3, \omega^2 = 1, \Omega^2 = 0.1$, and it has a time average of 2.85×10^{-10}.

use the solution of (8.44) as the initial guess of the "FindRoot" method in Mathematica. It is interesting to note that both figures 8.4 and 8.5 are identical. In order to distinguish them, we cannot rely exclusively on the graphs. We see the same for with a larger N and k in figures 8.6 and 8.7. The resemblance is independent of the oscillators' energy or coupling, as increasing Ω from 0.1 to 0.9 still results in entanglement entropies to be the same in the graphs. The pairs of graphs $[(8.4, 8.5), (8.6, 8.7)]$ between the approximate and the exact solution also follow the same pattern at which the entanglement entropy increases or decreases.

Both figures 8.4 and 8.5 and their corresponding time averages show that the order of entanglement entropy is around $O(10^{-10})$. In comparison, the absolute

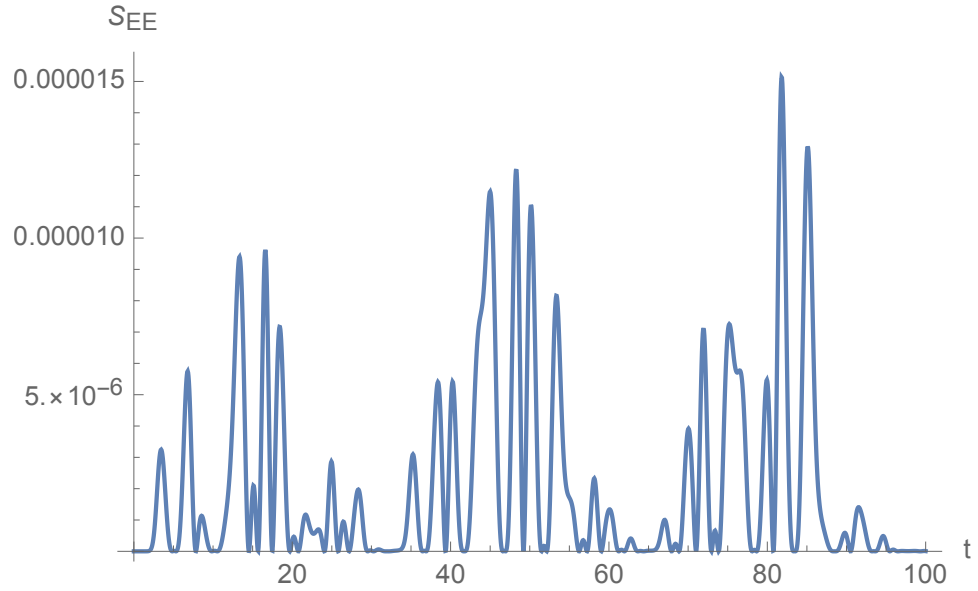

Figure 8.6: The entanglement entropy approximated with $N = 8$, $k = 4$, $\omega^2 = 1$, $\Omega^2 = 0.9$, and it has a time average of 2.11×10^{-6}.

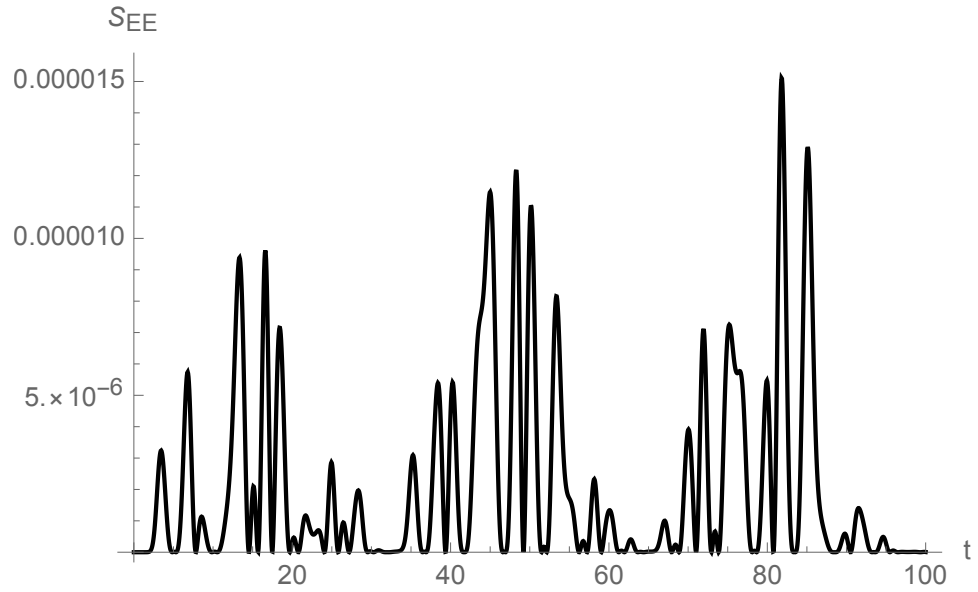

Figure 8.7: The exact entanglement entropy when $N = 8$, $k = 4$, $\omega^2 = 1$, $\Omega^2 = 0.9$, and it has a time average of 2.11×10^{-6}.

difference is of a much smaller order of $O(10^{-18})$. Hence, relative to the entanglement entropy, the difference is of the order $O(10^{-8})$. Similarly, for figures 7.6 and 7.7, the entanglement entropy order is $O(10^{-6})$, and the absolute difference is of the order $O(10^{-9})$. Therefore, relative to the entanglement entropy, the difference is of the order $O(10^{-3})$. We should keep in mind that the answer we obtained using the numerical method has a small degree of error that will contribute to the difference. If we want to decrease the error, we can always increase the numerical method's number of iterations.

The symmetry p of Γ always being positive allows finding the solution analytically using the symmetric part Γ_{sym} and using it as an initial guess of a numerical

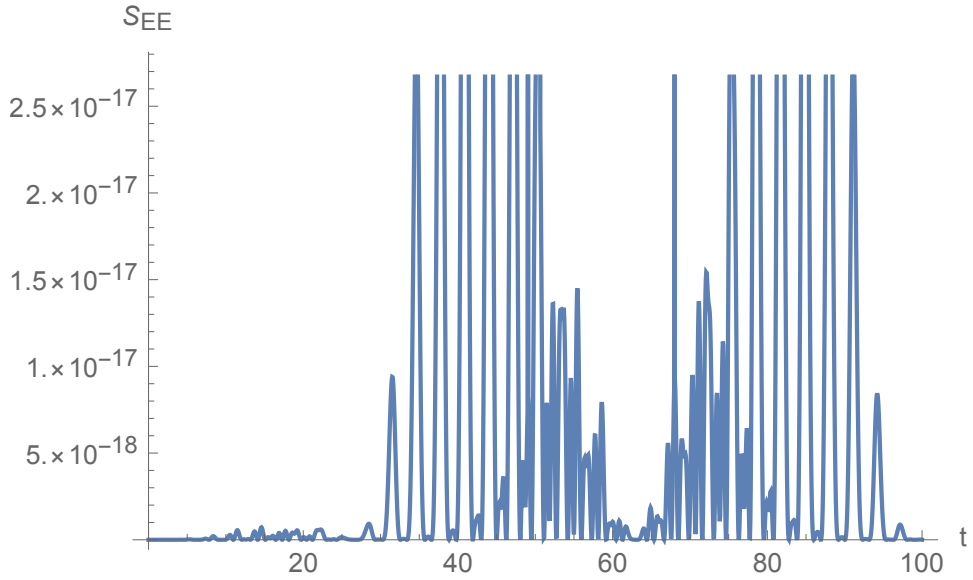

Figure 8.8: The absolute difference between the entanglement entropy obtained using the approximation and the exact solution with $N = 6$, $k = 3$, $\omega^2 = 1$, $\Omega^2 = 0.1$ and has a time average of 7.44×10^{-18}.

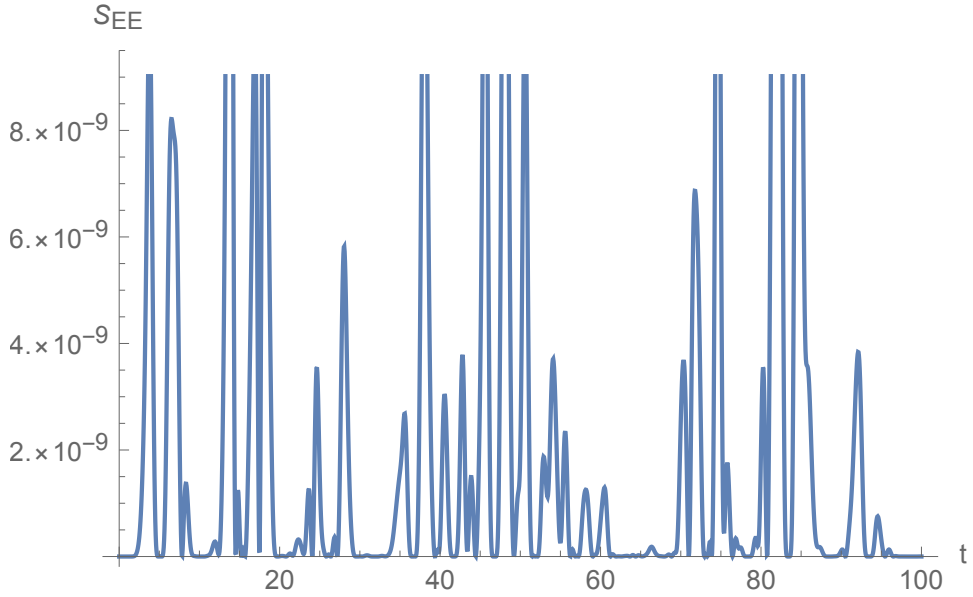

Figure 8.9: The absolute difference between the entanglement entropy obtained using the approximation and the exact solution with $N = 8$, $k = 4$, $\omega^2 = 1$, $\Omega^2 = 0.9$ and has a time average of 2.40×10^{-9}.

root finding method. Our analysis found that the approximate analytical solution and the slightly more accurate numerical solution differ insignificantly. It is also worth noting that both solutions behave in the same manner as to how they vary with time. Therefore, the analytical solution of equation (8.44) has the potential to offer meaningful physical insights. Since we are calculating the entanglement entropy, we are concerned with the determinant of $\mathcal{B}$ more than $\mathcal{B}$ itself. The analysis shows that the antisymmetric part of Gamma modifies the determinant of $\mathcal{B}$ to the point that fails to produce a noticeable change in the scale of the entanglement entropy.

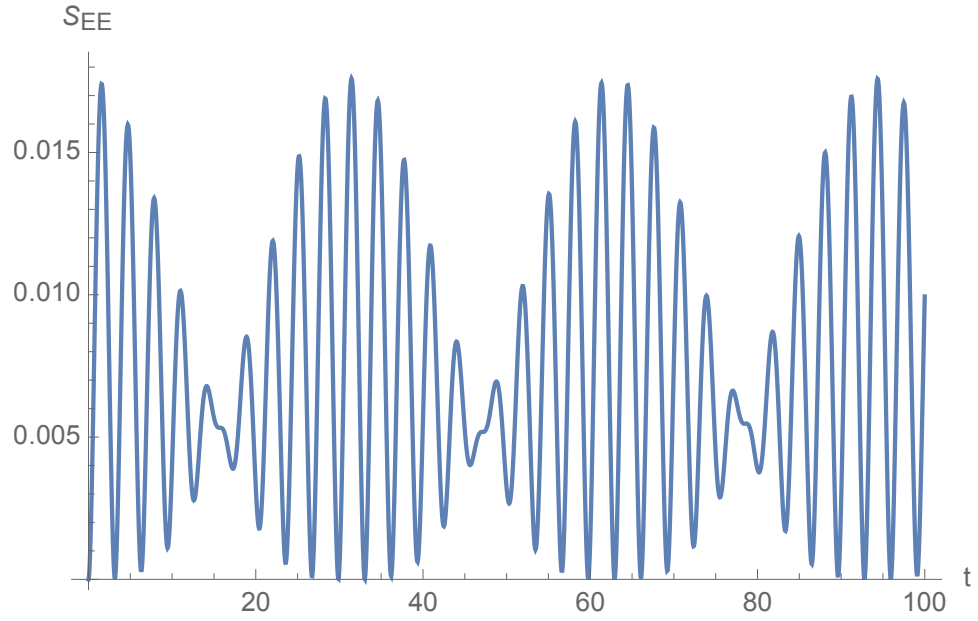

Figure 8.10: The entanglement entropy when $N = 2$, $k = 1$, $\omega^2 = 1$ and $\Omega^2 = 0.1$ with a time average of 7.34×10^{-3}.

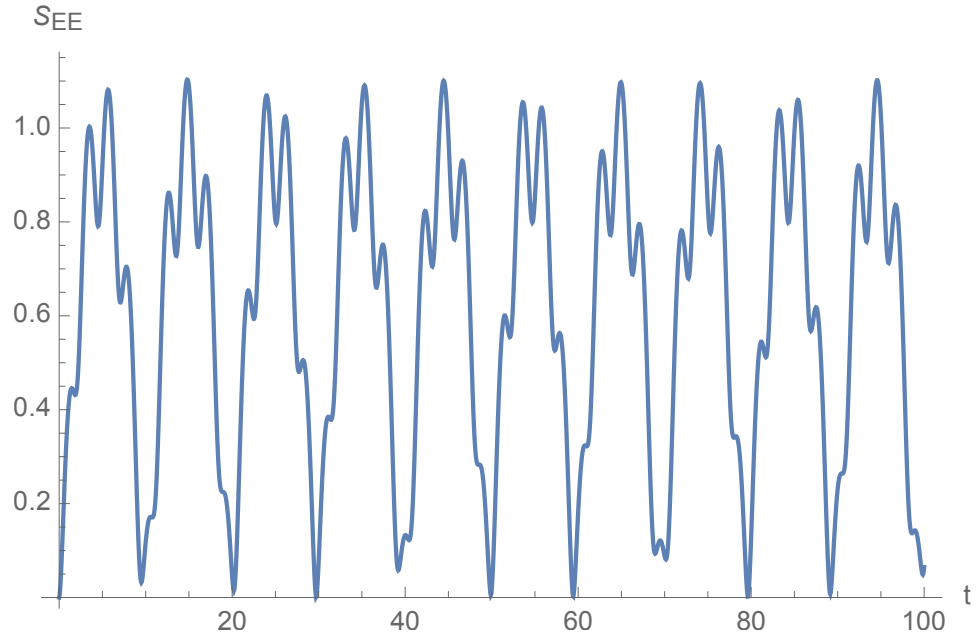

Figure 8.11: The entanglement entropy when $N = 2$, $k = 1$, $\omega^2 = 1$ and $\Omega^2 = 0.9$ with a time average of 0.615.

8.9 Properties of the Entanglement Entropy

- The entanglement entropy increases with the coupling term Ω.
- The entanglement entropy is consistent with the work by Ali and Moynihan[3] when $N = 2$, which is also shown in figures 7.1 and 7.2.

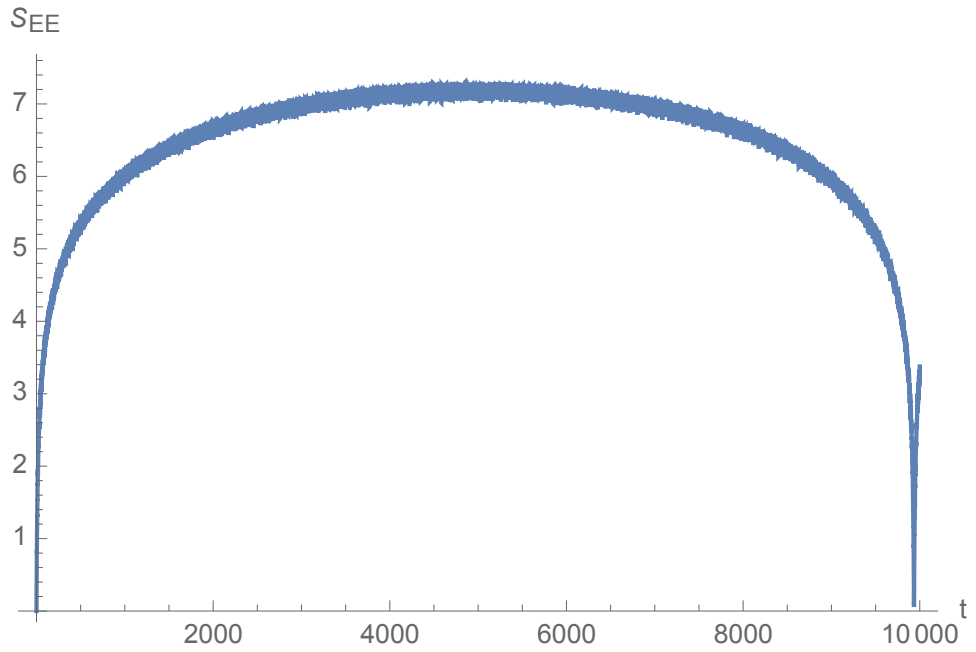

Figure 8.12: The entanglement entropy when $N = 10$, $k = 1$, $\omega^2 = 1$ and $\Omega^2 = 0.9999999$ with a time average of 6.47. Initially, there is some resemblance to the Page curve (4.3), which ends as our system is closed. This is likely due to $\mathcal{Z}_k \to \tilde{\omega}_k$ whenever $\Omega \to \omega$. Then the matrix $\mathcal{Z}$ in (8.25) is Hermitian and its symmetric part (8.24) used in our work is real. Therefore, our system is comparable to Srednicki's N oscillator work (6.4) as $\mathcal{A} \to \mathcal{A}^*$ and Γ becomes real and symmetric.

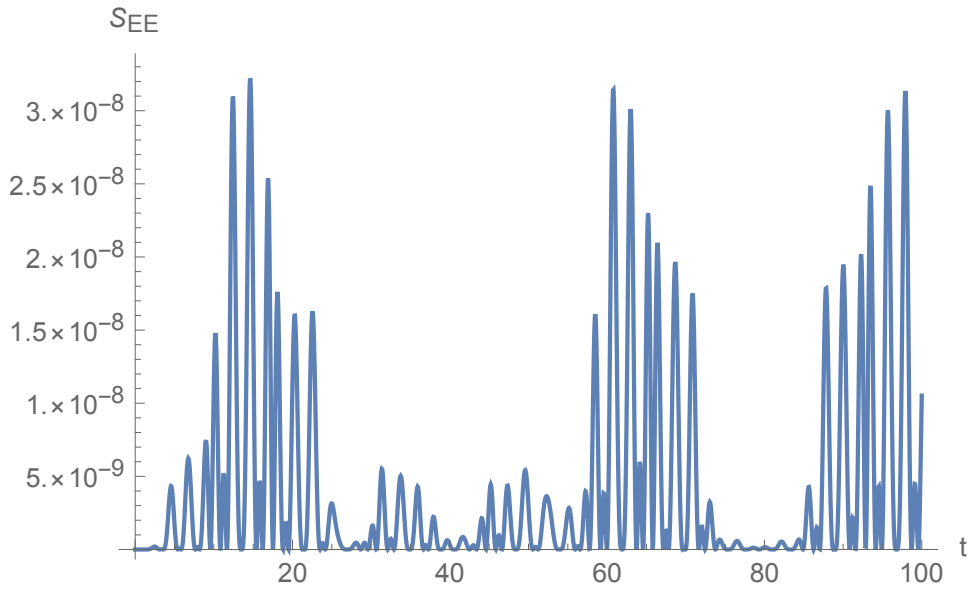

Figure 8.13: The entanglement entropy when $N = 8$, $k = 4$, $\omega^2 = 2$ and $\Omega^2 = 0.9$ with a time average of 4.19×10^{-9}.

We expect that the entanglement entropy shows the degree of interaction between the oscillators; therefore, increasing Ω should increase the entanglement entropy. Figures 8.10 and 8.11 demonstrate that the average entanglement entropy has gone up by an increase in Ω.

N	k	$\langle S_{EE} \rangle$
8	1	0.40×10^{0}
8	2	2.19×10^{-2}
8	3	4.16×10^{-4}
8	4	2.05×10^{-6}
10	1	0.40×10^{0}
10	2	2.34×10^{-2}
10	3	5.72×10^{-4}
10	4	6.74×10^{-6}
10	5	2.56×10^{-8}
20	3	9.29×10^{-4}

Table 8.1: The average of entanglement entropy $\langle S_{EE} \rangle$ with $\omega^2 = 1, \Omega^2 = 0.9$, and $\Delta t = 1000$.

- The entanglement entropy is always fluctuating and keeps dropping to zero and then continues to rise again. For some configurations such as 8.12, the timescale for the entanglement entropy to fall to zero can be extremely large.

Figure 8.12 shows that when Ω approaching ω; the entanglement entropy is of the highest order (compared to other graphs in this chapter) and slowly reaches a maximum value and then decreases back to zero.

- The entanglement entropy decreases with the kinetic term ω.

The kinetic term ω increases the degree of 'decoupling' of the oscillators. We have demonstrated one such situation by comparing 8.6 and 8.13.

- The entanglement entropy increases with $\frac{\Omega}{\omega}$.

Combining the properties of entropy related with ω and Ω, the subsystems of oscillators decouple when $\frac{\Omega}{\omega} \to 0$ and the oscillators couple most strongly when $\frac{\Omega}{\omega} \to 1$.

- The entanglement entropy also increases from zero continuously which is what we would expect from a sudden quench.

Suppose that our pure state Ψ_1 is a state on the Hilbert space $\mathcal{H}_{tot}$, which is bipartite as it can be factorized as $\mathcal{H}_{tot} = \mathcal{H}_{in} \otimes \mathcal{H}_{out}$, then we can find the eigenvalues of either ρ_{in} or ρ_{out} as they are equal regardless of which we trace out. We impose the restriction $k \leq N/2$ so that $|out| \leq \frac{1}{2}(|out| + |in|)$ to avoid repeating values of the entanglement entropy, where $|.|$ indicates the 'size' of the system[22] and is a measure of the number of oscillators in the system. Table 8.1 shows an interesting pattern of the way the average entanglement entropy changes with N and k.

- The entanglement entropy is maximal for a given N whenever $k = 1$ and $\Omega \to \omega$.
- The order of entanglement entropy decreases with k. This is a consequence of Page's theorem as the subsystems are close to being maximally entangled whenever $\frac{|out|}{|in|} \ll 1$.

- The order of entanglement entanglement depends mostly on k and decreases exponentially.

Chapter 9

Conclusion

One way to solve the black hole information paradox is to compute the Page curve; in other words, the problem is to find the time evolution of the entanglement entropy between the early and late radiation of a black hole. However, physicists are far from computing the Page curve, even in AdS/CFT or the BFFS Matrix Model. In the previous chapter (8), we designed a simple model motivated by the holographic principle that a black hole's intrinsic entropy is related with the the entanglement entropy that results from tracing out degrees of freedom. Since a pure state of a collapsing shell of photons has no entanglement entropy, it is comparable to a system of non-interactive harmonic oscillators. As the black hole's entropy begins to rise, so does the entanglement entropy of the quenched harmonic oscillators.

Moreover, for a specific time t, our quenched Hamiltonian's reduced density operator does not have the same form as that of Srednicki's time independent Hamiltonian. Therefore, the entanglement entropy of the quenched oscillators will not necessarily resemble the Bekenstein-Hawking entropy of a black hole. In contrast to Srednicki's N-oscillator work, the matrix equation we have to solve is not analytical (which we expect with periodic lattices)[13]. The fact that the entanglement entropy becomes mostly independent of N indicates that after regularization of a quantum field theory with appropriate limits to the Hamiltonian of the quenched oscillators, the theory is likely to be completely independent of N and, therefore, the infrared cutoff, which is common in both Srednicki and our work.

With more research, this model can be subject to many changes, including how the particles interact with each other. To get a more realistic model, we should probably rely on a "gradual" quench instead of a "sudden" quench by allowing the coupling Ω to be a function of time with $\Omega(0) = 0$. Furthermore, the entanglement entropy between the early and late radiation of a black hole increases linearly as the black hole starts to form. Our model needs refinement to reflect this property. As for our future project, we want to regularize a quantum field and modify our working to lead us more towards the time evolution of the entanglement entropy of the late and early radiation of a black hole.

Bibliography

[1] D. ”Harlow, “TASI Lectures on the Emergence of Bulk Physics in AdS/CFT,” *PoS*, vol. TASI2017, 2018. DOI: 10.22323/1.305.0002. arXiv: 1802.01040 [hep-th].

[2] T. Ali, A. Bhattacharyya, S. S. Haque, E. H. Kim, and N. Moynihan, “Time evolution of complexity: A critique of three methods,” *Journal of High Energy Physics*, vol. 2019, no. 4, Apr. 2019. DOI: 10.1007/jhep04(2019)087. [Online]. Available: https://doi.org/10.1007%2Fjhep04%282019%29087.

[3] T. Ali and N. Moynihan, “Entanglement entropy of the quenched double oscillator,” unpublished, 2018.

[4] M. Ammon and J. Erdmenger, *Gauge/gravity duality: foundations and applications*. Cambridge University Press, 2015.

[5] T. Banks, W. Fischler, S. Shenker, and L. Susskind, “M theory as a matrix model: A Conjecture,” *Phys. Rev. D*, vol. 55, pp. 5112–5128, 1997. DOI: 10.1103/PhysRevD.55.5112. arXiv: hep-th/9610043.

[6] A. Belin, J. De Boer, and J. Kruthoff, “Comments on a state-operator correspondence for the torus,” *SciPost Phys.*, vol. 5, no. 6, p. 060, 2018. DOI: 10.21468/SciPostPhys.5.6.060. arXiv: 1802.00006 [hep-th].

[7] S. M. Carroll, *Spacetime and Geometry: An Introduction to General Relativity*. Pearson, 2014.

[8] D. F. S. David J. Griffiths, *Introduction to Quantum Mechanics*, 3rd ed. 2018.

[9] A. Fitzpatrick, J. Kaplan, and M. T. Walters, *Universality of long-distance ads physics from the cft bootstrap*, Mar. 2014. [Online]. Available: http://old.inspirehep.net/record/1287645/plots.

[10] D. V. Fursaev, “Proof of the holographic formula for entanglement entropy,” *JHEP*, vol. 09, p. 018, 2006. DOI: 10.1088/1126-6708/2006/09/018. arXiv: hep-th/0606184.

[11] D. Harlow, *Jerusalem lectures on black holes and quantum information*, 2014. arXiv: 1409.1231 [hep-th].

[12] P. Hayden and J. Preskill, “Black holes as mirrors: Quantum information in random subsystems,” *JHEP*, vol. 09, p. 120, 2007. DOI: 10.1088/1126-6708/2007/09/120. arXiv: 0708.4025 [hep-th].

[13] T. He, J. M. Magan, and S. Vandoren, “Entanglement Entropy of Periodic Sublattices,” *Phys. Rev. B*, vol. 95, no. 3, p. 035130, 2017. DOI: 10.1103/PhysRevB.95.035130. arXiv: 1607.07462 [quant-ph].

[14] M. Headrick, “Lectures on entanglement entropy in field theory and holography.,” 2019.

[15] R. Jefferson and R. C. Myers, “Circuit complexity in quantum field theory,” *Journal of High Energy Physics*, vol. 2017, pp. 1–81, 2017.

[16] J. Kaplan, "Lectures on ads/cft from the bottom up,"
[17] C. Krishnan, *Quantum field theory, black holes and holography*, 2010. arXiv: 1011.5875 [hep-th].
[18] H. Liu and S. J. Suh, "Entanglement Tsunami: Universal Scaling in Holographic Thermalization," *Phys. Rev. Lett.*, vol. 112, p. 011 601, 2014. DOI: 10.1103/PhysRevLett.112.011601. arXiv: 1305.7244 [hep-th].
[19] D. A. Lowe and L. Thorlacius, "Ads-cft correspondence and the information paradox," *Physical Review D*, vol. 60, no. 10, Oct. 1999, ISSN: 1089-4918. DOI: 10.1103/physrevd.60.104012. [Online]. Available: http://dx.doi.org/10.1103/PhysRevD.60.104012.
[20] M. Natsuume, *AdS/CFT duality user guide*. Springer, 2015.
[21] T. Nishioka, S. Ryu, and T. Takayanagi, "Holographic entanglement entropy: An overview," *Journal of Physics A: Mathematical and Theoretical*, vol. 42, no. 50, p. 504 008, Dec. 2009, ISSN: 1751-8121. DOI: 10.1088/1751-8113/42/50/504008. [Online]. Available: http://dx.doi.org/10.1088/1751-8113/42/50/504008.
[22] Y. C. Ong, *Evolution of black holes in anti-de Sitter spacetime and the firewall controversy*. Springer, 2016.
[23] D. N. Page, "Time Dependence of Hawking Radiation Entropy," *JCAP*, vol. 09, p. 028, 2013. DOI: 10.1088/1475-7516/2013/09/028. arXiv: 1301.4995 [hep-th].
[24] M. E. Peskin and D. V. Schroeder, *An Introduction to Quantum Field Theory*. 1995.
[25] J. L. PETERSEN, "Introduction to the maldacena conjecture on ads/cft," *International Journal of Modern Physics A*, vol. 14, no. 23, pp. 3597–3672, Sep. 1999, ISSN: 1793-656X. DOI: 10.1142/s0217751x99001676. [Online]. Available: http://dx.doi.org/10.1142/S0217751X99001676.
[26] M. Rabinowitz, *Black hole paradoxes*, 2004. arXiv: astro-ph/0412101 [astro-ph].
[27] E. Rieffel and W. Polak, *Quantum Computing: A Gentle Introduction*. The MIT Press, 2014.
[28] S. Ryu and T. Takayanagi, "Holographic derivation of entanglement entropy from the anti–de sitter space/conformal field theory correspondence," *Physical Review Letters*, vol. 96, no. 18, May 2006, ISSN: 1079-7114. DOI: 10.1103/physrevlett.96.181602. [Online]. Available: http://dx.doi.org/10.1103/PhysRevLett.96.181602.
[29] B. Schumacher and M. D. Westmoreland, *Quantum processes, systems, and information*. Cambridge University Press, 2010.
[30] Srednicki, "Entropy and area.," *Physical review letters*, vol. 71 5, pp. 666–669, 1993.
[31] L. Susskind, *Black holes and holography*, 2007. [Online]. Available: https://www.perimeterinstitute.ca/images/files/black_holes_and_holography_course_notes.pdf.
[32] B. Ydri, *Quantum black holes*, 2017. arXiv: 1708.00748 [hep-th].
[33] B. Zwiebach, *A first course in string theory*. Cambridge University Press, 2017.

Appendix A

Gaussian Integrals

A.1 Single Variable Gaussian Integrals

This appendix will contain various Gaussian integrals required to work through this paper. x and y are real variables. a and b are complex constants with $\mathrm{Re}\,(a) > 0$ and $z = x + iy$ is a complex variable. All limits of the integrals with are from $-\infty$ to $+\infty$.

$$\int \exp\left(-ax^2 + bx\right) dx = \sqrt{\frac{\pi}{a}} \exp\left(\frac{b^2}{4a}\right) \tag{A.1}$$

We will attempt to evaluate the following integral. First, we note that the Jacobian determinant of the transformation is

$$\begin{aligned} dz^* dz &= \left| \begin{pmatrix} \frac{\partial z}{\partial x} & \frac{\partial z}{\partial y} \\ \frac{\partial z^*}{\partial x} & \frac{\partial z^*}{\partial y} \end{pmatrix} \right| dxdy \\ &= \left| \begin{pmatrix} 1 & i \\ 1 & -i \end{pmatrix} \right| dxdy \\ &= -2i dxdy. \end{aligned}$$

Now,

$$\begin{aligned} &\int \frac{dz^* dz}{-2i} \exp\left(-a|z|^2 + bz^* + b^* z\right) = \\ &\int\int \exp\left(-a\left(x^2 + y^2\right) + b\left(x - iy\right) + b^*\left(x + iy\right)\right) dxdy \\ &= \int \exp\left(-ax^2 + 2\,\mathrm{Re}\,(b)\right) dx \int \exp\left(-ay^2 + 2\,\mathrm{Im}\,(b)\right) dy \\ &= \sqrt{\frac{\pi}{a}} \exp\left(\frac{\mathrm{Re}\,(b)^2}{a}\right) \sqrt{\frac{\pi}{a}} \exp\left(\frac{\mathrm{Im}\,(b)^2}{a}\right). \end{aligned}$$

Therefore,

$$\int \frac{dz^* dz}{-2i} \exp\left(-a|z|^2 + bz^* + b^* z\right) = \frac{\pi}{a} \exp\left(\frac{|b|^2}{a}\right). \tag{A.2}$$

A.2 Multivariable Gaussian Integrals

We only need one multivariable Gaussian integral, which can be proved by using diagonalization and the results from A.1. Let x and J be n dimensional real vectors such that $x, J \in R^n$, $dx = \prod_i x_i$ and A be a $n \times n$ complex symmetric matrix, such that $A^T = A$ and A has a positive definite real part. Then,

$$\int \exp\left(-\frac{1}{2}x^T A x + Jx\right) dx = \sqrt{\frac{(2\pi)^n}{detA}} \exp\left(\frac{1}{2}J^T A^{-1} J\right). \tag{A.3}$$

Appendix B

Graphical Representation of Entanglement Entropy with Mathematica 12.0

In this appendix, we have written down our original code that was used to produce the graphs of chapter (8). The approximation procedure is computationally a lot more efficient than the exact solution. The following shows the portion of the code identical for both exact and approximate solutions.

```
Remove["Global*"]
$Messages = {};
n = Input["Enter number of oscillators N:"];
traced = Input["Enter number of oscillators to be traced out:"];
μ = Exp[-2πI/n];
inputFlag = True;
Λ = 1/Sqrt[n] Table[μ^((a-1)(b-1)), {a, n}, {b, n}];
ωTilde[k_] = Sqrt[ω^2 + Ω^2 Cos[2πk/n]];
ω = √Input["Enter ω sqaured:"];
Ω = √Input["Enter Ω squared:"];
time = Input["Enter time interval:"];
str = StringForm["N=1, Traced=2, ω^2=3, Ω^2=4", n, traced, ω^2, Ω^2];
S = {{0, 0}};
If[n ≥ traced&&ω > Ω&&ω > 0&&Ω > 0&&n ≥ 2&&n == Round[n]&&
traced == Round[traced], Do[
z[k_] = -Iωτilde[k]Cot[ωτilde[k]t] + ωτilde[k]^2/(ωSin[ωτilde[k]t]^2 - Iωτilde[k]Cos[ωτilde[k]t]Sin[ωτilde[k]t]);
v = Table[z[k - 1], {k, n}];

mZ = 1/2(ConjugateTranspose[Λ].DiagonalMatrix[v].Λ +
Transpose[ConjugateTranspose[Λ].DiagonalMatrix[v].Λ]);
If[traced < n/2, traced = n - traced];
mA1 = mZ[[1;;traced, 1;;traced]];
mB = mZ[[traced + 1;;n, traced + 1;;n]];
mC1 = mZ[[1;;traced, traced + 1;;n]];
```

$\alpha = 2\text{Re}[\text{mA1}];$
$\text{mA2} = \text{mB} - \text{Transpose}[\text{mC1}].\text{Inverse}[\alpha].\text{mC1};$

$\Gamma = \frac{1}{2}(\text{Transpose}[\text{mC1}].\text{Inverse}[\alpha].\text{Conjugate}[\text{mC1}] +$
$\text{ConjugateTranspose}[\text{Transpose}[\text{mC1}].\text{Inverse}[\alpha].\text{Conjugate}[\text{mC1}]]);$
$\Gamma\text{s} = \frac{1}{2}(\Gamma + \text{Transpose}[\Gamma]);$
$\text{gRoot} = \text{MatrixPower}[\Gamma\text{s}, 1/2];$
$\text{mC2} = \text{Inverse}[\text{gRoot}].(\text{mA2} + \text{Conjugate}[\text{mA2}]).\text{Inverse}[\text{gRoot}];$
$\text{sol} = \frac{1}{2}\text{gRoot}.(\text{mC2} + \text{MatrixPower}[\text{mC2.mC2} - 4\text{IdentityMatrix}[n - \text{traced}], 1/2]).\text{gRoot};$

The following portion of code is for the exact solution:

$l = \text{Flatten}\left[\text{Table}\left[\{x_{i,j}, \text{sol}[[i,j]]\}, \{i, n - \text{traced}\}, \{j, n - \text{traced}\}\right], 1\right];$
$\text{mX} = \text{Table}\left[x_{i,j}, \{i, n - \text{traced}\}, \{j, n - \text{traced}\}\right];$
$\text{sol} = \text{mX}/.\text{FindRoot}[\text{mA2} + \text{Conjugate}[\text{mA2}] - \Gamma.\text{Inverse}[\text{mX}].\text{Transpose}[\Gamma] == \text{mX}, l,$
$\text{WorkingPrecision} \to \text{MachinePrecision} + 1, \text{MaxIterations} \to 100];$
$\beta = \frac{\text{Det}[\Gamma]}{\text{Det}[\text{sol}]};$
$S = \text{Append}\left[S, \left\{t, -\frac{((1-\beta)\text{Log}[1-\beta]+\beta\text{Log}[\beta])}{(1-\beta)}\right\}\right];$
$\text{If}[\text{Det}[\Gamma]==0, S[[\text{Length}[S]]] = \{t, 0\}]$
$, \{t, 0.05, \text{time}, 0.05\}], \text{inputFlag} = \text{False};]$
$\text{If}[\text{inputFlag} == \text{False}, \text{Print}[\text{“Incorrect Input.”}]]$
$\text{If}\left[\text{inputFlag}, \text{ListLinePlot}\left[S, \text{AxesLabel} \to \{\text{t}, \text{"}S_{\text{EE}}\text{"}\}, \text{PlotLegends} \to \text{Placed}[\text{str}, \text{Above}],\right.\right.$
$\left.\left.\text{PlotStyle} \to \text{Black}, \text{PlotRange} \to \text{Full}\right]\right]$

The following portion of code is for the approximate analytical solution:

$\beta = \frac{\text{Det}[\Gamma]}{\text{Det}[\text{sol}]};$
$S = \text{Append}\left[S, \left\{t, -\frac{((1-\beta)\text{Log}[1-\beta]+\beta\text{Log}[\beta])}{(1-\beta)}\right\}\right];$
$\text{If}[\text{Det}[\Gamma]==0, S[[\text{Length}[S]]] = \{t, 0\}]$
$, \{t, 0.05, \text{time}, 0.05\}], \text{inputFlag} = \text{False};]$
$\text{If}[\text{inputFlag} == \text{False}, \text{Print}[\text{“Incorrect Input.”}]]$
$\text{If}\left[\text{inputFlag}, \text{ListLinePlot}\left[S, \text{AxesLabel} \to \{\text{t}, \text{"}S_{\text{EE}}\text{"}\}, \text{PlotLegends} \to \text{Placed}[\text{str}, \text{Above}],\right.\right.$
$\left.\left.\text{PlotRange} \to \text{Full}\right]\right]$